1-1-2016

Portable X-Ray Fluorescence Measurement Viability In Organic Rich Soils: Pxrf Response As A Function Of Organic Matter Presence

Roozbeh Ravansari
Wayne State University,

PORTABLE X-RAY FLUORESCENCE MEASUREMENT VIABILITY IN ORGANIC RICH SOILS: PXRF RESPONSE AS A FUNCTION OF ORGANIC MATTER PRESENCE

by

ROOZBEH RAVANSARI

THESIS

Submitted to the Graduate School

of Wayne State University

Detroit, Michigan

in partial fulfilment of the requirements

for the degree of

MASTER OF SCIENCE

2016

MAJOR: GEOLOGY

Approved By:

_____

Advisor Date

DEDICATION

Dedicated to my mom, brother, sisters and girlfriend.

You guys rock.

ACKNOWLEDGEMENTS

I am forever grateful to Larry Lemke, my graduate advisor. I was lucky enough to have met him during my graduate studies at Wayne State University, and even more lucky to have had him as my graduate advisor. I can honestly say that he has had a huge impact on my life.

I would like to thank Shawn P. McElmurry of the Wayne State University department of engineering for serving on my master's committee and also for allowing me to use his lab. He also presented me with many side opportunities to grow professionally for which I am grateful.

I would like to thank Mark M. Baskaran of the Wayne State University department of geology for serving on my master's committee and also for allowing me to use his lab. He provided me with different perspectives for which I am thankful.

I would like to thank my girlfriend Junghyun Lee for agreeing to do the illustrations presented in this thesis and more importantly for always encouraging me to better myself. Her love and support helped me through graduate school and I am forever grateful for that.

I would also like to thank the Wayne State University College of Liberal Arts, the Wayne State Office of Vice President for Research, and the USDA (Grant Funding # 2015-70001-23424) for providing me with financial assistance in the form of a graduate research assistantship. The position helped me develop my leadership, research and professional skills.

Finally, I would like to thank Geoffrey Cook of the University of California San Diego, Scripps Institution of Oceanography for keeping in touch with me even after I had already graduated and for encouraging me to pursue a master's degree.

TABLE OF CONTENTS

LIST OF TABLES

LIST OF FIGURES

Chapter 1

Introduction

1.0 Introduction

There has been a recent boom in the popularity of urban gardening and urban farming (Weindorf et al., 2012), raising questions about health risks associated with legacy contamination in urban settings such as Detroit, Michigan. Trace metal contamination of crop soils is an important concern because their presence may have negative health impacts if consumed via adhesion to produce or inhaled via garden dust. In many instances, gardens operating in urban settings lack the financial capabilities to have their soils tested via relatively expensive acid digestion analysis methods. Recently, the use of the portable X-ray fluorescence (pXRF) analytical method to measure metal concentrations in soils was formalized by the United States Environmental Protection Agency (USEPA, 2007b). pXRF offers urban gardeners a potentially faster and less expensive way to ensure their soil trace metal content falls below regulatory guidelines. Nonetheless, it is important to fully understand pXRF reliability and accuracy in the context of its use in urban farm settings.

Soils are heterogeneous by nature (USEPA, 2007b) and soils in general contain varying amounts of organic matter. Soil organic matter can range from as low as 1% in desert environments to as much as 90% or more in low wet areas (Troeh, 2005) and can reach as high as 20% in farming environments. Higher organic matter content is desirable to farmers because its presence on cultivated lands provides nutrients that stimulate crop growth. As such, many farmers, both rural and urban alike, boost the productivity of their crops by improving their soils through organic matter addition in the form of compost or other soil amendments. Although the influence of soil characteristics such as soil heterogeneity and moisture content on pXRF metal measurements have been documented (Tjallingii et al., 2007), the effect of variable organic matter content is not well understood. The overall aim of this investigation is to explore the effect of organic matter content on the ability of pXRF to accurately determine trace metal content in soils. This

chapter provides background information on XRF and soil metal measurement supporting the formulation of a hypothesis predicting an expected response to varying soil organic matter content.

1.1 Fluorescence and XRF Theory

X-rays, a form of electromagnetic ionizing radiation, were first discovered in 1895 by Wilhelm Roentgen, a German physicist (Jenkins, 1988). Since then, X-rays have proven useful in a wide range of fields including medical applications developed after doctors observed they could be used to examine the human body for bone fractures and foreign objects. This application of X-rays was widely used in World War I to save tens of thousands of lives (Jenkins, 1988). Since then X-rays have found applications beyond the medical field including, but not limited to, organic and inorganic elemental analysis. In his pioneering work, Verne Birks demonstrated that elemental analyses could be performed by bombarding an object with high energy X-rays and examining the resulting fluorescence spectrum (Jenkins, 1988). The field of X-Ray fluorescence (XRF) was thus born and since then many advancements have been made to the instrumentation and methods for performing elemental analyses.

Ionizing radiation is the driving force behind the fluorescence elemental analysis technique. Typically one of two different excitation (ionizing radiation) sources are utilized in XRF instruments. Some XRF instruments contain radioactive materials such as Cd-109, Fe-55 or Am-241 which are used as a direct source for ionizing radiation (Potts, 1999). The most commonly used ionizing radiation source in modern instruments however, is the X-Ray generating tube. The tube generates X-rays by accelerating electrons through the application of a potential difference between a cathode and an anode located at the ends of the tube. The acceleration and subsequent rapid deceleration of the electrons results in the emission of X-rays which are then used to excite the atoms of the sample being analyzed. Tube based instruments have several advantages over their radioactive material bearing counterparts due to safety concerns, regulatory barriers and procedures involved with the handling of radioactive materials (Shand and Wendler, 2014). With tube based instruments these concerns are less of an issue because ionizing radiation is only produced when the instrument is in operation.

Within the broader category of tube based X-Ray fluorescence instrumentation, two types of XRF instruments exist: energy dispersive and wavelength dispersive XRF instruments. Wavelength dispersive XRF involves manipulation of the fluorescence photons emitted from the sample being analyzed by putting a crystal between the sample and the detector resulting in diffraction of the fluorescence photons (Lachance and Claisse, 1995). The different wavelengths are thus isolated by diffraction and can be analyzed by the instrument at higher resolutions through rotation of the crystal at precise angles. This gives wavelength dispersive XRF more precision than the energy dispersive XRF, but it also makes it more expensive because it requires more internally moving parts than energy dispersive XRF. In contrast, energy dispersive XRF operates by varying the potential difference between the anode and cathode within the X-Ray tube in order to manipulate the energy levels of the incident X-Ray beam (Goulding and Jaklevic, 1973). The excited atoms of the sample then emit characteristic radiation which are picked up by the instrument's detector. The detector in this case is able to pick up both counts (number of incident photons) and energies (energy of the incident photons). In certain instruments it is also common practice to place filters between the beam source and the sample in order to further manipulate the incident beam.

XRF instruments operate on the principle of fluorescence, which is a phenomenon where atoms emit characteristic spectral lines when hit with high energy X-rays. Electrons orbiting the protons of atoms are quantized in that they can only be found at specific energy levels. These orbits, associated with the different energy levels, are classified and commonly referred to as the K,L,M and N shells of an atom (Lachance and Claisse, 1995). The X-rays excite and knock out the atom's electrons located in a certain shell and an electron of higher energy falls to a lower energy shell to fill the vacancy resulting in a characteristic spectral emission known as fluorescence.

When the energy of an impinging X-Ray equals the critical excitation energy for an element there is a sharp increase in the amount of X-Rays absorbed by the given element and thus a sharp increase in characteristic fluorescence X-Rays. Many XRF instruments take advantage of this phenomenon by placing

energy filters between the X-Ray source and the sample so as to filter out the excitation energies of the elements of lesser interest. In many instances, the filters segregate the source X-Rays into three spectral energy fields (high, medium and low filters). These filters enhance the performance of the XRF processor executing computations for translating counts per second picked up by the detector into concentration measurements.

Rayleigh scattering, also referred to as coherent scattering, occurs when an X-Ray hits an electron and the energy is coherently scattered in a different direction (Figure 1.1a). Consequently, no energy is lost, but the trajectory of the impinging X-Ray changes. Compton scattering, also referred to as incoherent scattering, occurs when an X-Ray hits an electron and ejects it from its orbit (Figure 1.1b). During Compton scattering, the impinging X-Ray retains some of its energy after the collision and ejection. Incoherent scattering thus results in a modification of both trajectory and energy of the impinging X-Ray. Incoherent scattering may affect XRF measurements and is addressed by XRF manufacturers at the factory by performing calibrations on internal standards (Kenna et al., 2011).

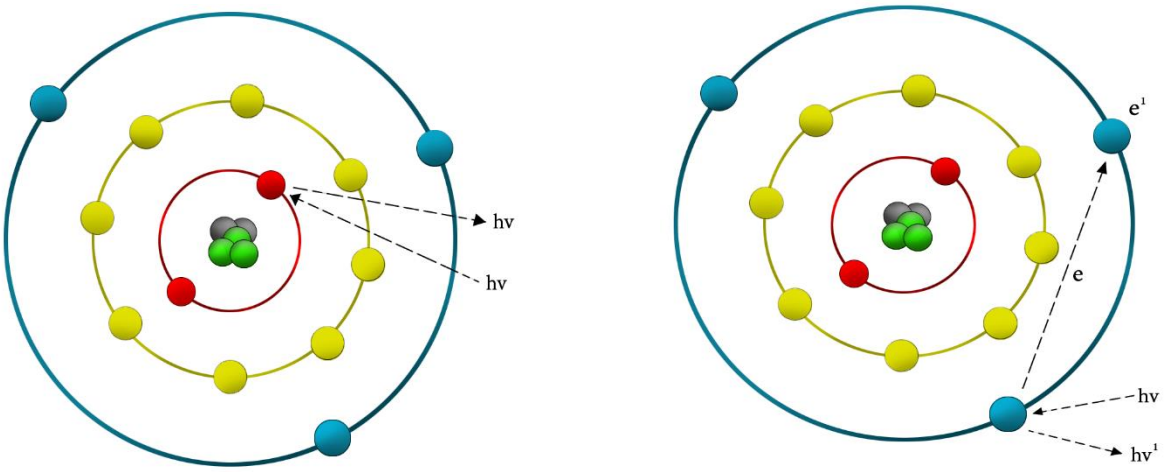

Figure 1.1 Scattering of incident X-rays: (a) Rayleigh scattering; (left), (b) Compton scattering; (right).

1.2 XRF analysis sequence

The sequence of events involved in X-Ray fluorescence analysis begins when a high energy X-Ray beam irradiates a portion of the sample. Subsequently, the electrons for which the energy of the incident X-Ray photon is higher than the electron binding energy are subject to ejection from atoms comprising the sample (Figure 1.2). Higher energy electrons fall to fill the vacancies left over by the ejected electrons. Because energy is conserved, a spectral emission is generated with a wavelength corresponding to the energy lost from the higher energy electron as it transitions from a higher state to a lower energy state. The characteristic fluorescence photon unique to the element is detected by the XRF instrument. Finally, XRF analytical algorithms transform the measured intensity of the fluorescence for each element into a mass concentration, typically in parts per million (mg/kg) for trace elements or % for major elements. Because the fluorescence intensity of any given element within the sample may vary at any given moment in time, the intensities are averaged over a prescribed length of time so as to maximize accuracy and minimize variability related to the probabilistic excitement of atoms by incident X-rays.

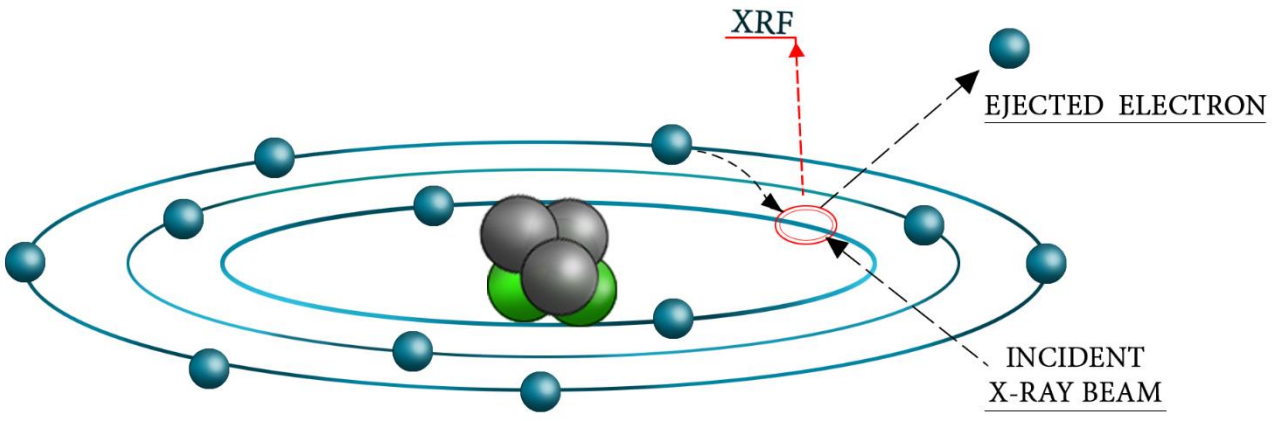

Figure 1.2 Generation of X-Ray fluorescence through electron ejection by incident photon.

1.3 XRF Advantages

With technological advancements and miniaturization of integrated circuitry, the portability of XRF analyzers has become feasible (Iwanczyk and Patt, 1999). The portable X-Ray fluorescence (pXRF) instrument is used to determine the elements present within samples. The pXRF instrument has many advantages over other methods currently available for metal analyses of soils. First and foremost, the instrument itself costs considerably less than an inductively coupled mass spectrometer (ICPMS). ICPMS analyses are also time consuming, expensive, and destructive because acid digestion of the soil sample is required.

With the pXRF, samples can be analyzed in-situ as well as in a controlled laboratory environment. They can be analyzed quickly (Kalnicky and Singhvi, 2001), economically, and non-destructively which make pXRF an attractive method of analysis for soils in both academia and industry alike (Shand and Wendler, 2014). The cost effectiveness of the pXRF makes it an attractive method for determining soil trace metal presence and concentrations at urban farms (Weindorf et al., 2012). The accuracy and reliability of pXRF has important implications for anyone applying the X-Ray fluorescence technique for determinations of soil trace metal content.

1.4 Factors affecting XRF soil measurements

Other factors affecting XRF measurements include object geometry (Löwemark et al., 2011), soil moisture content (Böning et al., 2007) and soil heterogeneity (Tjallingii et al., 2007). X-rays are photons which behave like light in that the X-Ray intensity attenuates by a factor of $1/r^2$ where r is the distance between the emission source and detector (Shand and Wendler, 2014). The XRF generates information on elemental abundances by bombarding the sample with X-rays and measuring the intensities of the resulting fluorescence photons from the sample. If the surface of the object is irregularly shaped, it may affect the measurement because the XRF algorithms assume a flat surface over the area of incidence for the X-ray beam. XRF measurements may also be affected by soil moisture content which is why drying soil samples prior to analysis is recommended (EPA 2007b). Soil heterogeneity refers to the variability in the

composition of soils, it is inherently present in all soil samples (Ramsey, 1998), i.e. there is a fundamental non-uniformity to the spatial arrangement of the atoms comprising the sample arising from random mixing of atoms and molecules during soil formation. Soil heterogeneity can be mitigated by sample sieving prior to analysis and by repeating XRF measurements in triplicate. Shaking of soil sample vials between measurements is also recommended (EPA 2007b).

1.5 Prior Studies

The USEPA (2007) recommends the use of confirmatory sample analysis for pXRF quality control, however inconsistencies between analytical methods for soil trace metal content determinations are widely recognized. For example, Brumbaugh et. al (2013), measured two different National Institute of Standards and Technology (NIST) soil standards for which comparisons were drawn between XRF, ICPMS and NIST certified values. Their results demonstrated inconsistency between XRF and ICPMS measurements. Similarly, Congiu et al. (2013), demonstrated inconsistencies between XRF and ICPMS in trace metal soil contaminant measurements. Shand and Wendler (2014) reported inconsistencies between pXRF measurements made on standard materials and their certified values. They recognized that organic matter causes complications to pXRF measurements and concluded that the realm of pXRF could benefit from the creation of certified standards on a continuum of organic matter content which could be used for calibration of pXRF instruments.

The use of X-Ray fluorescence has been employed to assess XRF measurement reliability within highly contaminated soils. Radu and Diamond (2009) compared lead, arsenic, copper and zinc XRF and AAS (atomic abortion spectrometry) measurements made on soils obtained from areas with past mining activity near Silvermines, Ireland. The results of their investigation revealed strong correlation between the two analytical methods but discrepancies between individual measurements (Radu and Diamond, 2009). Some of the measurements made on the same samples using the different analytical methods were not within each other's 2σ confidence interval. The authors concluded that pXRF could be use in lieu of more expensive analytical methods to determine the *presence* of contaminants within potentially highly

contaminated soils. The results of their individual measurements however revealed discrepancies which suggest that a different approach must be taken if precise measurements are required (beyond simply confirming presence).

The feasibility of pXRF for soil trace metal measurements within a peri-urban agricultural setting was conducted by Weindorf et al. in 2012. The findings of their study suggest that portable X-Ray fluorescence shows promise for use in agricultural soils; however, there were discrepancies between the standard certificate values for the reference materials used in the investigation and the pXRF measurements (Weindorf et al., 2012). The results of the investigation suggest a different approach is required to render accurate values when using portable X-Ray fluorescence within the context of urban agricultural settings. Accurate pXRF measurements are crucial to contamination determination investigations because accurate measurements are required for determining whether the levels of a trace metal contaminant present exceed or fall below regulatory action levels as this may have health connotations for people consuming the vegetables grown within the soil.

Recognizing the error prone nature of X-Ray fluorescence, some have called for the constant monitoring and calibration (Kenna et al., 2011) of pXRF performance and measurements by continually running standards between set numbers of measurements (Brand and Brand, 2014). In samples requiring homogenization, the addition of sodium fluorescein dye to monitor mixing has been widely used (e.g., VanCott et al., 1999) and is still in use today (USEPA, 2007b) because it is thought not to affect the measurements to a high degree.

1.6 Hypothesis

Factors affecting discrepancies between pXRF measurements of soil standards and their certificate values have been traditionally attributed to heterogeneity and matrix interference effects. However, the effects of organic matter fraction on XRF measurements have not been thoroughly investigated. The purpose of this investigation is to quantify the effect of increasing organic matter fraction on pXRF measurements for the following thirteen elements: arsenic, chromium, copper, iron, manganese, lead, rubidium, strontium, thorium, titanium, vanadium, zinc, and zirconium.

It is hypothesized that **pXRF metal concentration measurements are attenuated with increasing soil organic matter in proportion to the fraction of organic matter present.** This effect is expected to be different for individual elements, however, depending on the similarities of electron transition energy peaks that they may share with carbon and oxygen, the primary elemental components of organic matter.

To evaluate this hypothesis, a series of laboratory experiments was designed to investigate the effects of organic matter on pXRF trace metal measurements. The experiments involved an organic free soil with known metal concentrations that was subsequently spiked with three organic matter surrogates of varying proportions. Chapter 2 of this thesis describes the materials, laboratory methods and experimental design in detail. Relevant equations and results from XRF measurements are reported in Chapter 3. Conclusions and a discussion are presented in Chapter 4 along with recommendations for future research.

Chapter 2

Materials and Methods

2.0 Introduction

To determine the effects of organic matter on pXRF soil metal measurements, a sample of Natural Resources Canada (NRCan) Till-1 standard reference soil was expunged of organic matter and subsequently incrementally spiked with increasing organic matter surrogate material. Plots of pXRF measured metal concentration versus organic matter fraction for each organic matter surrogate were generated for comparison with theoretical response curves based on dilution of the soil with organic matter. This chapter provides information on the pXRF instrument, the Till-1 standard, the chosen organic matter surrogates, and a detailed series of procedures outlining the steps taken to conduct the experiments.

2.1 Materials and Instrumentation

Several soil standard reference materials (SRM) with certified metal concentrations are available for verification of laboratory analytical methods. These include National Institute of Standards and Technology (NIST) standard NIST-2586, NIST-2709a, NIST-2711a and an SiO2 blank. NRCan standards include Till-1, Till-2, Till-3, and Till-4 derived from glacial soils and tills in Ontario and British Columbia. The Till-1 standard was selected for this investigation because NRCan certificate SRM contained more detailed information compared to available NIST standards, including information on organic matter content. Among the four NRCan standards, the Till-1 standard was chosen because it contained most elements of interest in sufficient quantities above the detection limit of the pXRF instrument.

Table 2.1 provides Till-1 standard certificate values for the 13 elements of investigation. The Natural Resources Canada Till-1 standard itself was collected 25 kilometers north-west of Lanark Ontario, Canada near Joe Lake (NRCan, 1995).

Table 2.1 Natural Resources Canada Till-1 standard certificate values and organic matter fraction.(NRCan, 1995)

Element	Certificate (mg/kg)	Organic Matter %
As	18	6.3
Cr	65	
Cu	47	
Fe	48100	
Mn	1420	
Pb	22	
Rb	44	
Sr	291	
Th	5.6	
Ti	5990	
V	99	
Zn	98	
Zr	502	

Three organic matter surrogates were chosen for the experiment: cellulose, carbon (graphite powder), and sugar (Table 2.2).

Table 2.2 Organic matter surrogate information table

Surrogate	Source	Description	Chemical Formula
Cellulose	Sigma Aldrich Labs	Cellulose Powder	$C_6H_{10}O_5$
Carbon	Sigma Aldrich Labs	Graphite Powder	C
Sugar	Meijer	Meijer's brand confectioner's powdered sugar	$C_{12}H_{22}O_{11}$

The experiment was initially carried out with confectioners' sugar because it was a readily available powdered form of organic matter with a grain size of less than 250 microns. Initial pilot experiments using confectioners' sugar and local garden soils were used to explore the feasibility of using organic matter surrogates for this investigation. Results of subsequent, better controlled experiments using confectioners' sugar and the Till-1 reference soil are reported here. Graphite powder was acquired from Sigma Aldrich labs and is certified to be 99.98% pure carbon. Its grain size is less than 250 microns. Cellulose powder was also acquired from Sigma Aldrich labs although its certificate did not contain purity information. Prior to its use, the cellulose powder was passed through a 250 micron mesh to remove grains larger than 250 microns. Samples were digested using USEPA Method 3051 (2007a) and ICP-MS measurements were carried out on all three organic matter surrogates to confirm the absence of the metals of interest to this study.

The pXRF instrument used for these experiments was the Niton XL3t GOLDD+ analyzer which was used in conjunction with its laboratory stand in desktop mode to increase precision and repeatability while performing analyses (Figure 2.1). The X-Ray generating tube contains a silver (Ag) anode and reaches 50 keV while in operation. The detector is a geometrically optimized large area drift detector and its resolution is 185 electron volts. The radius of its primary X-Ray beam is 8mm in diameter; however, it also allows the operator to choose the "small spot" option which makes the beam 3mm in diameter. This is typically used if the analyst is attempting to analyze a specific crystal within a rock. The instrument can be set to a variety of modes including metal alloys mode, electronics alloy mode, mining mode and soil mode. For this study, the instrument was operated in soils mode with the 8mm diameter option enabled to improve the measurements of the instrument.

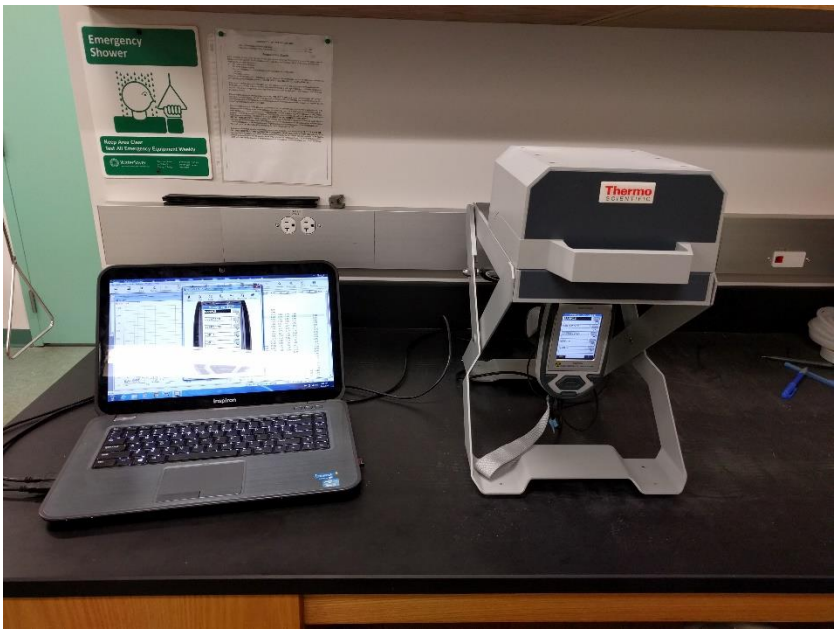

Figure 2.1 The pXRF instrument loaded into its desktop stand and interfaced with a computer.

2.2 XRF Analysis Vial Preparation Method

XRF analysis vials were prepared for use in many of the subsequent procedures (Figure 2.2). The 37 ml XRF analysis vials are made of polypropylene and serve as containers for the soil samples being analyzed. The following steps were followed when preparing XRF vials for analysis.

1. Obtain clean polypropylene tubes with caps.
2. Puncture a hole in the cap with a diameter of ~20mm.
3. Rinse the cap and the tube with deionized water. Air dry them.
4. Once dry, pour the sample to be analyzed via XRF into the tube. Ensure the height of sample within the tube is no less than 20mm in the tube.
5. Place a 4 micron thick "XRF Thin Film Circle" made by Premier Lab Supply (Model #: TF-240-255) on top of the tube's entrance paying careful attention to keeping it clean and free of any potential contamination.
6. Pop the cap back onto the analysis vial securing the sample within the tube. The tube is now prepared for XRF analysis and can be turned upside down to place on the XRF stand for analysis.

The XRF analysis vials are sealed with the 4 micron thick sheet of polypropylene film to minimize signal attenuation (Compton scattering) which may result from radiation traveling between the sample and the XRF detector.

Figure 2.2 Prepared XRF vials: Side view pictured left, top view pictured right.

2.3 XRF Analysis Method

More than 700 pXRF analyses were performed throughout the investigation using a standard operating procedure for the pXRF instrument. The following steps were adhered to when performing pXRF analyses. The pXRF was set to soils mode in the pXRF settings console prior to analyses. A dosimeter ring was worn whenever the pXRF was in operation to monitor radiation exposure levels and ensure a safe lab environment. Standards were run before the start of analyses for the day, after every 10 samples, and at the conclusion of analyses for the day in order to check for instrumental drift. The standards used for this purpose were the NIST 2709a, NIST 2586, Till-4 and an SiO_2 blank. System checks must be performed each time the pXRF is turned on.

1. The XRF vial was turned upside down and gently tapped on the surface of the XRF analyzer 10 times.
2. The center of the hole in the cap of the XRF vial (sealed with the 4 micron thick polypropylene film) was aligned with the center of the pXRF analyzer window on the test stand.
3. The stand was shut and the latch was locked to ensure no radiation leaked out of the analysis chamber.
4. The pXRF was operated remotely via a computer connection. Each analysis was set to a 3 minute (180 second) duration. Thus, dwell time included 60 seconds in each of the low, medium, and high energy filter modes.

Considerations

- Attention is to be paid between each step throughout the experiment to avoid contamination of the sample and/or XRF analyzer itself. Do not allow dust on the XRF analyzer screen or the analysis vial thin film as this will affect XRF measurements.

2.4 Organic Matter Determination and Expulsion

It is necessary to determine and remove the organic matter fraction (%) from the Till-1 standard used for the experiments in this investigation. This was achieved by following the instructions set forth in ASTM Method 2974 – 14 (ASTM, 2014). A "burn" of the sample is performed by placing the sample in an oven set at 550 degrees Celsius to remove any organic matter through combustion and associated volatilization. The following steps were adhered to when determining OM fraction and performing the burn.

1. Determine the mass of an empty clean porcelain dish. The dish should have a high surface area to allow the soil sample to be spread out so as to avoid trapping any organic matter from exposure to oxygen when the furnace is turned on.
2. Evenly spread a thin coat of the NIST Till-1 sample in the porcelain dish and determine the mass of the entire dish.
3. Place the dish in a muffle furnace and increase the temperature to 550 degrees Celsius to burn off the organic matter content of the soil, leave the sample in the furnace overnight.
4. Remove the sample from the furnace and let the sample cool at room temperature. After it cools down, determine the mass of the specimen.
5. From the recorded mass data, determine % organic matter composition of the sample.
6. Save the sample for use in the subsequent "Incremental Organic Matter Spiking Method" section of the experimental design.

Considerations

- Attention is to be paid between each step throughout the experiment to avoid contamination of the sample.

2.5 Cellulose Sieving Method

The cellulose sieving method served as a preparatory step for the subsequent procedures which use cellulose. The cellulose being used must be sieved down to 250 microns in order to ensure that the cellulose grains are comparable to the grains from the Till-1 standard.

1. Line a ro-tap catcher pan with paper and prepare a ro-tap mesh stack with a 250 micron mesh as the last sieve before the catcher pan.
2. Pour cellulose into sieve and turn on ro-tap for 10 minutes.
3. Remove, label and store the cellulose <250 micron fraction for use in the subsequent sections of this experiment.

The ro-tap catcher pan was lined with paper to minimize potential for metal contamination making its way from the pan to the sample being analyzed.

2.6 Incremental Organic Matter Spiking Method (Dry Method)

After removal of the organic matter (Section 2.4), the standard sample was incrementally spiked with organic matter surrogate (cellulose/carbon/sugar) and analyzed via XRF in order to determine the XRF response to increasing OM fraction. This method utilized dry surrogate material as opposed to wetting the sample after the homogenization step (Section 2.7).

The carbon pXRF analyses were performed twice in a row in batch mode prior to shaking the sample. This was done to acquire the information required for the detailed analysis of variance (ANOVA) (Section 2.9) which was conducted to decipher the geochemical variability, heterogeneity variability and analytical variability components (Ramsey, 1998).

The resulting fraction of organic matter was calculated using this equation:

$$OMAfter = \frac{(OMBefore * SampleWeight) + SurrogateAdded}{SampleWeight + SurrogateAdded} \quad (2.1)$$

where “OM After” is the fraction of organic matter within the sample after addition of OM, “OM Before” is the fraction of organic matter present in the sample, “Sample Weight” is the mass of the sample before addition of surrogate, and “Surrogate Added” is the mass of the surrogate added to the sample.

1. Draw a line associated with a 20mm sample depth on two polypropylene XRF analysis vials. Weigh, label and record the masses of the empty vials for use in calculations.
2. Fill one of the vials to the indicated line with only the chosen organic matter surrogate and perform an XRF analysis on the contents in triplicate shaking the vial for 10 seconds between runs.
3. Fill the other vial to the indicated line with the burned Till-1 sample, record the Sample Weight for use in calculations then analyze the sample in triplicate with the pXRF instrument shaking the vial for 10 seconds between runs.
4. Remove sample and pour it in its entirety into the mixing beaker. Place the beaker on the scale and record the vessel mass in grams.
5. Add approximately 0.5 grams of the organic matter surrogate into the vessel and weigh and record the vessel once more after spiking it with the organic matter surrogate. The difference between the vessel weight before and after OM addition represent the surrogate added.
6. Put a piece of paper over the lid of the beaker and then put an appropriately sized rubber stopper over the beaker. Hold it closed tightly.
7. Shake the sample so as to mix the added cellulose in the sample. This serves as a premix step.
8. Pour beaker contents onto a 30cm x 30cm piece of construction paper and homogenize following the procedure described by Piorek (1998).
9. Roll the sample over on itself 20 times to ensure homogeneity of the sample.

10. Pour the sample into the vial up to the 20mm line. Save and label the excess leftover materials in individual vials for potential further investigation. Record the weight of the sample for use in calculations.
11. Perform XRF analysis in triplicate on the spiked sample shaking the vial for 10 seconds between runs.
12. Repeat steps 4 through 11 until the sample has been spiked to desired organic matter content.

Considerations

- Standards must be run in triplicate before start and after finish of the experiment.
- Standards should also be run in triplicate between every 10 triplicate measurements to allow the analyst to check and correct for instrumental drift if it occurs (Brand and Brand, 2014).
- Additional individually saved and labeled materials from this experiment should be saved to allow the analyst the option of analyzing said samples via different analytical methods including ICPMS using different digestion methods to determine how organic matter content affects recoverability of trace metals and to draw comparisons between XRF and other analytical method measurements.
- Attention is to be paid between each step throughout the experiment to avoid contamination of the sample.
- Careful tapping of containers should be performed so as to minimize mass loss between vessel transfers.

2.7 Incremental Organic Matter Spiking Method (Wet Method)

The “Wet Method” organic matter spiking method was developed to coat the sediment grains from the standard with cellulose. This was done to mimic the behavior of organic matter in natural samples, i.e., organic matter coating sediment grains and was used to provide a comparison with the experiments using the addition of dry cellulose as an organic matter surrogate. The resulting fraction of organic matter was calculated using Equation 2.1.

1. Obtain a burned Till-1 sample devoid of organic matter. Draw a line associated with a 20mm sample depth on a polypropylene XRF analysis vials. Weigh, label and record the mass of the empty vial for use in calculations. Put Till 1 sample into the XRF analysis vial up to marked 20mm line and prepare for XRF.
2. Analyze the sample 3 times using the XRF. Shake before and between runs.
3. Pour the sample into a beaker (Note empty beaker weight for calculations). Weigh the entire contents of the beaker + soil.
4. Put approximately 0.5 grams of cellulose in the beaker and record the new weight.
5. Put a piece of paper over the lid of the beaker and then put a rubber stopper over the beaker. Hold it closed tightly.
6. Shake the sample so as to mix the added cellulose. This step serves as a premix.
7. Pour beaker contents onto a 30cm x 30cm piece of construction paper.
8. Roll the sample over on itself 20 times to ensure homogeneity of the sample.
9. Pour contents into drying porcelain dish. Record weight of porcelain dish + soil.
10. Add approximately 15-20 ml of deionized water to porcelain dish. Stir to homogeneity by mixing with a clean straw. Shake and tap straw at the end of stirring to prevent mass loss.
11. Put porcelain dish in an oven set to ~90 degrees Celsius to evaporate the sample.
12. After sample is dry (minimum 6 hours), remove it from the oven. Let the sample cool and equilibrate with ambient atmosphere for at least 30 minutes. Weigh the porcelain dish once more

and compare with previous measurement to ensure no critical mass loss has occurred in the drying step.

13. Transfer the porcelain dish contents from the dish to a sieving pan. Use a 250 micron mesh. Use a clean plastic straw to scrape off any contents which may be adhering to the bottom of the porcelain dish. Line the sieving capture pan with paper to catch the sample.
14. Transfer the pan contents from the sieve capture pan to an XRF analysis tube. Weigh and record the new weight of the XRF analysis tube for use in calculations (equation 2.1, “Sample Weight”).
15. Prepare tube for XRF analysis and shake it before and between runs for 10 seconds.
16. Run each sample 3 times then begin the process again by referring to step 3 of this procedure.

Considerations

- Standards must be run in triplicate before start and after finish of the experiment.
- Standards should also be run in triplicate between every 10 sets of triplicate measurements to allow the analyst to check and correct for instrumental drift if it occurs.
- Additional individually saved and labeled materials from this experiment should be saved to allow the analyst the option of analyzing said samples via different analytical methods including ICPMS using different digestion methods to determine how organic matter content affects recoverability of trace metals and to draw comparisons between XRF and other analytical method measurements.
- Attention is to be paid between each step throughout the experiment to avoid contamination of the sample.
- Careful tapping of containers should be performed so as to minimize mass loss between vessel transfers.

2.8 Digestion and Dilution Procedure for ICPMS Sample Prep

Digestions and dilutions were performed on carbon, sugar and cellulose samples adhering to EPA digestion method 3051a (Microwave assisted 70% nitric acid). Specific digestion and dilution steps created by Michael Bickel and revised by Shawn P. McElmurry for use in the Wayne State University College of Engineering McElmurry lab can be found in Appendix A. Briefly, approximately 0.5g of sample was digested with concentrated nitric acid in a microwave for 15 minutes. The digested sample was then diluted and centrifuged, followed by filtration and further dilution in preparation for ICP-MS analysis. Prepared ICP-MS samples were analyzed by the Wayne State University Department of Chemistry Lumigen Laboratory in Detroit, Michigan using an Agilent 7700x instrument.

2.9 ANOVA: Carbon

A nested analysis of variance (ANOVA) (Ramsey, 1998) was conducted on the carbon samples (Section 2.6) to determine what fraction of the variance exhibited in the pXRF measurements can be attributed to geochemical variability, sample heterogeneity, and analytical variability (Figure 2.3). Geochemical variance refers to the variability from sample to sample and is where one would expect to find the greatest % of attributable variability in response to changes in the independent variable (organic matter fraction). Variance attributable to sample heterogeneity results from small scale variability of soil material within the sample vials. It arises because the XRF beam does not sample the entire volume of each vial. Thus, sample heterogeneity is assessed by shaking each vial between runs. Analytical variance refers to the instrument's measurement variability in running exactly identical samples. It was assessed by measuring every shaken sample twice in batch mode on the XRF. The fully nested ANOVA was conducted using the Minitab statistical software package.

The nesting pattern used for the ANOVA is depicted as a flow chart below.

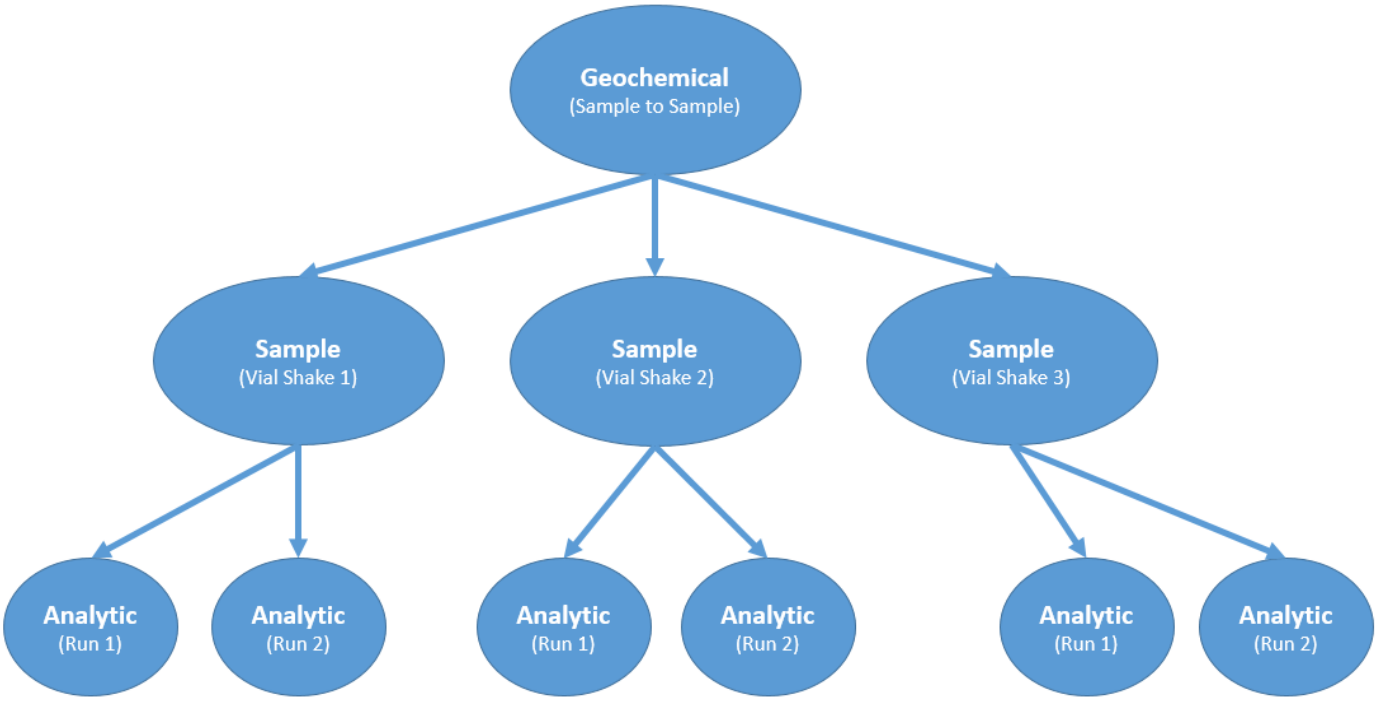

Figure 2.3 ANOVA nesting pattern

2.10 Regression Statistical Significance Analysis

Regressions and plots comparing organic matter fraction to pXRF responses were prepared and computed using Microsoft Excel spreadsheet software. Regression statistical significance tests were performed using Minitab statistical analysis software to compare different regressions to one another. The various regression comparisons performed are listed in Table 2.3. Rendered P values less than .01 were considered significant, indicating different regression slopes or intercepts.

Table 2.3 Regressions Statistical Significance Tests

OM Type vs Theoretical Line	Cellulose vs Theoretical
	Carbon vs Theoretical
	Sugar vs Theoretical
Repeatability	Dry Run 1 vs Dry Run 2
Coating	Dry 1 vs Wet
Elemental Dependence	Carbon vs Cellulose
	Carbon vs Sugar
	Cellulose vs Sugar

2.11 Summary

This chapter highlighted the procedures and materials used to obtain information on the effects of organic matter surrogates on pXRF measurements. In the following chapter, the results of these experiments are presented in the form of plots for each type of organic matter surrogate used (cellulose, carbon, sugar).

Chapter 3

Results

3.0 Introduction

The results of the experiments are presented in this chapter. Results from separate measurements made on the Till-1 SRM and individual OM surrogates are presented first. OM addition experiment results are presented in subsections based on each of the thirteen different elements of interest. Separate graphs showing the theoretical pXRF response along with experimental results for the incremental addition of cellulose, carbon, and sugar are included. The chapter concludes with a detailed analysis of variance for the carbon dilution runs followed by a table summarizing the regression coefficients for each of the plots presented in this chapter.

3.1 Till-1 OM Determination Results

Table 3.1 lists the experimental loss on ignition organic matter determinations for the Till-1 standard following the procedures set forth in ASTM D 2974-14 (ASTM, 2014). Four separate trials were conducted associated with the preparation of Till-1 soil for use with cellulose dry, cellulose wet, carbon, and sugar experiments. The combusted standard material used in trial 4 was split into two portions that were used to conduct the cellulose dry 2 and cellulose wet experiments.

Table 3.1 Experimental organic matter concentration for Till-1 Standard.

Trial		Organic Matter %
1	Cellulose Dry 1	6.4
2	Carbon	6.4
3	Sugar	6.4
4*	Cellulose Dry 2 Cellulose Wet	6.1

Table 3.2 lists the adjusted certificate values for the Till-1 standard accounting for organic matter mass loss after combustion using a value of 6.4% for mass loss (Table 3.1). Element concentrations before combustion were obtained from the Till-1 certificate (NRCan, 1995). The indicated errors are associated with the 2σ confidence interval.

Table 3.2 Till-1 reference values before and after combustion.

Element	Certificate Values Before Combustion (mg/kg)	Adjusted Values After Combustion (mg/kg)
As	18 +/- 2	19
Cr	65 +/- 12	69
Cu	47 +/- 8	50
Fe	48100 +/- 4400	51384
Mn	1420 +/- 150	1517
Pb	22 +/- 6	24
Rb	44 +/- 12	47
Sr	291 +/- 20	311
Th	5.6 +/- 1	6.0
Ti	5990 +/- 420	6399
V	99 +/- 20	106
Zn	98 +/- 20	105
Zr	502 +/- 116	536

3.2 Cellulose, Carbon, Sugar ICPMS Measurements

ICPMS analyses following EPA digestion procedure 3051a were performed in duplicate on cellulose, carbon and sugar samples to detect and quantify the presence of any elements of interest in this study. This was done to ensure elemental concentrations were not enhanced through the addition of surrogate material in the experimental process. ICPMS results were below detection limit for all elements of interest to this investigation with the exception of iron (Table 3.3).

Table 3.3 ICPMS measured concentrations in surrogate organic matter samples.

Element*	Detection Limit (ppm)	Cellulose (ppm)	Carbon (ppm)	Sugar (ppm)
As	4	-	-	-
Cr	4	-	-	-
Cu	5	-	-	-
Fe	5	151	49	60
Mn	4	-	-	-
Pb	4	-	-	-
Rb	4	-	-	-
Sr	4	-	-	-
Th	*	*	*	*
Ti	5	-	-	-
V	5	-	-	-
Zn	11	-	-	-
Zr	4	-	-	-

*Note: ICPMS laboratory was unable to generate reliable results for Thorium.

3.3 Cellulose, Carbon, Sugar XRF Measurements

XRF analyses were also performed on cellulose, carbon and sugar to ensure samples were void of elements of interest (Table 3.4). This was done to ensure that elemental levels were not significantly concentrated through the addition of organic matter surrogate material. Analyses were performed in triplicate on sugar and 10 times on carbon and cellulose.

Table 3.4 pXRF average measured concentrations in surrogate organic matter samples.

Element	Detection Limit (ppm)	Cellulose (ppm)	Carbon (ppm)	Sugar (ppm)
As	7	-	-	-
Cr	22	-	-	-
Cu	13	26 +/- 5	-	-
Fe	N/A	147	-	-
Mn	50	-	-	-
Pb	8	-	-	-
Rb	3	-	-	-
Sr	3	-	-	-
Th	4	-	-	-
Ti	4	-	36 +/- 29	-
V	25	-	-	-
Zn	10	-	-	-
Zr	4	12	10	8

3.4 Till-1 After Combustion XRF Measurements

Table 3.5 contains information for the Till-1 measurements made at zero percent organic matter content. Comparisons are drawn between the average pXRF value and the corrected certificate values. The average for all pXRF measurements among the different experimental runs fall within 20% of their certificate values for each of the thirteen metals investigated.

Table 3.5 pXRF measurements of Till-1 standard at zero percent organic matter.

Sample	XRF Detecion Limit	Cellulose 1 (ppm)	Cellulose 2 (ppm)	Cellulose Wet (ppm)	Carbon (ppm)	Sugar (ppm)	Average (ppm)	Certificate Adjusted (ppm)	% Difference
As	7	20	20	22	20	20	**20.3**	**19.0**	**6.94%**
Cr	22	63	59	62	58	57	**59.7**	**69.0**	**-13.5%**
Cu	13	58	63	62	56	60	**59.9**	**50.0**	**19.7%**
Fe	N/A	46895	46717	46758	46601	45152	**46425**	**51384**	**-9.65%**
Mn	50	1518	1597	1528	1519	1435	**1519**	**1517**	**0.15%**
Pb	8	24	26	23	25	23	**24**	**24**	**0.74%**
Rb	3	42.5	42.3	42.6	41.7	41.7	**42.2**	**47.0**	**-10.3%**
Sr	3	306	306	304	299	300	**303**	**311**	**-2.58%**
Th	4	6.24	5.74	6.32	5.45	7.20	**6.19**	**6.00**	**3.17%**
Ti	4	5716	5715	5568	5273	5389	**5532**	**6399**	**-13.5%**
V	25	117	121	118	109	116	**116**	**106**	**9.61%**
Zn	10	100	102	100	98	95	**99**	**105**	**-5.66%**
Zr	4	518	506	495	500	499	**504**	**536**	**-6.04%**

3.5 Experimental Results

Results from experiments measuring elemental concentrations within the Till-1 sample after the addition of varying fractions of organic matter surrogates are presented in Figures 3.1 -3.39. These plots include a curve showing the theoretical dilution effect resulting from the addition of variable fractions of the organic matter surrogate beginning with the certified concentration at 0% OM. This curve assumes that OM consisting of C, O, and H atoms does not interfere with the pXRF metal measurements. The error bars depicted on the graphs show +/- 2 standard deviations as recorded by the XRF instrument. The cellulose graph contains data for three cellulose runs (dry 1, dry 2, wet) because the experiment was conducted multiple times using cellulose to determine repeatability. The linear regressions presented on the cellulose plots are listed in the following order: dry cellulose run 1, dry cellulose run 2, and wet cellulose run.

3.5.1 Arsenic [As]

As expected, the pXRF arsenic signal drops off in response to the addition of OM for each of the different organic matter surrogates used (Figures 3.1-3.3). Results among the cellulose experiments (dry 1 vs. dry 2 and dry 1 vs. wet) are repeatable, as indicated by regression significance testing results (see Section 3.7). However, cellulose regression coefficients (slope and intercept) differ from theoretical predictions based on OM dilution. With the exception of the intercept for sugar, carbon and sugar regressions also differ from theoretical predictions based on dilution.

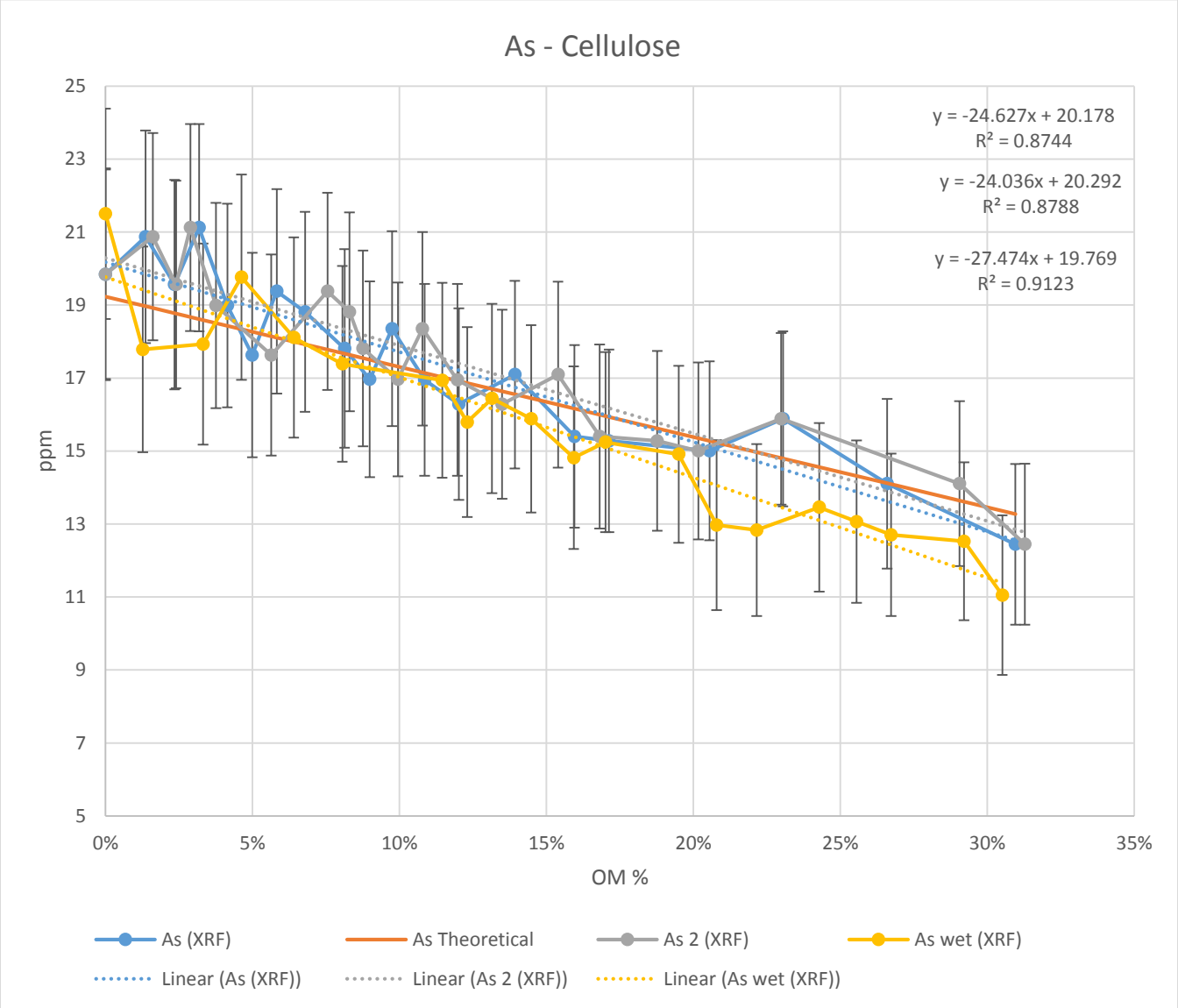

Figure 3.1 Arsenic concentration versus cellulose organic matter fraction.

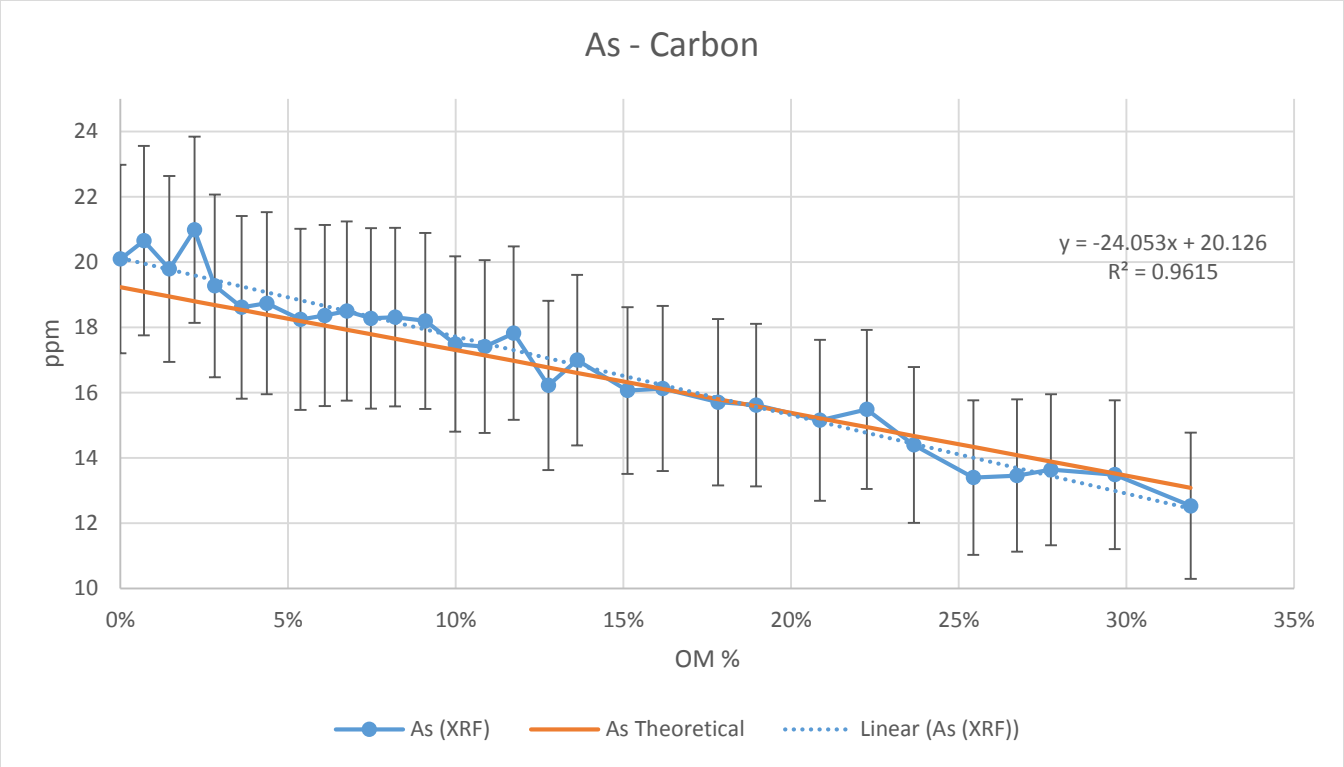

Figure 3.2 Arsenic concentration versus carbon organic matter fraction.

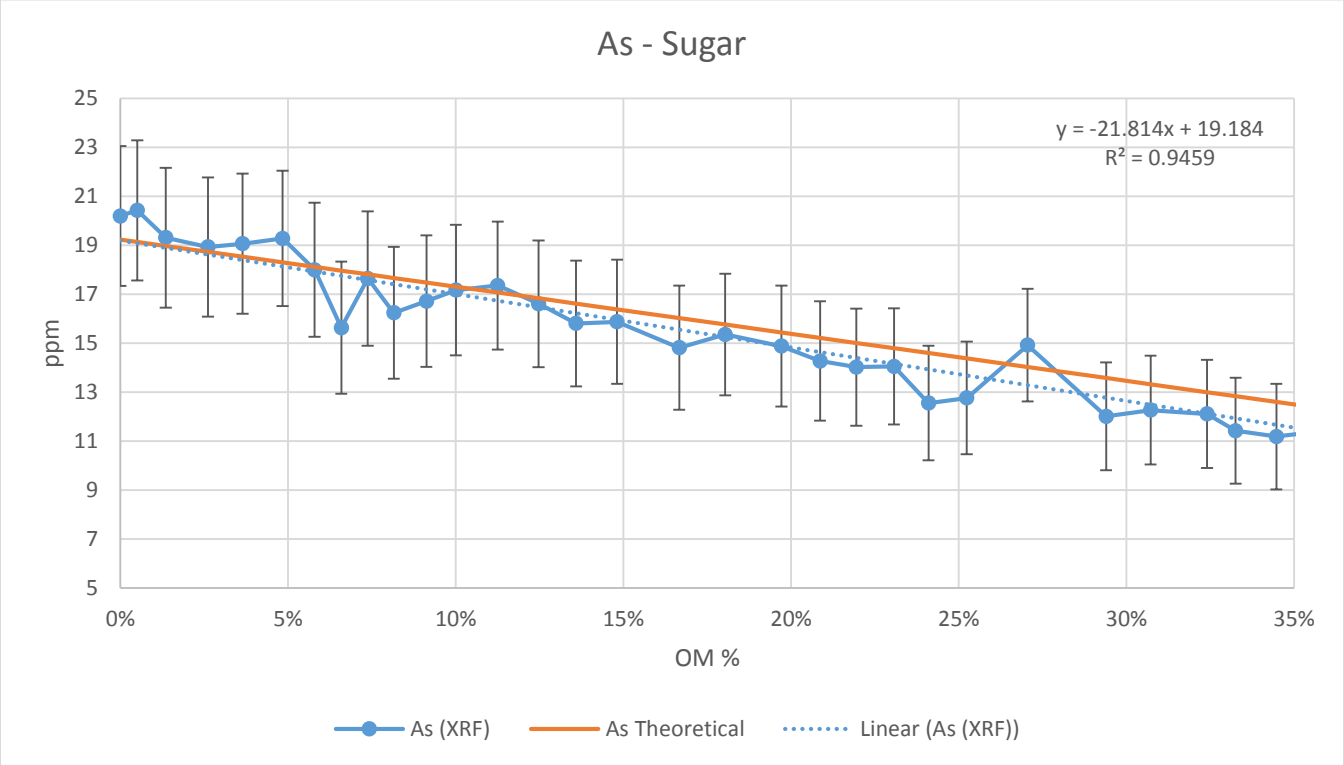

Figure 3.3 Arsenic concentration versus sugar organic matter fraction.

3.5.2 Chromium [Cr]

Chromium concentrations measured with the pXRF fall below the theoretical dilution line for dry cellulose, carbon and sugar (Figures 3.4-3.6). There is repeatability between the dry cellulose runs, however the wet cellulose run differs significantly from the dry cellulose runs. In fact, the regression for the wet cellulose run was positive while the other two dry runs were negative. This is likely attributable to the method employed in spiking the sample with surrogate. Sieves were used after drying of cellulose to ensure grain size remained below 250 microns. It is postulated that the sieve, which contained 15% chromium when tested by the Niton pXRF using metal analysis mode, sequentially spiked the sample with trace amounts of chromium as an inadvertent result of the sieving process (Section 2.7). This may explain why the slope for the wet cellulose line was positive while the dry cellulose results (which were not sieved between incremental cellulose additions) were negative

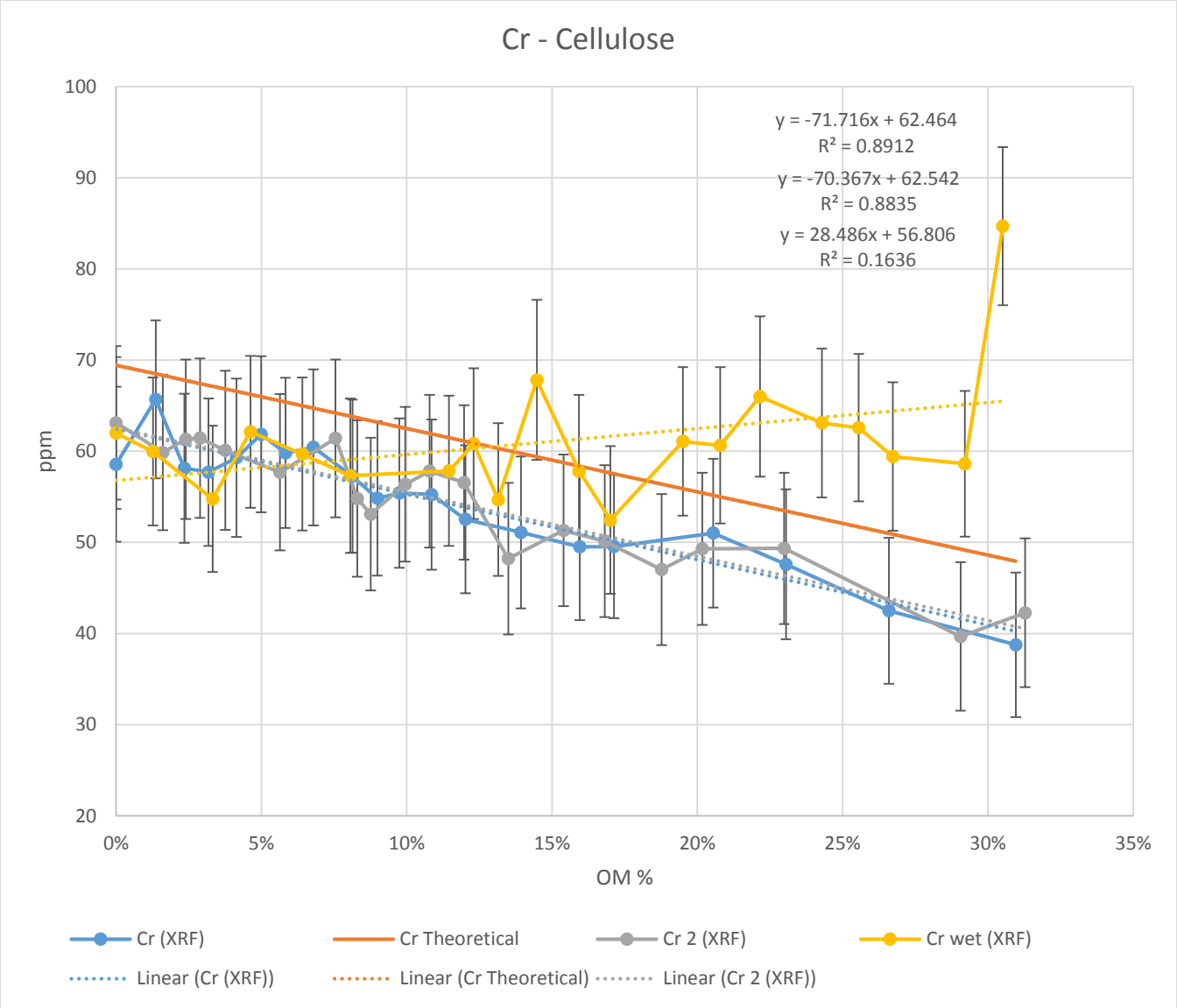

Figure 3.4 Chromium concentration versus cellulose organic matter fraction.

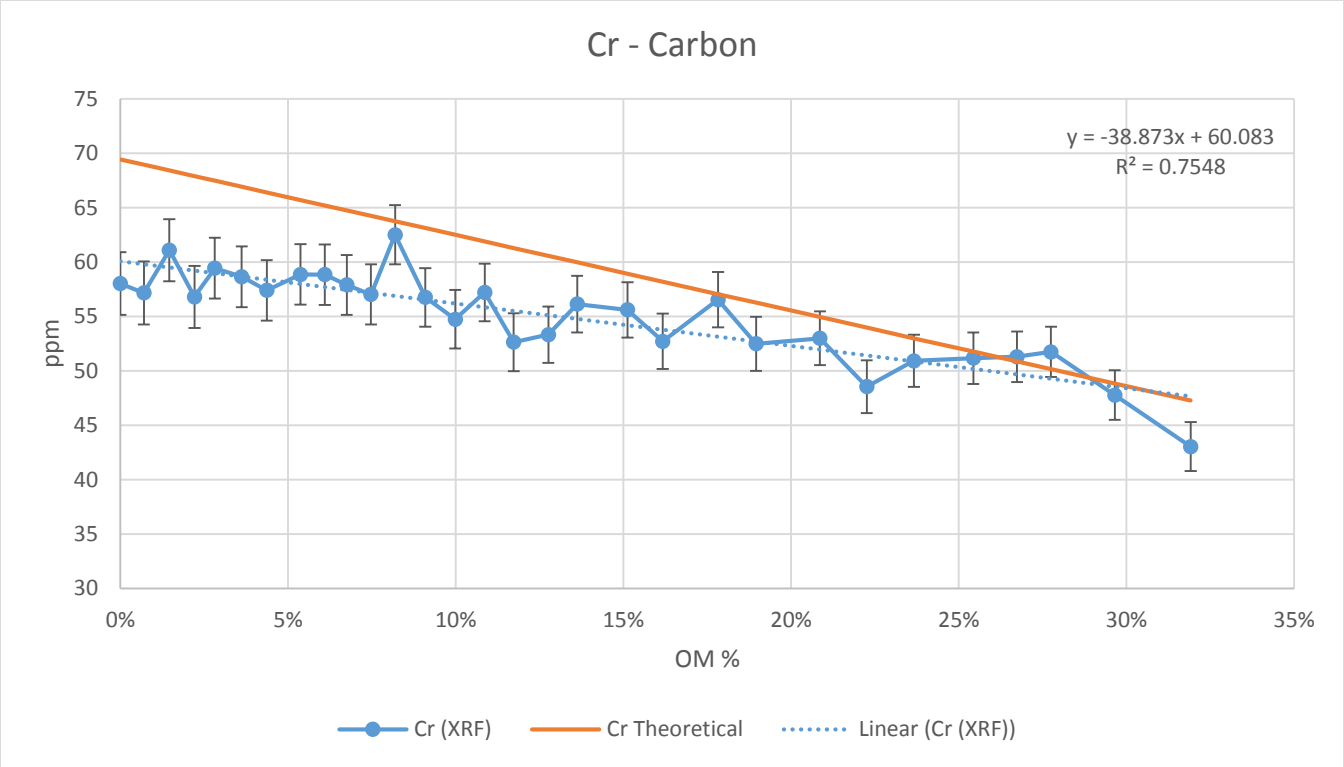

Figure 3.5 Chromium concentration versus carbon organic matter fraction.

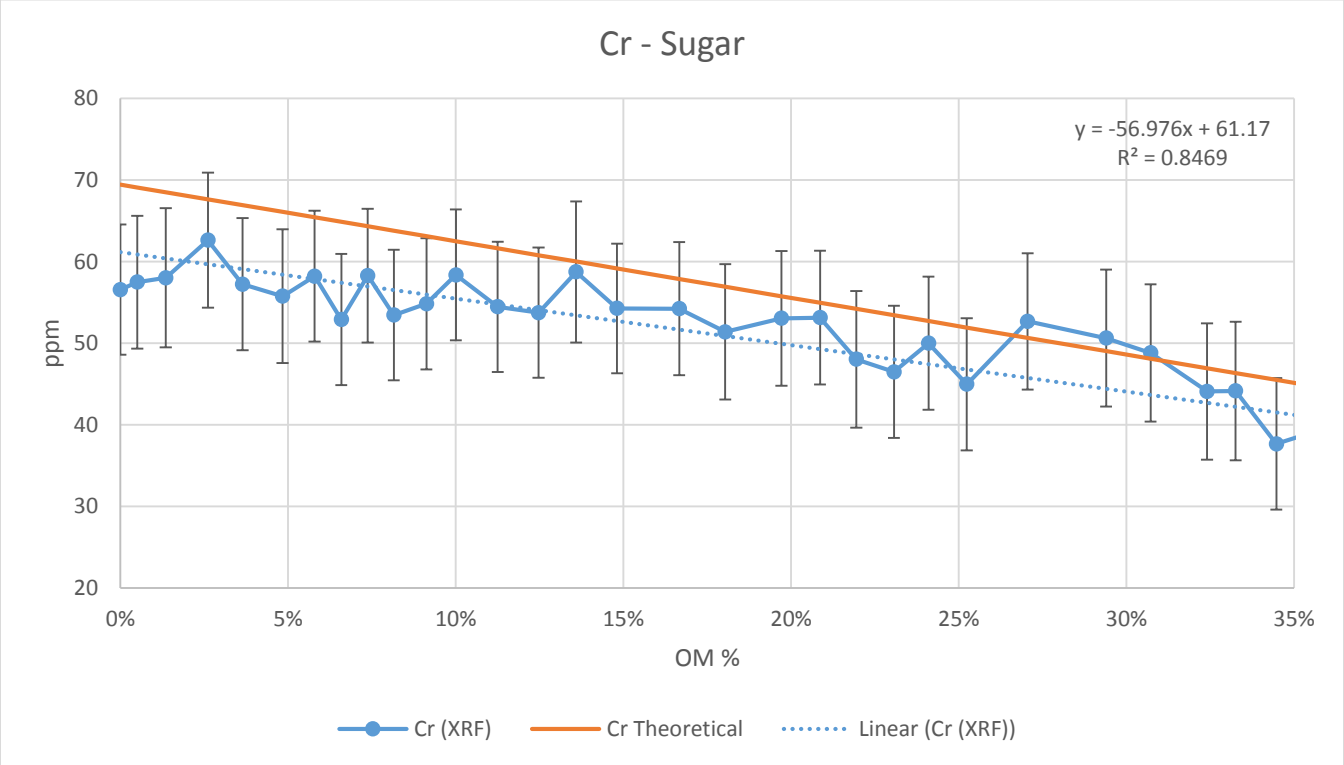

Figure 3.6 Chromium concentration versus sugar organic matter fraction.

3.5.3 Copper [Cu]

Copper pXRF concentrations exceed the theoretical dilution line for cellulose (up to approximately 25% OM surrogate), carbon and sugar (Figures 3.7-3.9). Statistical regression analysis (Section 3.7) indicates that cellulose, carbon and sugar regressions differ from theoretical predictions based on dilution. Although there is repeatability between the dry cellulose runs, the wet and dry cellulose runs generate different slopes.

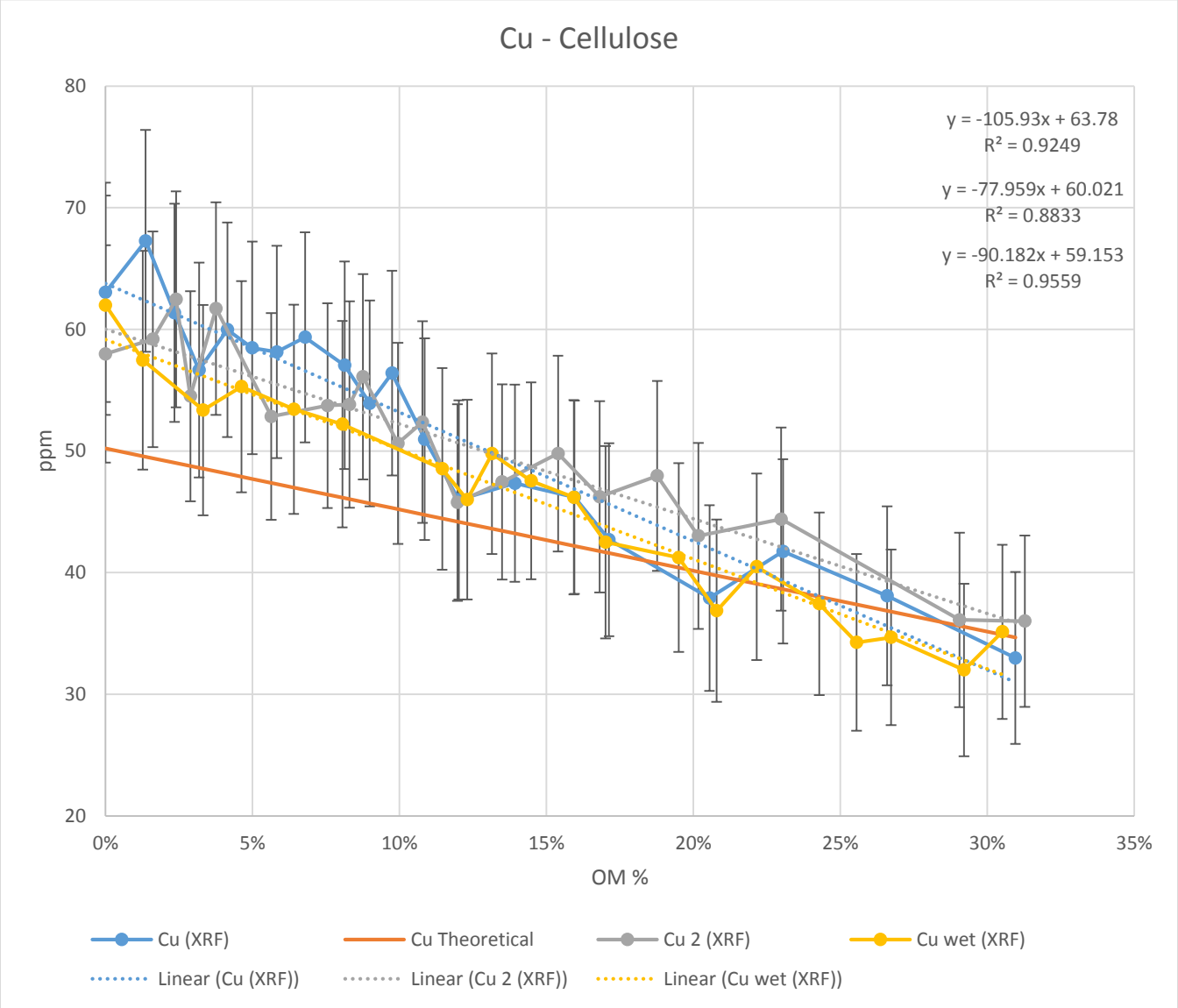

Figure 3.7 Copper concentration versus cellulose organic matter fraction.

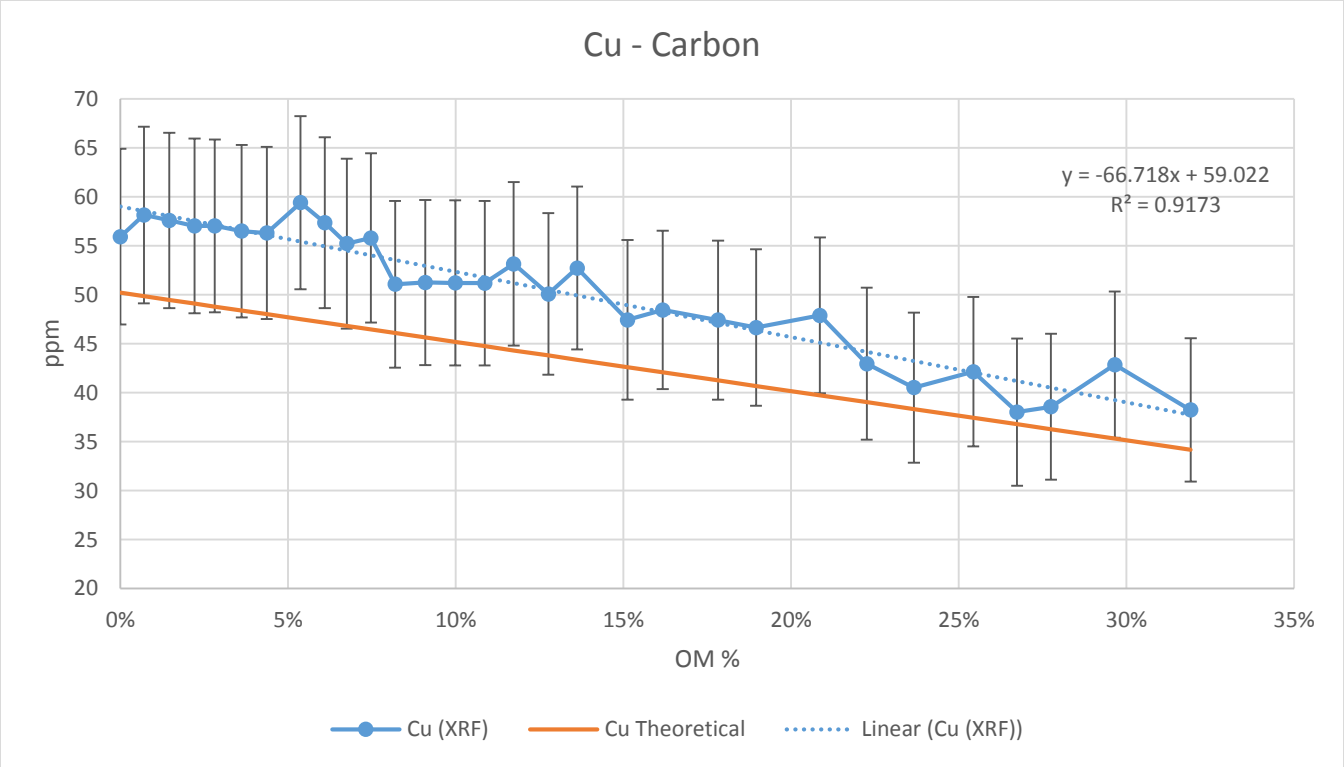

Figure 3.8 Copper concentration versus carbon organic matter fraction.

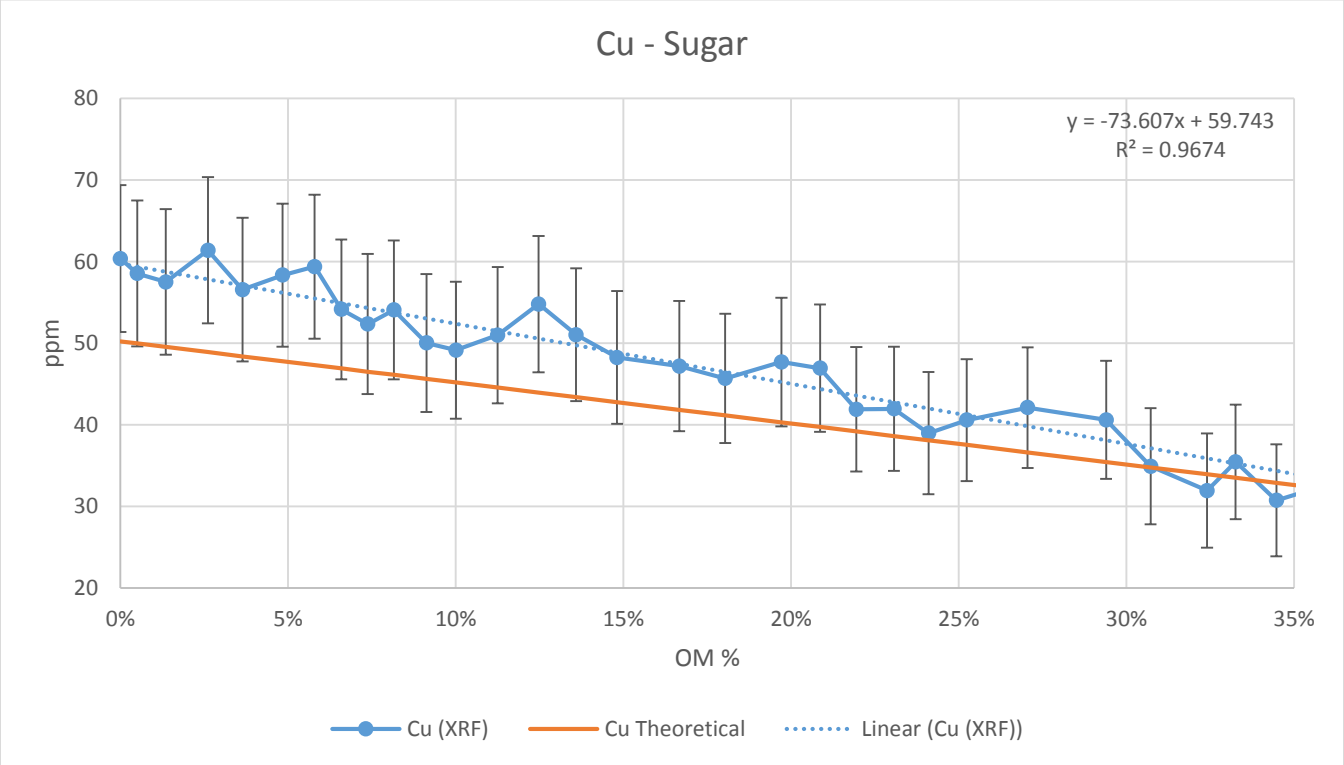

Figure 3.9 Copper concentration versus sugar organic matter fraction.

3.5.4 Iron [Fe]

Iron pXRF concentrations consistently undershoot the theoretical dilution line for cellulose, carbon and sugar (Figures 3.10-3.12). Although there is repeatability amaong the cellulose runs (dry 1 vs. dry 2 and dry 1 vs. wet), slopes and intercepts for these experiments differ from the theoretical curve. Slopes and intercepts for carbon and sugar also differ from the theoretical dilution line.

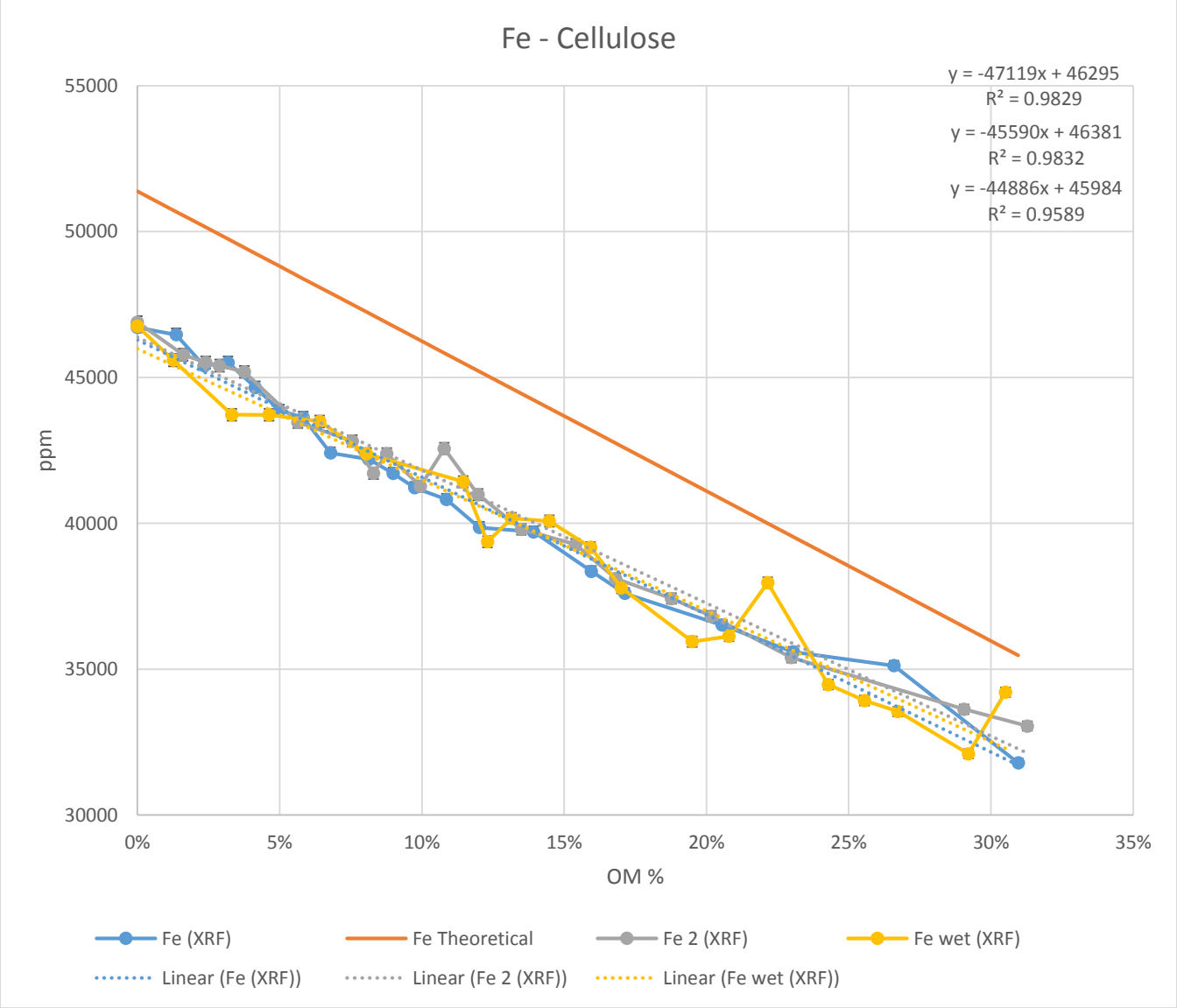

Figure 3.10 Iron concentration versus cellulose organic matter fraction.

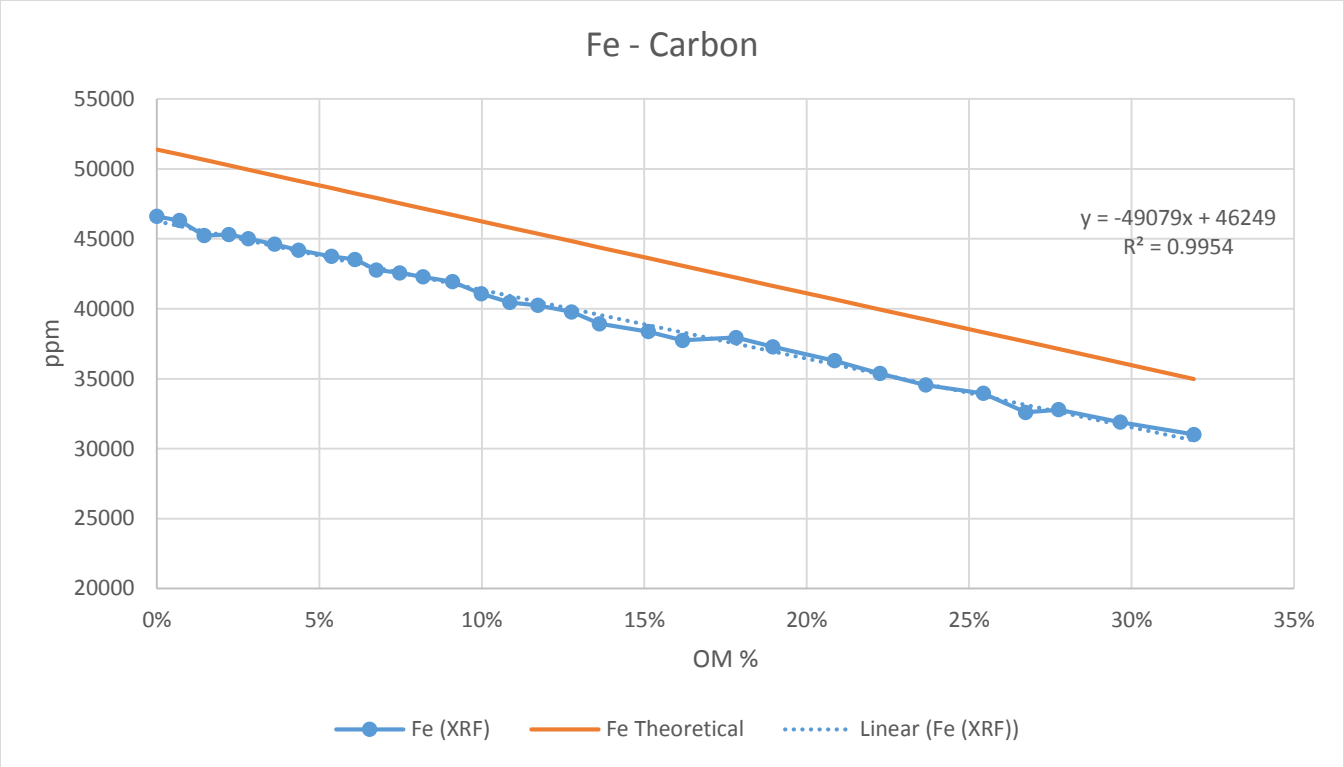

Figure 3.11 Iron concentration versus carbon organic matter fraction.

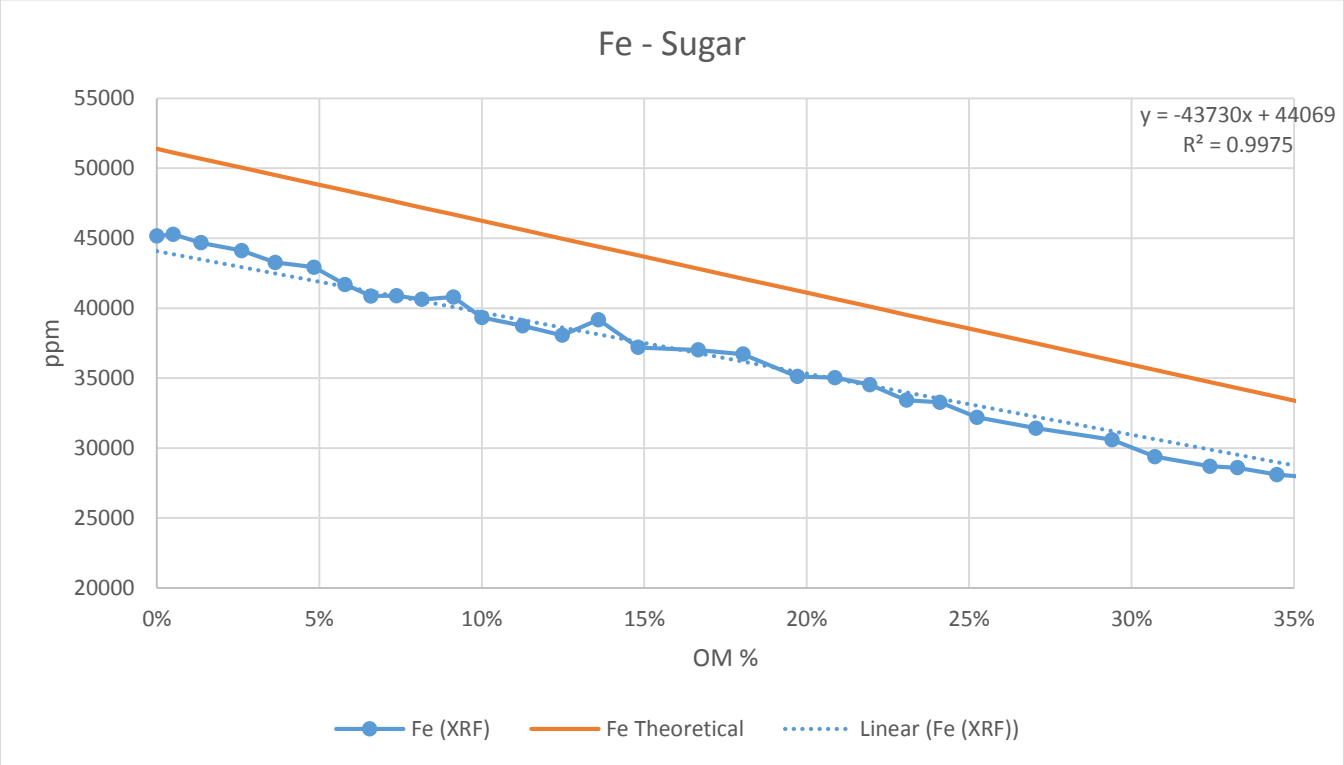

Figure 3.12 Iron concentration versus sugar organic matter fraction.

3.5.5 Manganese [Mn]

The manganese signal almost consistently undershoots the theoretical dilution line for cellulose, carbon and sugar (Figures 3.13-3.15), although intercepts at 0% OM are not statistically different for cellulose or carbon (Section 3.7). There is repeatability between the dry cellulose runs however, the wet and dry cellulose run intercepts are different. The carbon, sugar and cellulose runs have different slopes and intercepts.

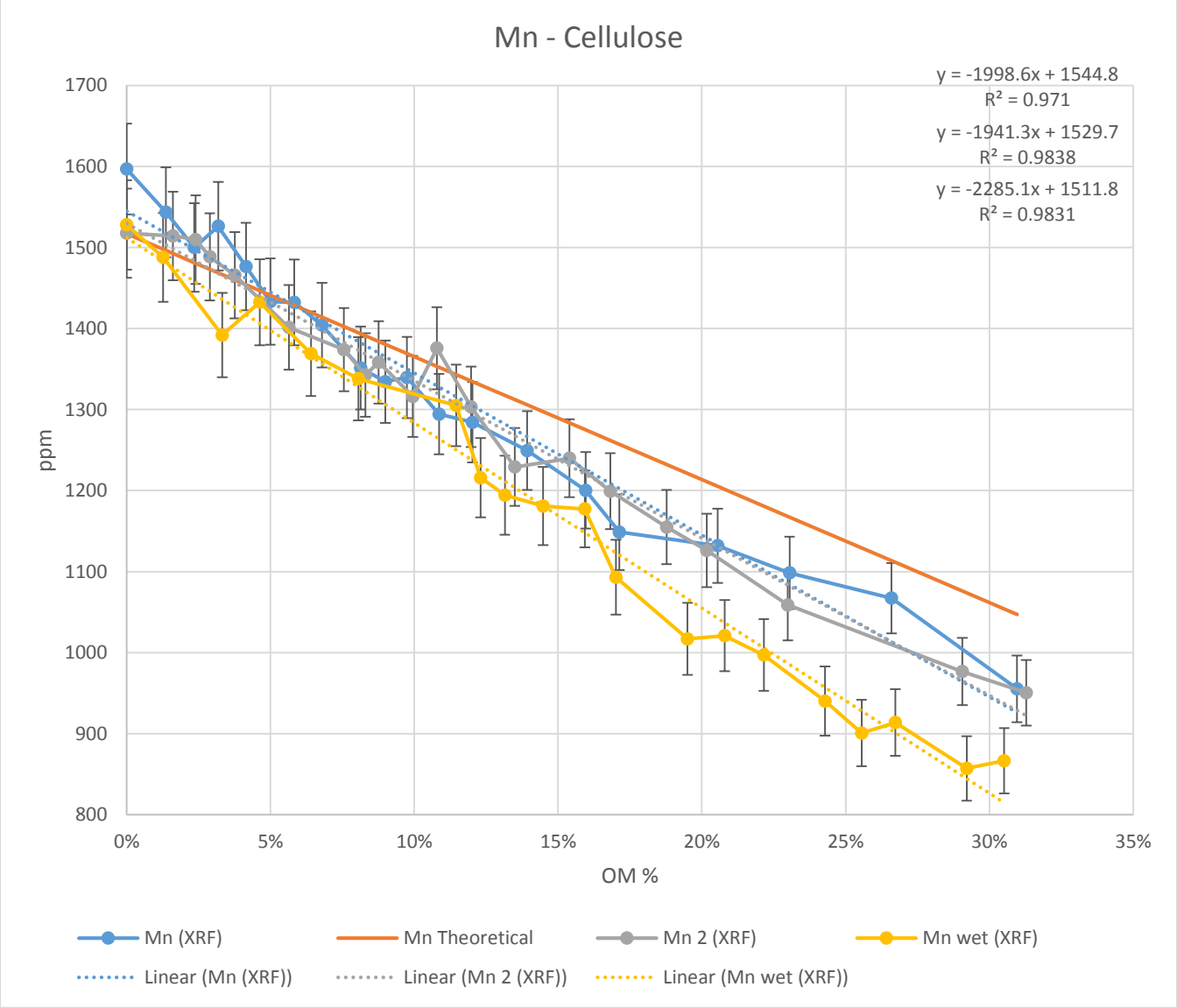

Figure 3.13 Manganese concentration versus cellulose organic matter fraction.

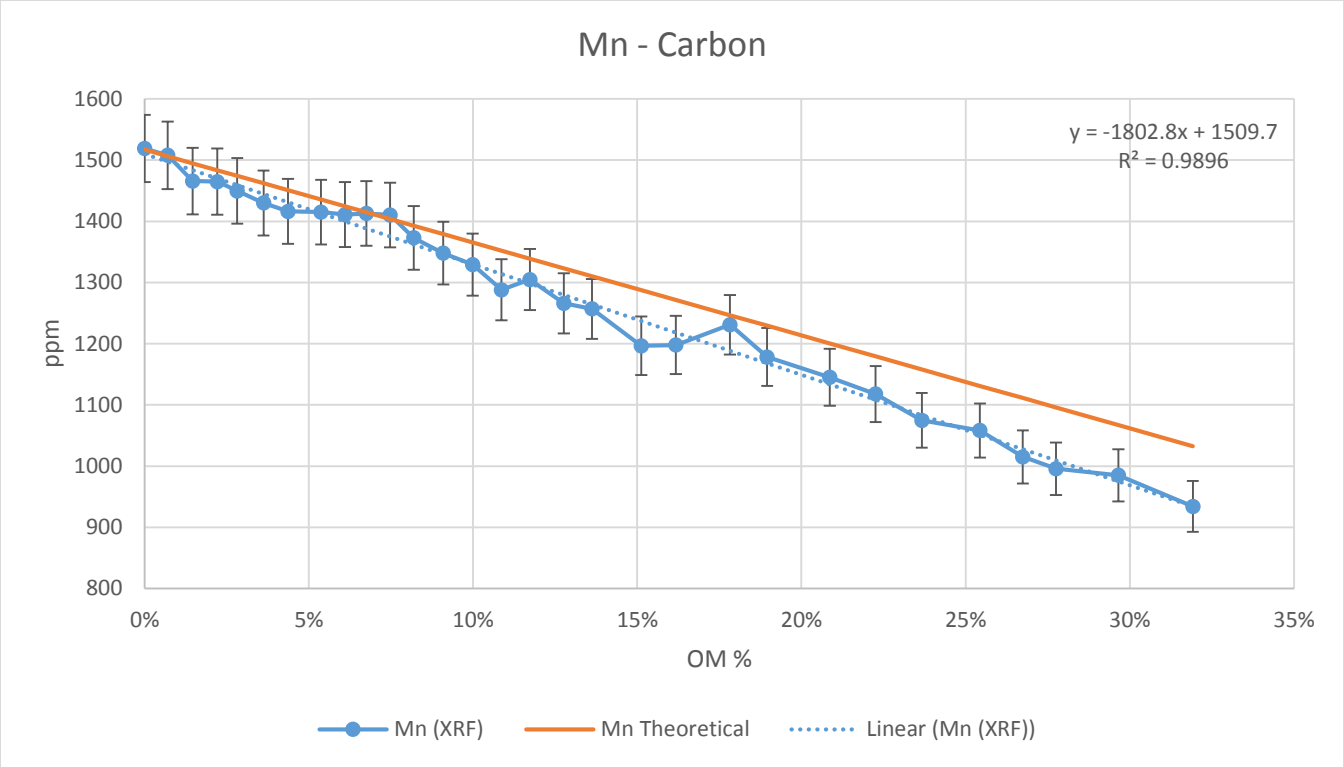

Figure 3.14 Manganese concentration versus carbon organic matter fraction.

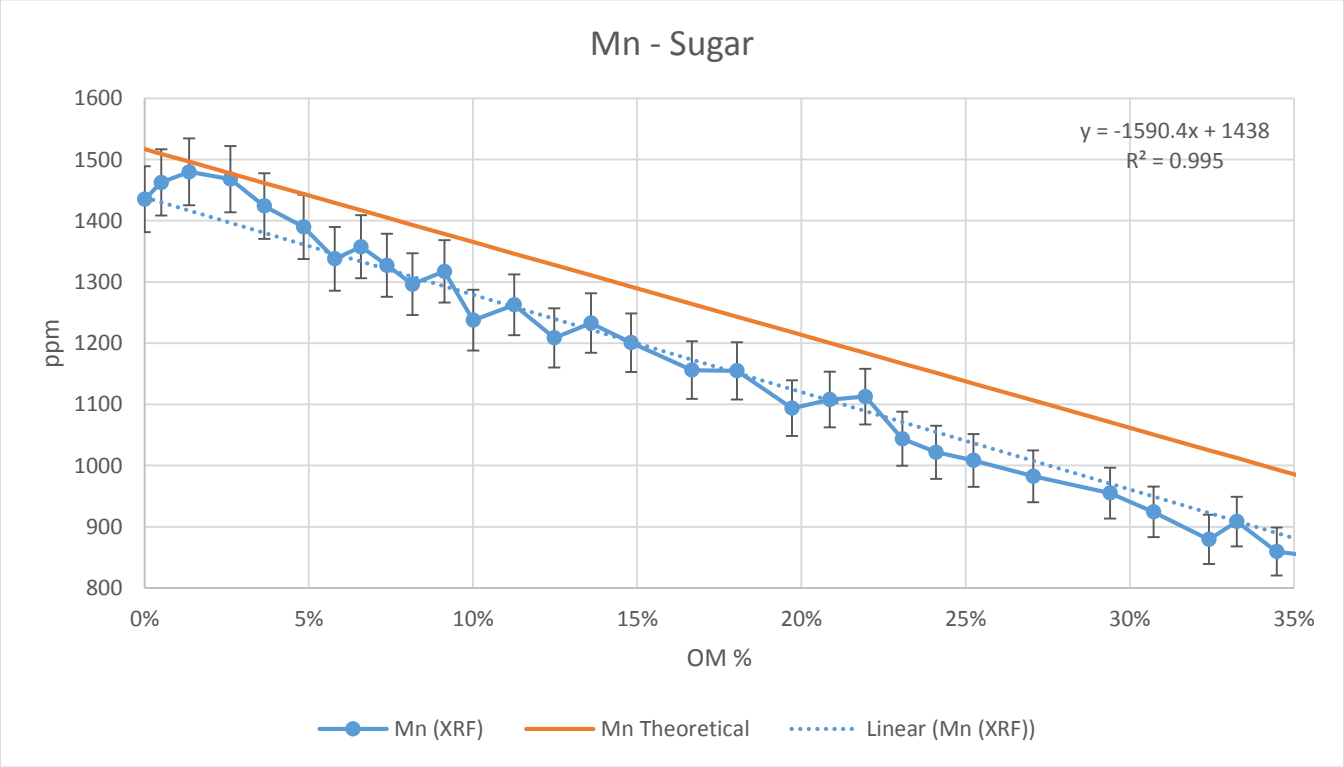

Figure 3.15 Manganese concentration versus sugar organic matter fraction.

3.5.6 Lead [Pb]

Lead pXRF concentrations agree well with the theoretical dilution lines for cellulose, carbon and sugar (Figures 3.16-3.18). With the exception of the intercept for sugar, statistical regression analysis (Section 3.7) indicates that cellulose, carbon and sugar regressions are not statistically different from theoretical predictions based on dilution. Repeatability is demonstrated between the dry cellulose runs, as well as the wet and dry cellulose runs. Slopes and intercepts for cellulose, carbon, and sugar all differ from each other.

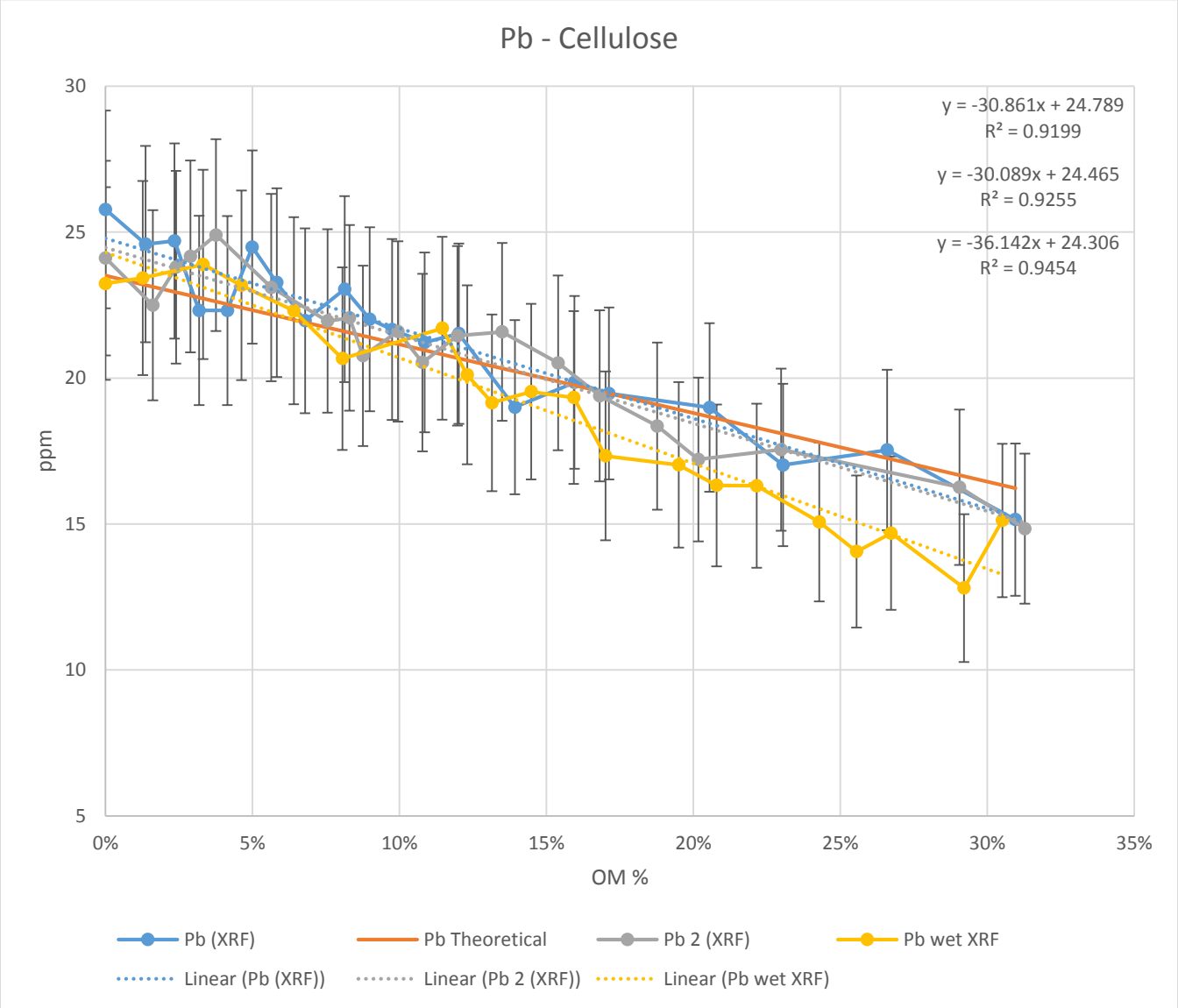

Figure 3.16 Lead concentration versus cellulose organic matter fraction.

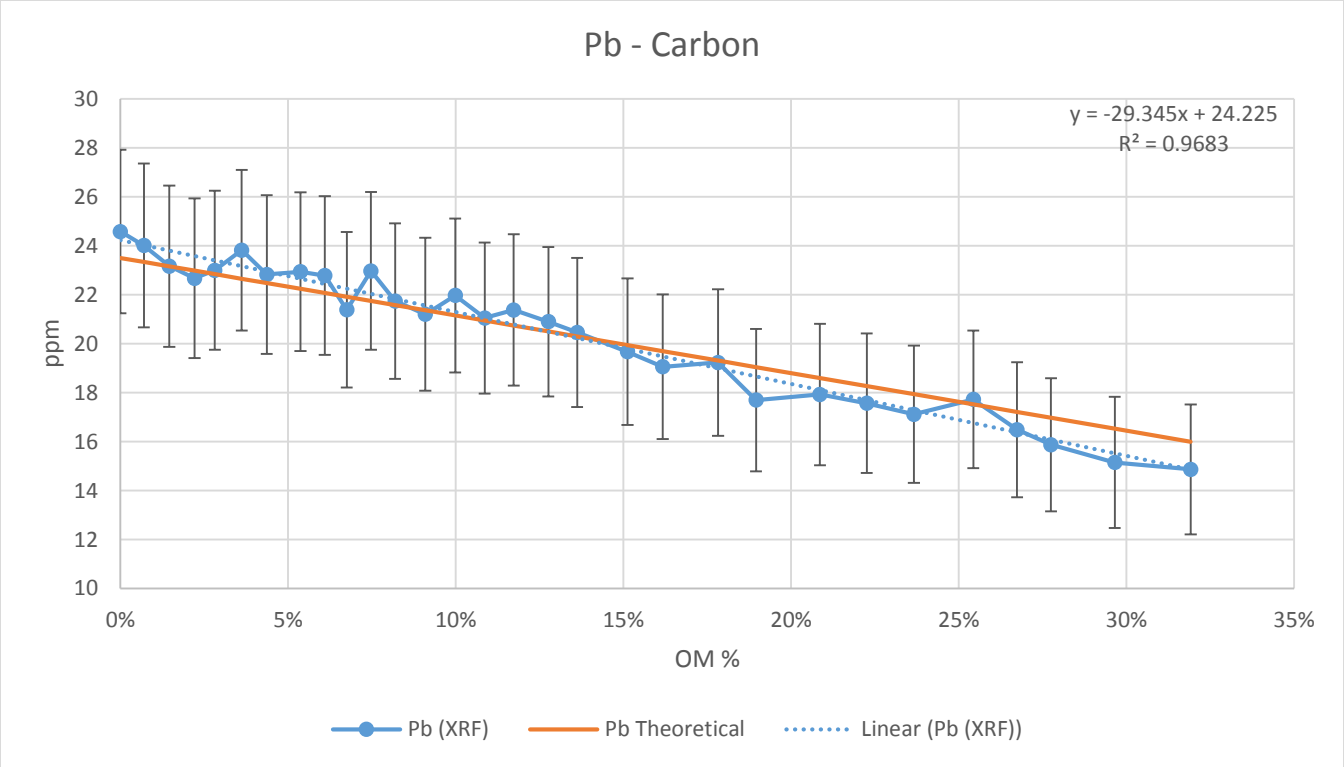

Figure 3.17 Lead concentration versus carbon organic matter fractio

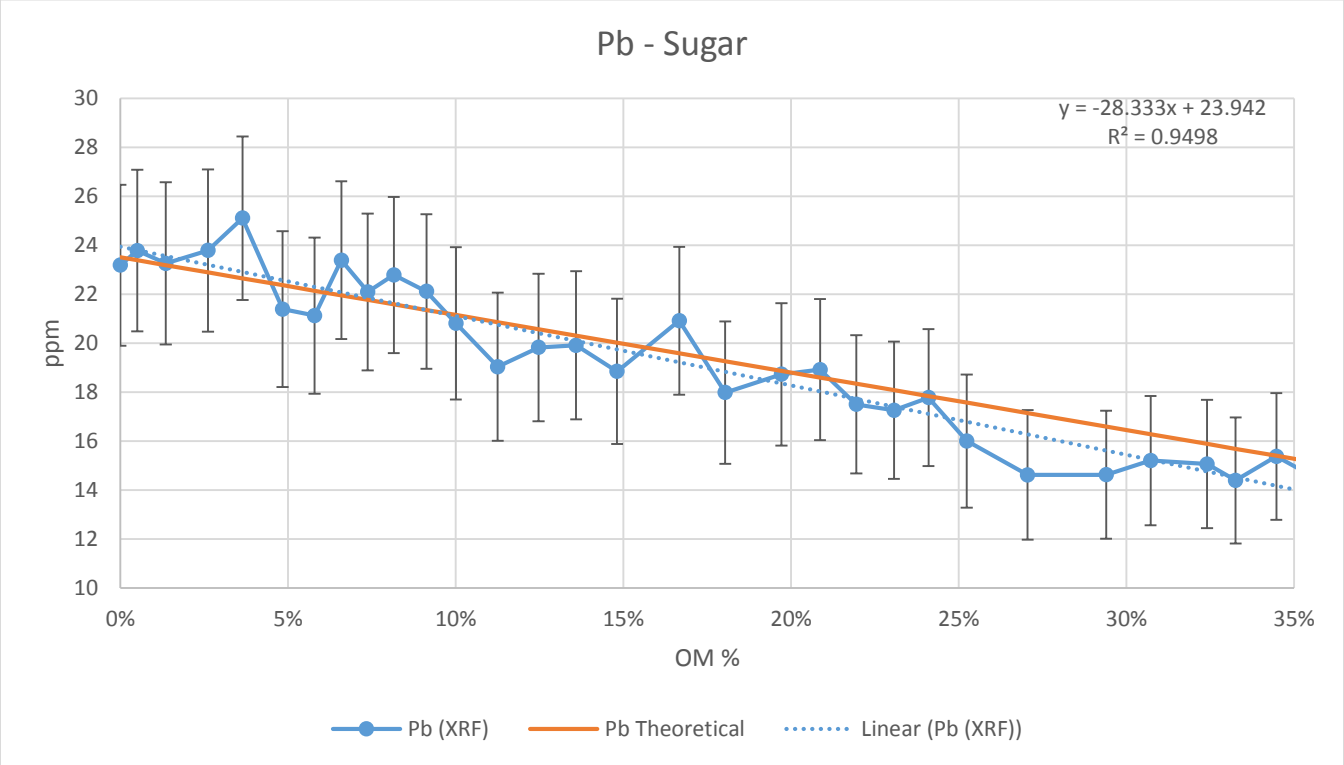

Figure 3.18 Lead concentration versus sugar organic matter fraction.

3.5.7 Rubidium [Rb]

With the exception of the slope for cellulose, linear regression coefficients for pXRF rubidium concentrations differ from theoretical predictions for cellulose, carbon, and sugar, consistently undershooting the theoretical dilution line (Figures 3.19-3.21). Results between dry cellulose runs were repeatable, but wet vs. dry cellulose runs yielded different slopes.

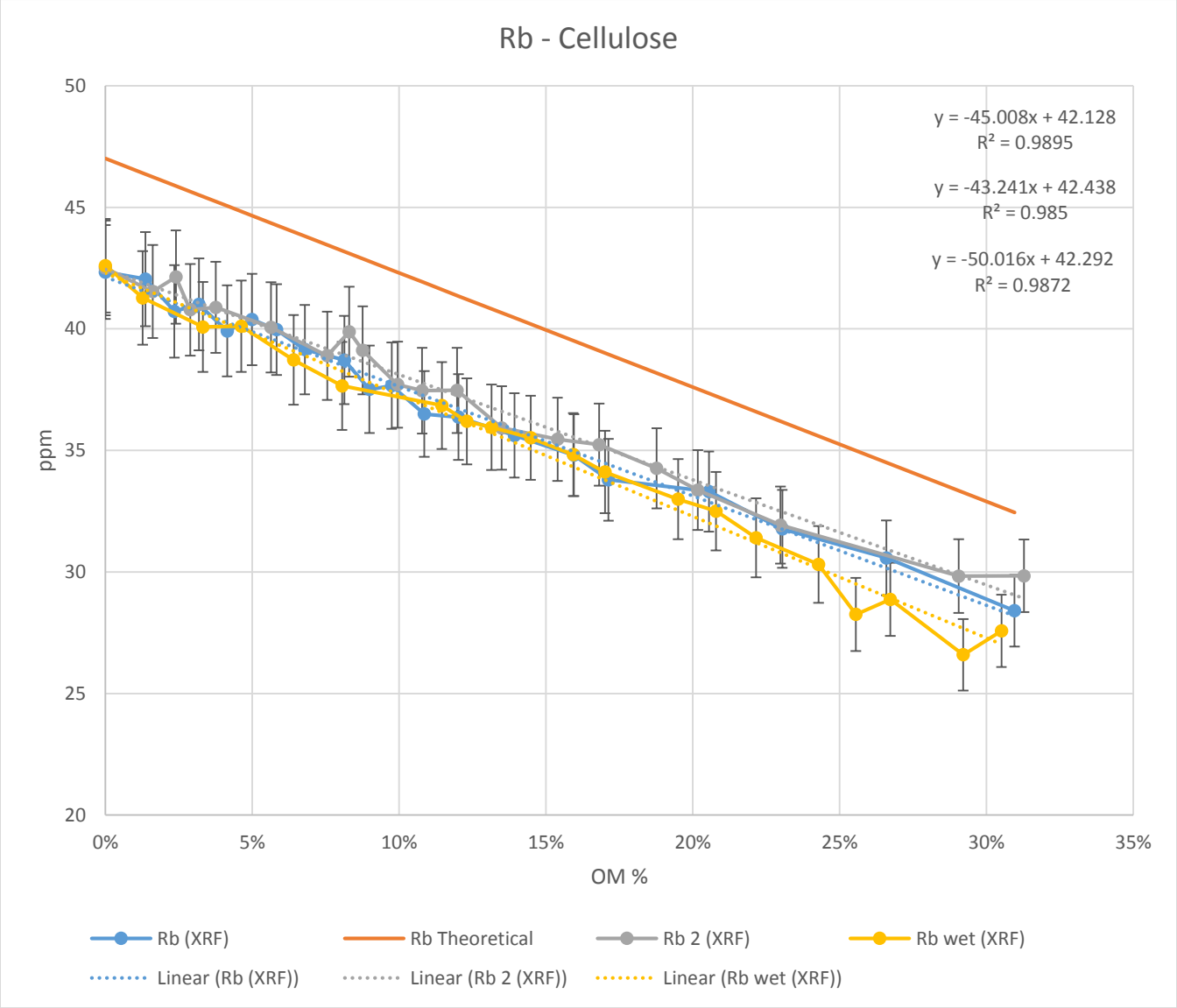

Figure 3.19 Rubidium concentration versus cellulose organic matter fraction.

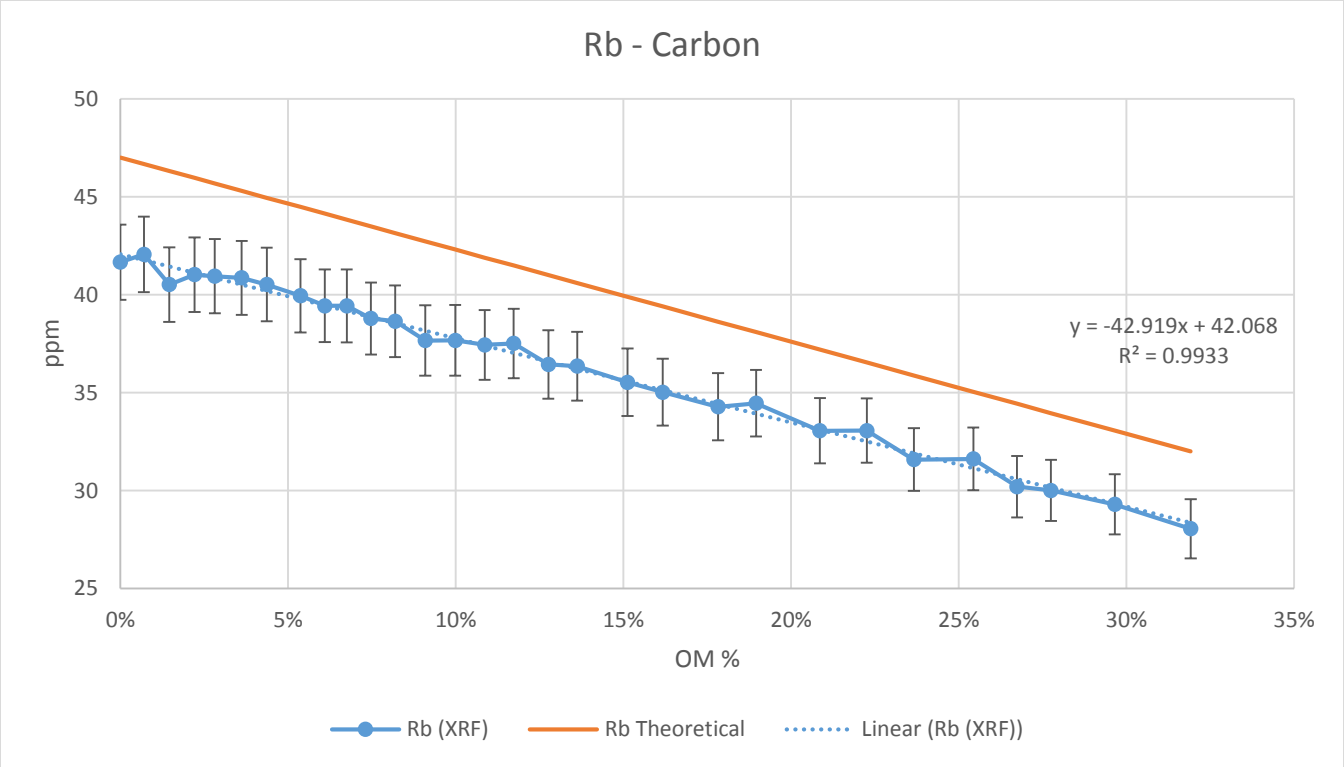

Figure 3.20 Rubidium concentration versus carbon organic matter fraction.

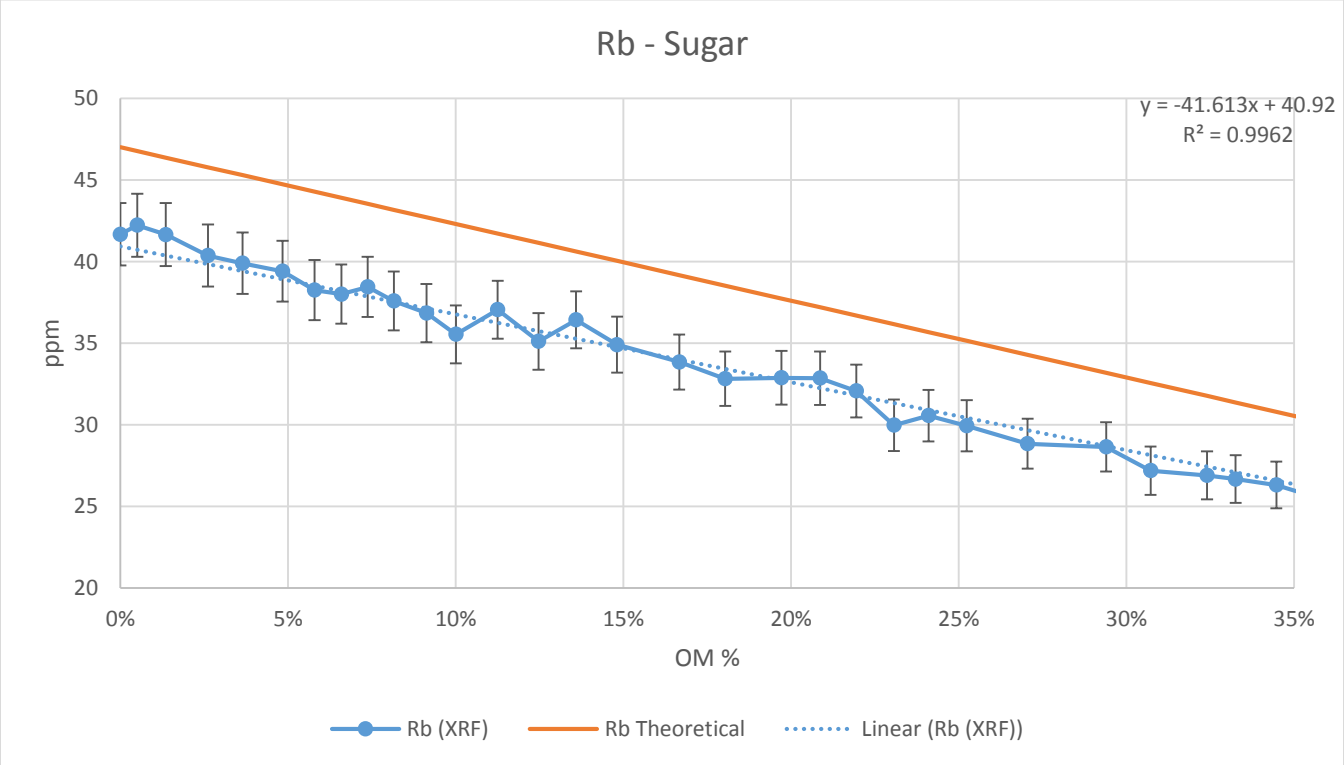

Figure 3.21 Rubidium concentration versus sugar organic matter fraction.

3.5.8 Strontium [Sr]

Strontium pXRF concentrations generally fall below the dilution lines for cellulose, carbon, and sugar (Figures 3.22-3.24). Regression lines yield statistically different coefficients from the dilution line, with the exception of the slope for cellulose. Dry cellulose experimental results yielded repeatable slopes but different intercepts. Dry vs. wet cellulose experiments were not statistically different.

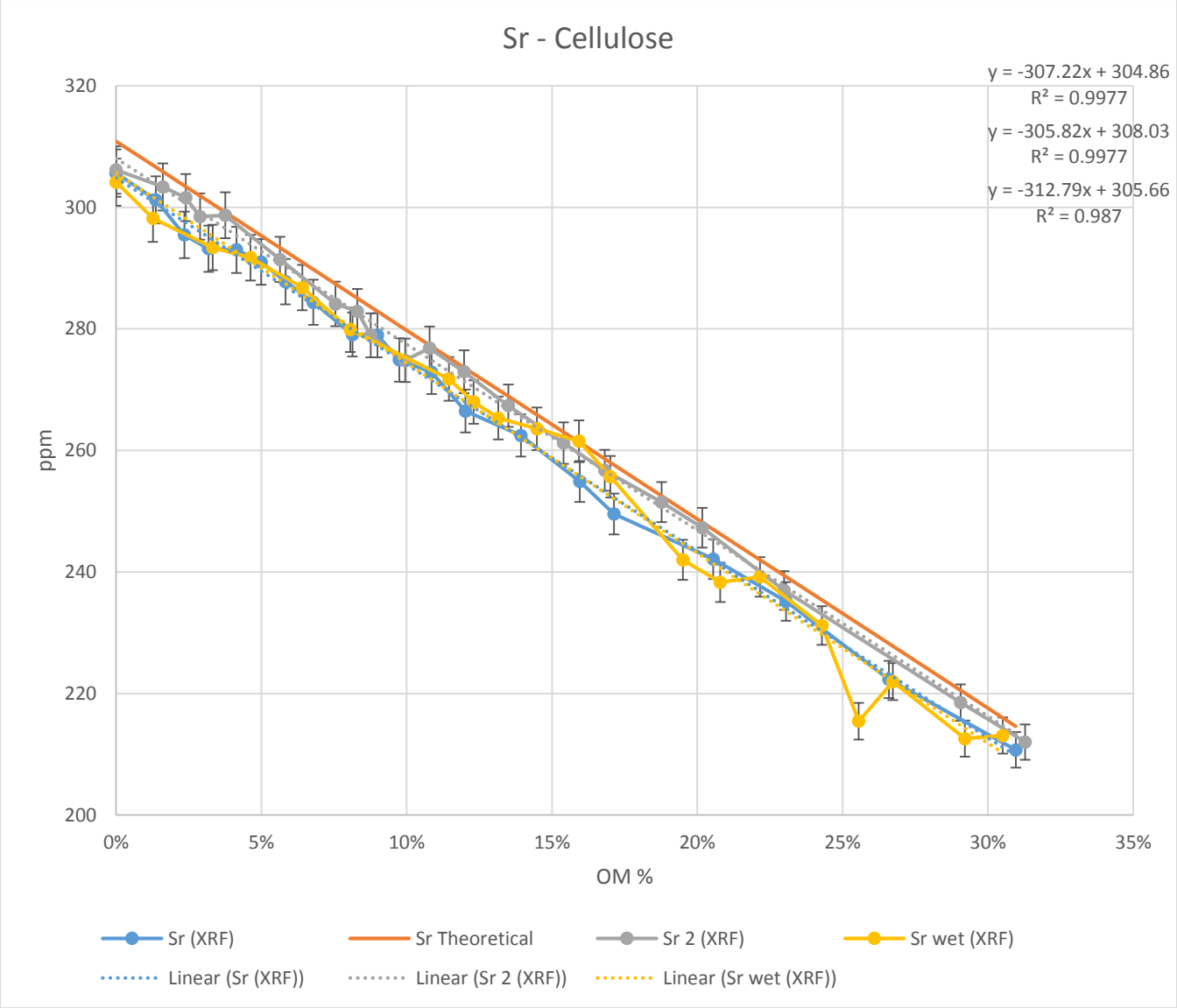

Figure 3.22 Strontium concentration versus cellulose organic matter fraction.

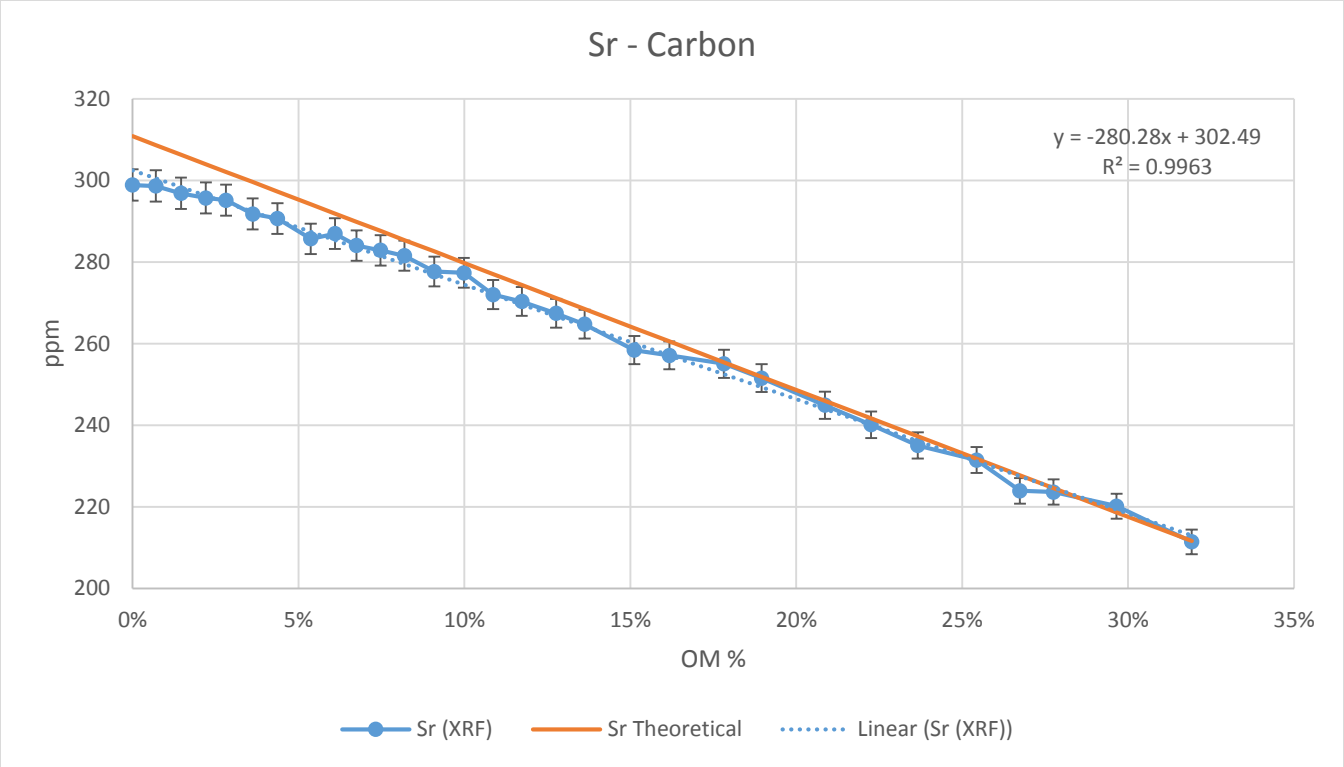

Figure 3.23 Strontium concentration versus carbon organic matter fraction.

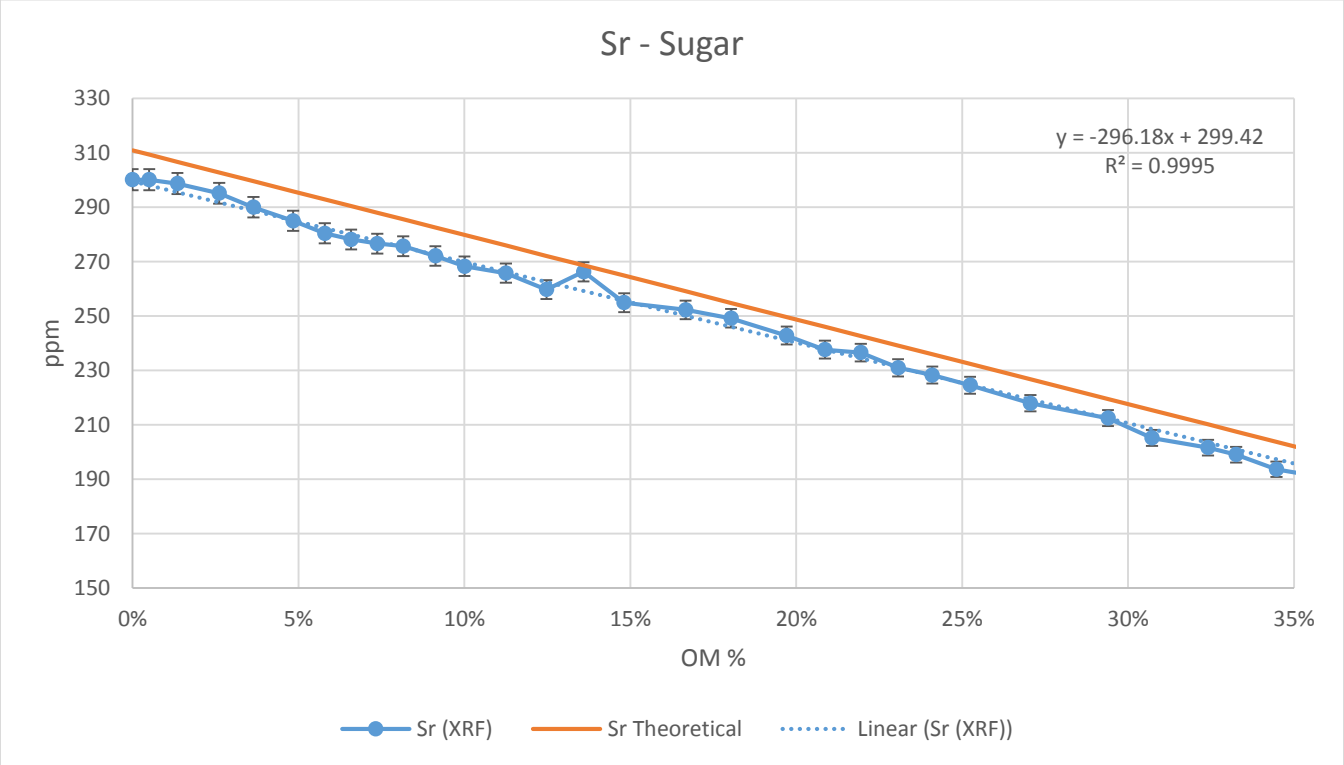

Figure 3.24 Strontium concentration versus sugar organic matter fraction.

3.5.9 Thorium [Th]

Thorium pXRF concentrations generally fall below theoretical concentrations for cellulose, carbon, and sugar (Figures 3.25-3.27). Except for the cellulose slope, slopes and intercepts of cellulose, carbon, and sugar regressions were not significantly different from the dilution line, however. Repeatability was demonstrated for dry cellulose experiments as well as for dry vs. wet cellulose.

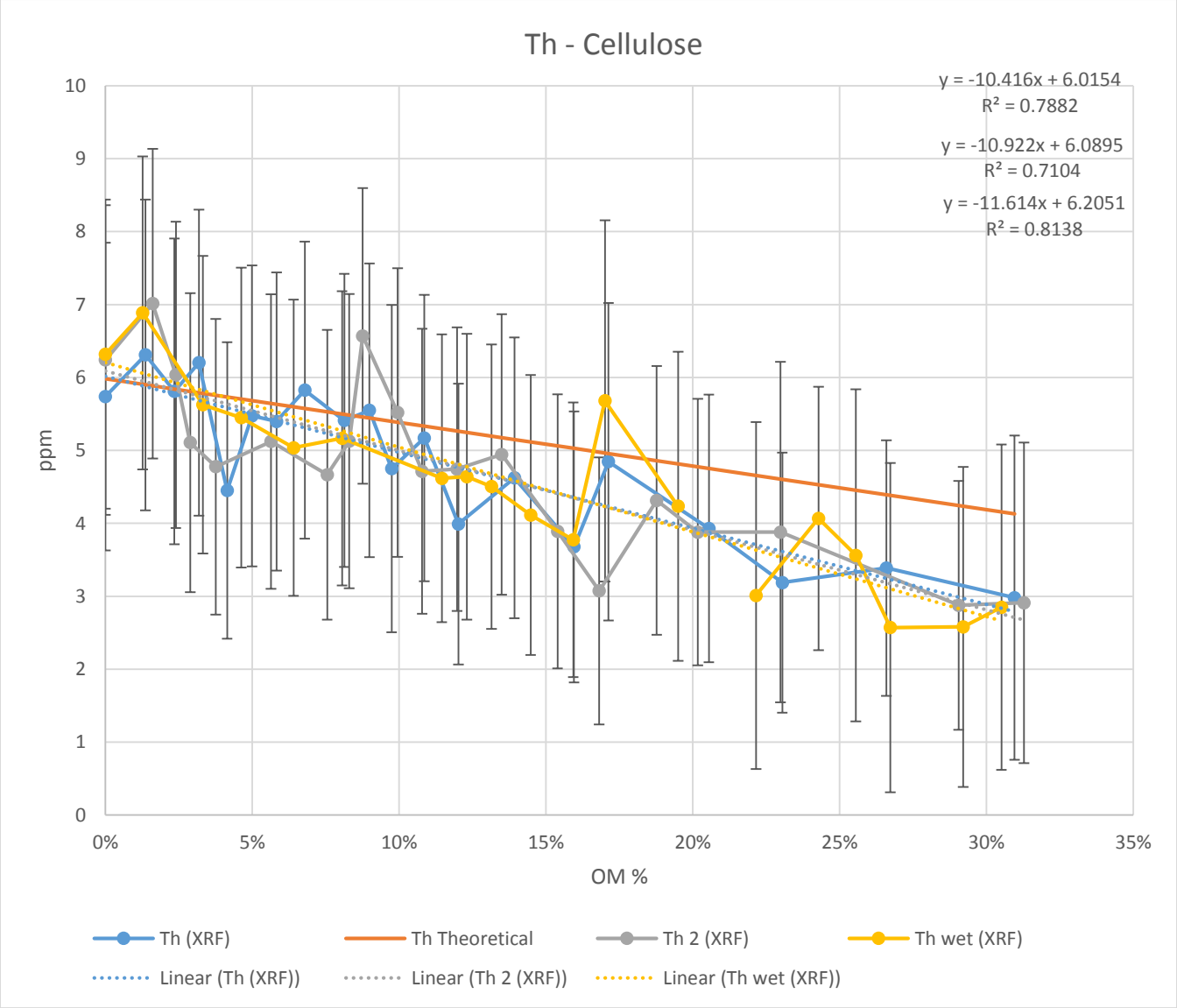

Figure 3.25 Thorium concentration versus cellulose organic matter fraction.

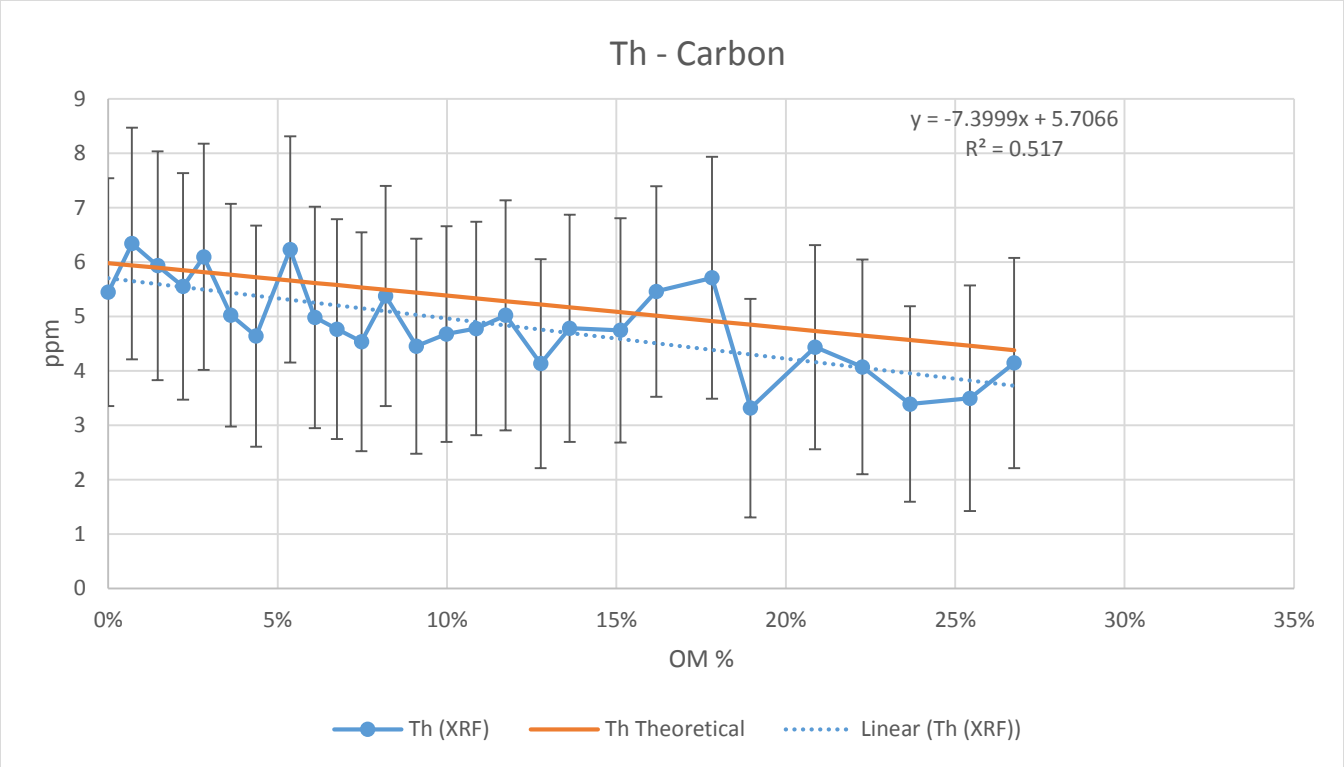

Figure 3.26 Thorium concentration versus carbon organic matter fraction.

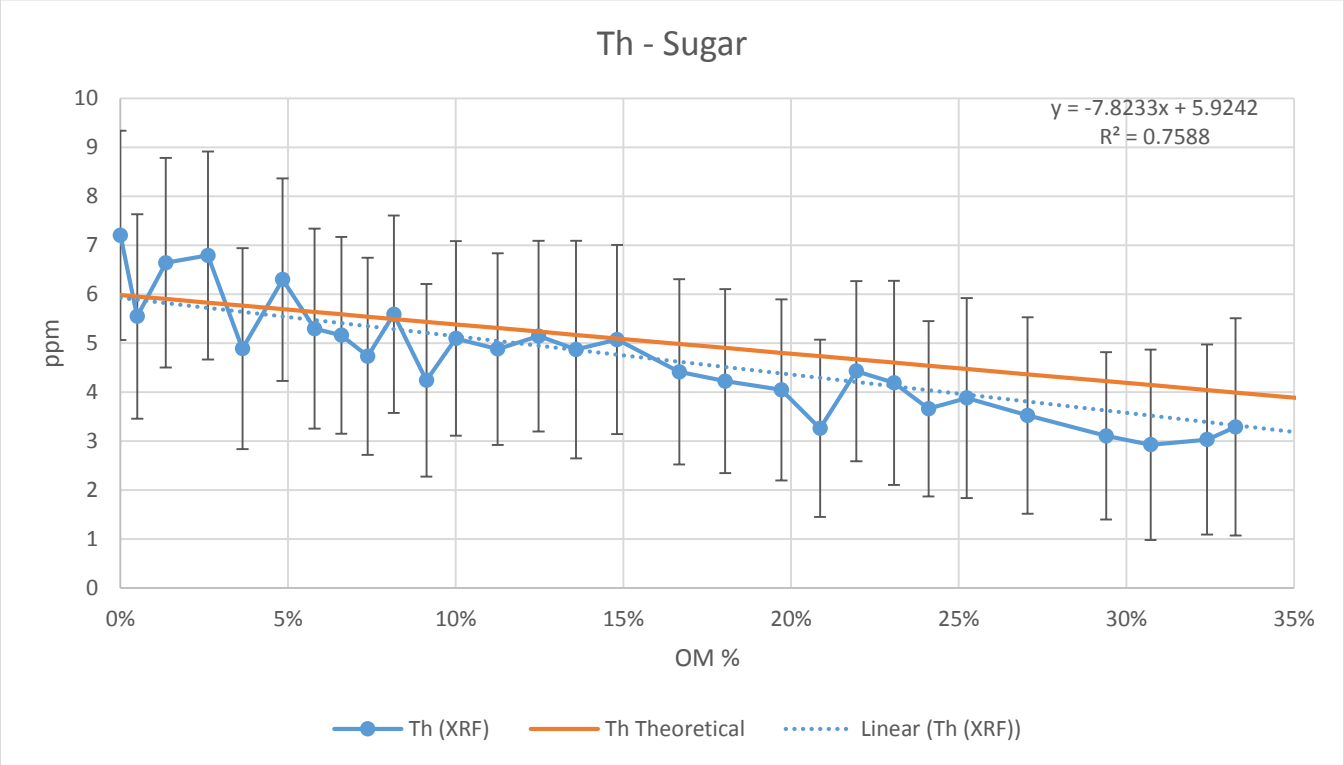

Figure 3.27 Thorium concentration versus sugar organic matter fraction.

3.5.10 Titanium [Ti]

Titanium pXRF concentrations both exceeded and fell below predicted concentrations for cellulose, carbon, and sugar (Figures 3.28-3.30). Although sugar had a similar intercept, the remaining slopes and intercepts were statistically different from the dilution line for cellulose, carbon, and sugar. Dry cellulose results were repeatable, while the wet vs. dry cellulose experiment yielded a different (positive) slope with the same intercept.

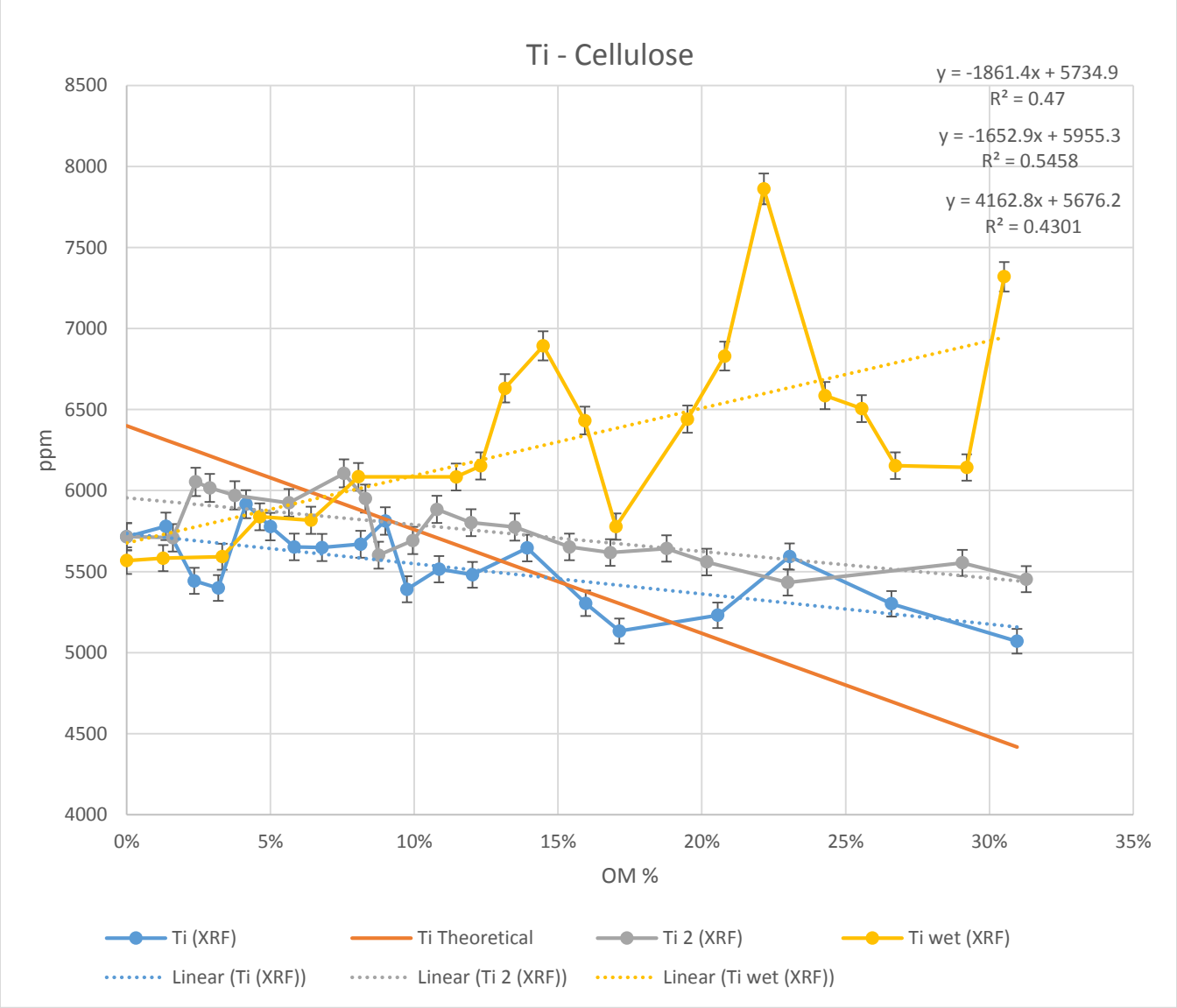

Figure 3.28 Titanium concentration versus cellulose organic matter fraction.

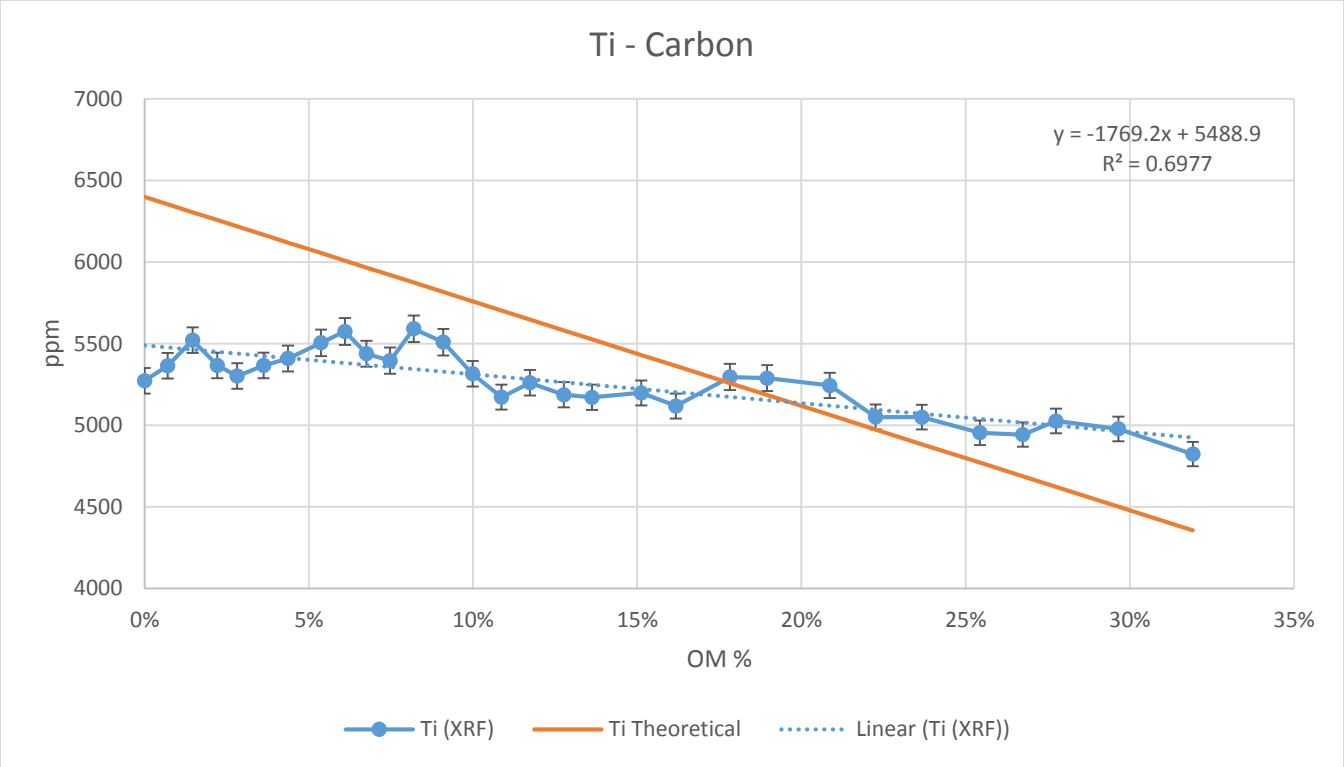

Figure 3.29 Titanium concentration versus carbon organic matter fraction.

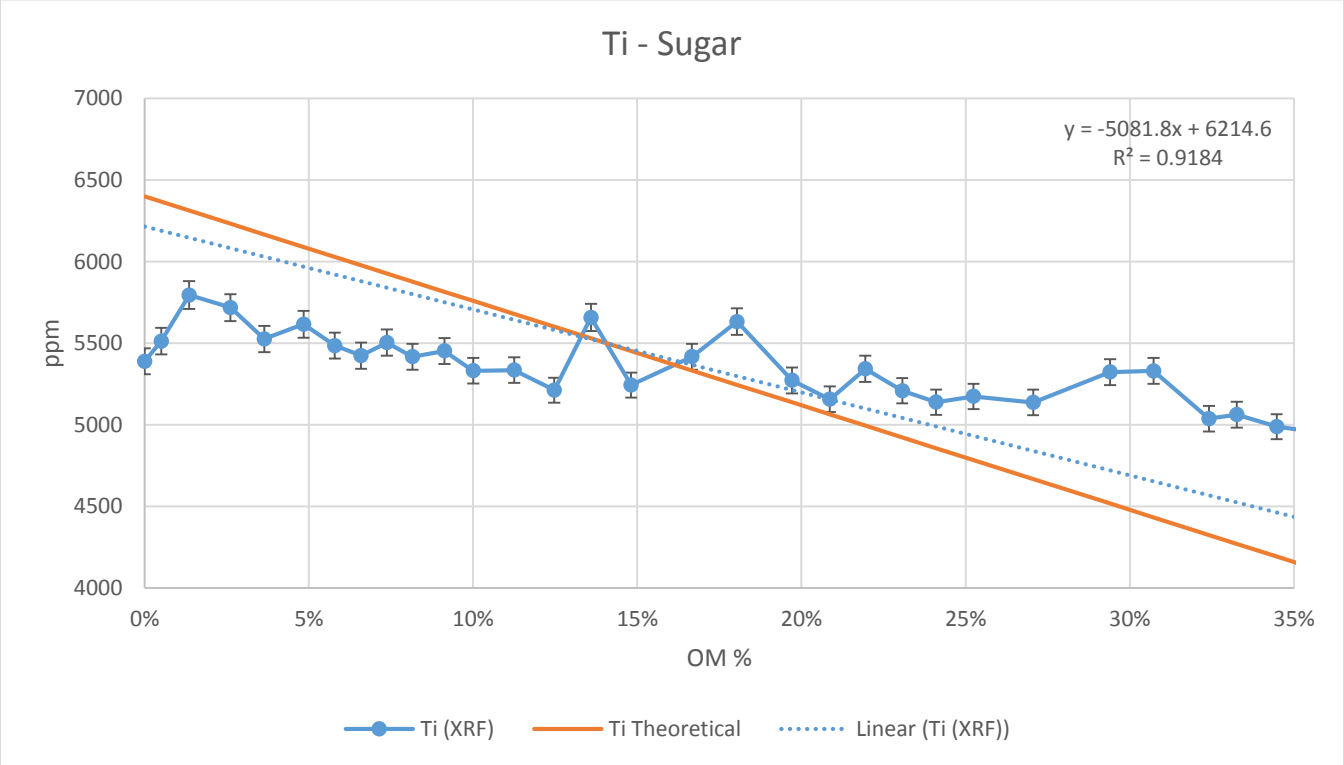

Figure 3.30 Titanium concentration versus sugar organic matter fraction.

3.5.11 Vanadium [V]

Vanadium pXRF concentrations exceed the theoretical predictions for cellulose, carbon, and sugar (Figures 3.31-3.33). Regression analysis (Section 3.7) indicates that slopes and intercepts are different from the dilution line for cellulose, carbon, and sugar. Although the dry vs. wet experiment yielded statistically significant similar regression coefficients, results from the dry1 and dry2 experiments were not repeatable. Consistent over estimation of the theoretical value may be attributable to the wide error margins which are due to the many peak similarities between oxygen and vanadium (Table 4.1). Consequently, this may also explain why the vanadium signal is overestimated by pXRF instrument with the addition of cellulose organic matter surrogate.

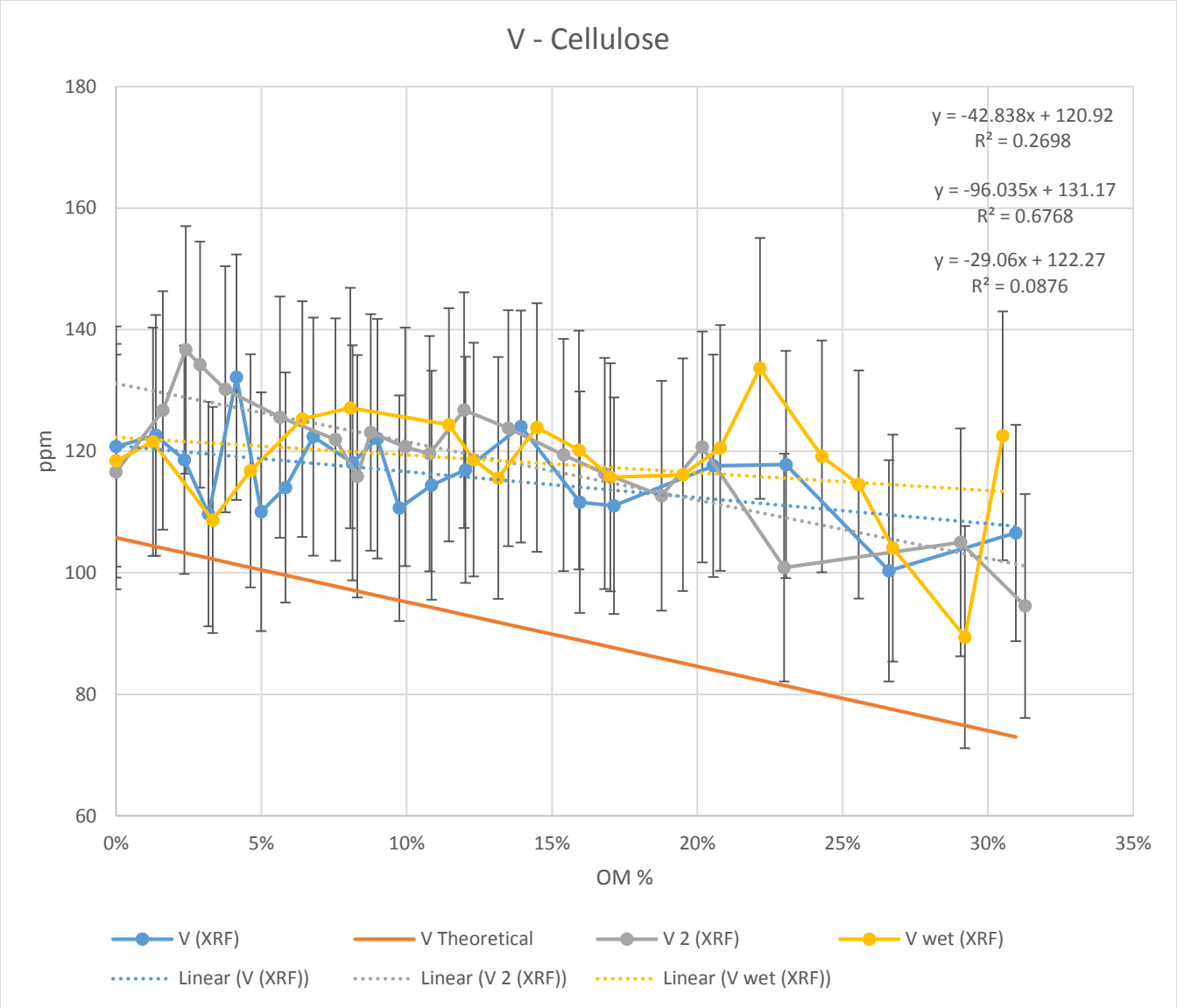

Figure 3.31 Vanadium concentration versus cellulose organic matter fraction.

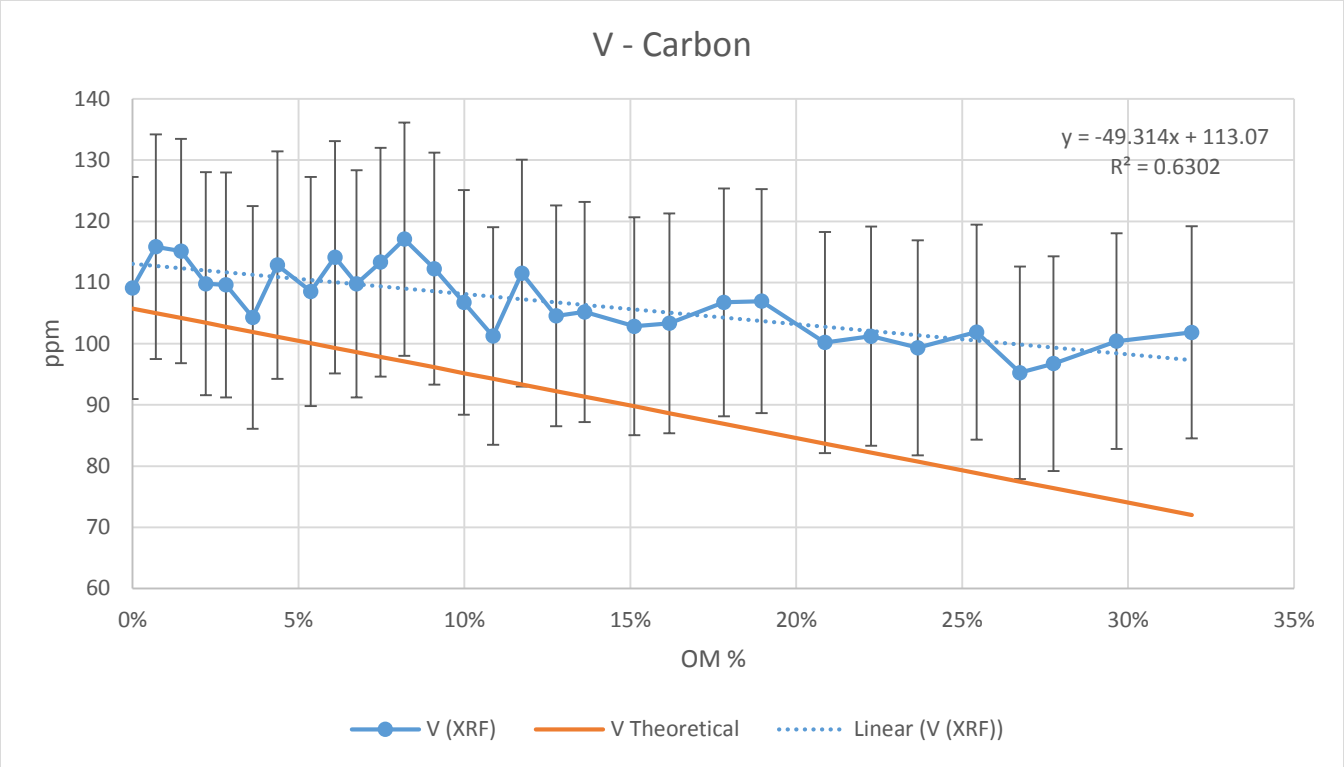

Figure 3.32 Vanadium concentration versus carbon organic matter fraction.

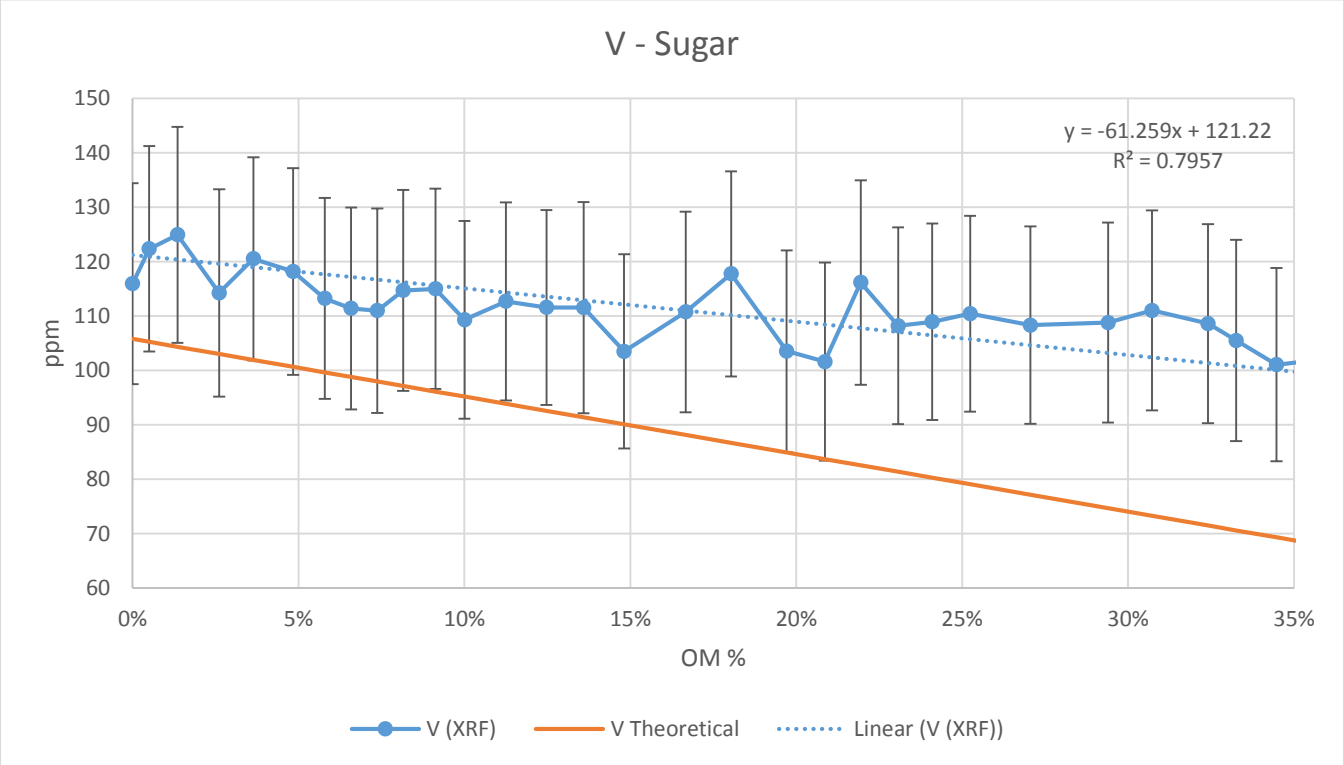

Figure 3.33 Vanadium concentration versus sugar organic matter fraction.

3.5.12 Zinc [Zn]

The zinc pXRF response undershoots the theoretical dilution line in all three cellulose runs (Figure 3.34). There is repeatability among the three separate zinc cellulose runs. The zinc pXRF response also undershoots the theoretical dilution line for the both carbon and sugar (Figures 3.35 and 3.36, respectively). Regression statistical analysis (Section 3.7) indicates that regression slopes agree with the dilution curve for all OM surrogates, although each yields a different intercept for zinc. Results for dry cellulose experiment were repeatable, as were the dry vs. wet experiment.

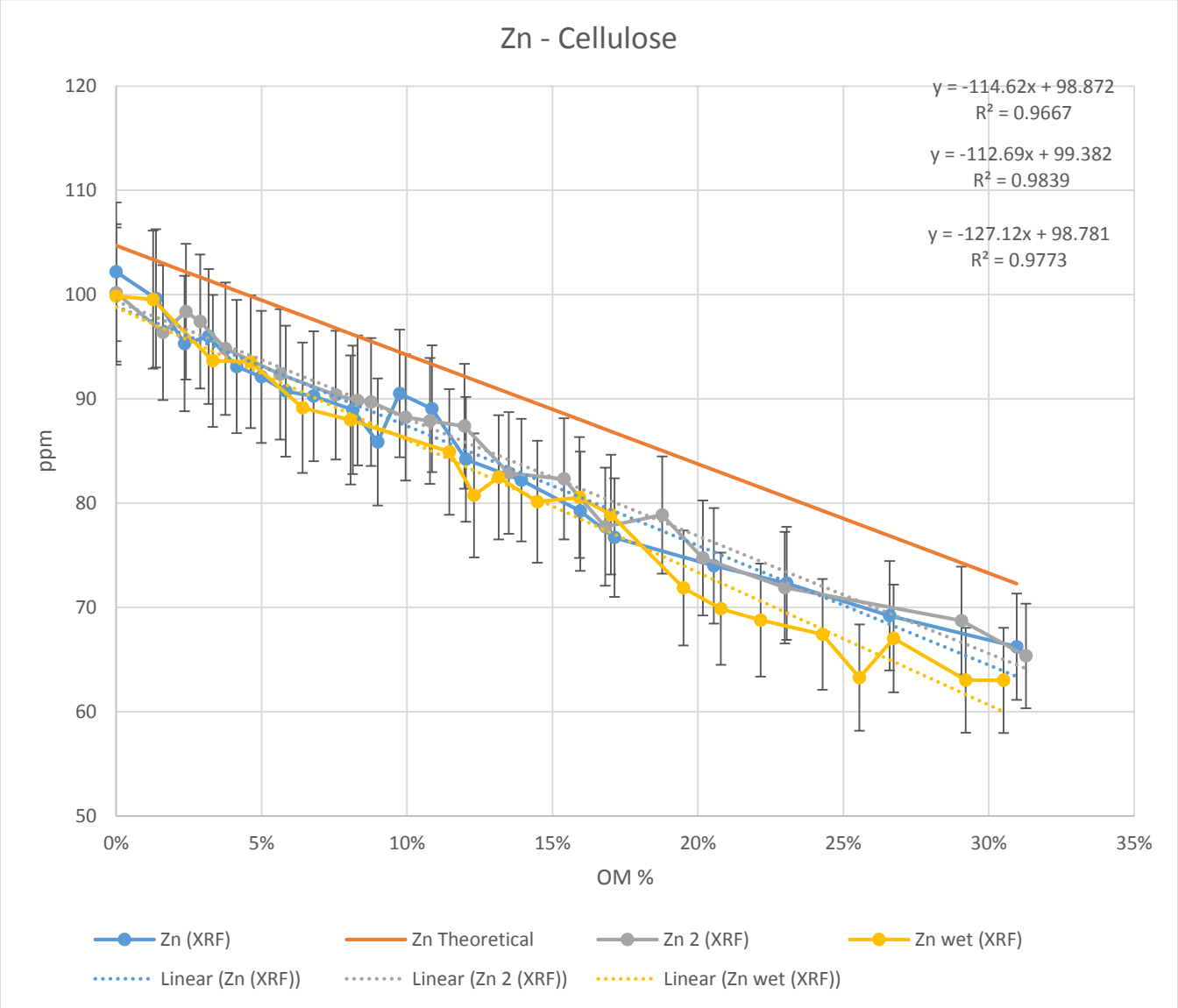

Figure 3.34 Zinc concentration versus cellulose organic matter fraction.

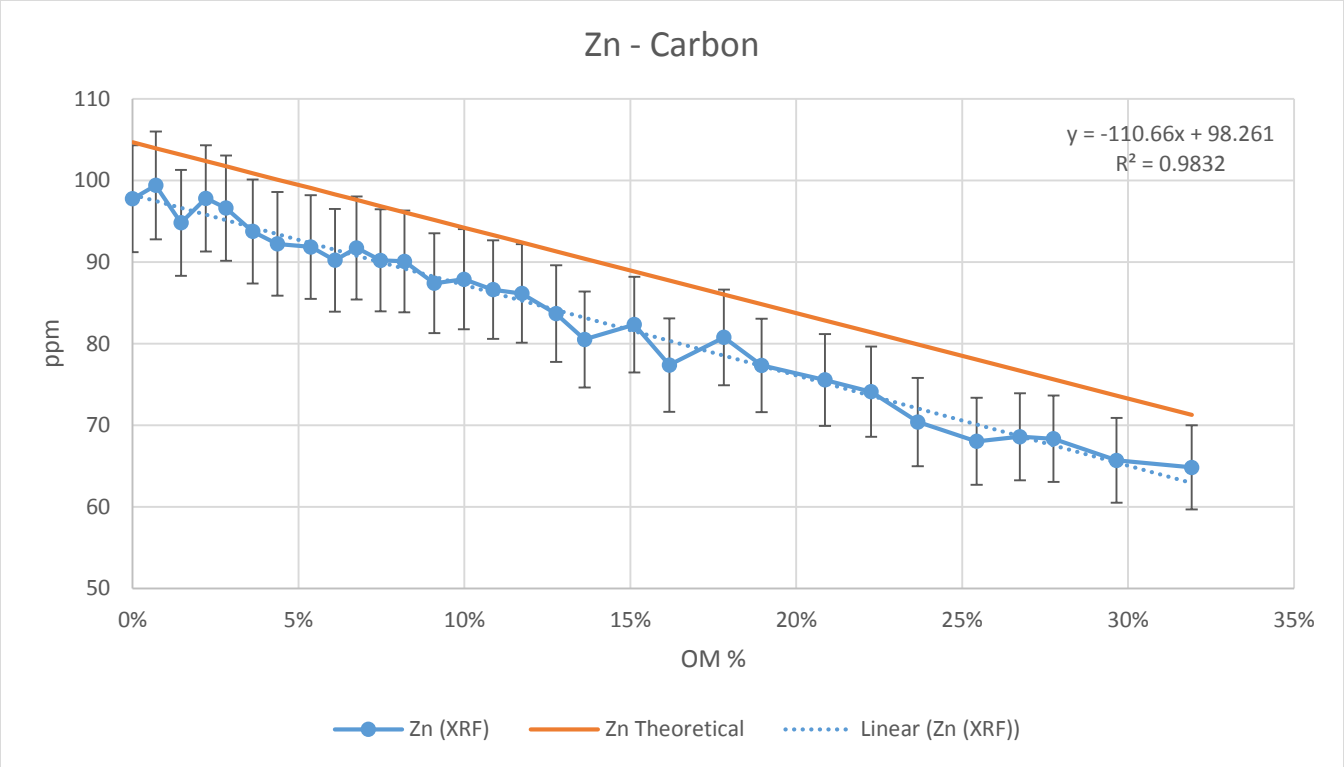

Figure 3.35 Zinc concentration versus carbon organic matter fraction.

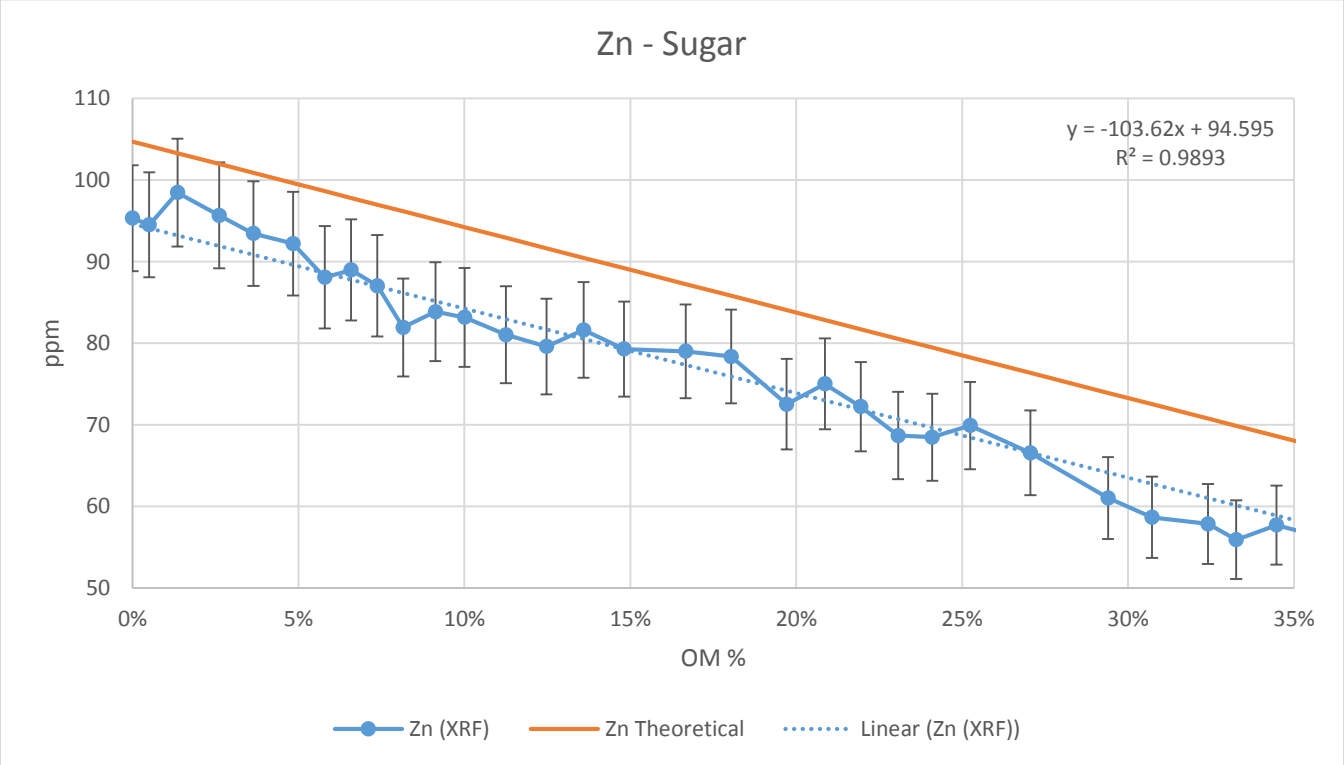

Figure 3.36 Zinc concentration versus sugar organic matter fraction.

3.5.13 Zirconium [Zr]

The zirconium pXRF response falls below the theoretical dilution line for dry cellulose (Figure 3.37), carbon (Figure 3.38) and sugar (Figure 3.39). In the wet cellulose experiment it falls below the theoretical line until approximately 12% cellulose content after which it exceeds it (Figure 3.37). Slopes and intercepts for all three OM surrogates differ from the theoretical dilution line (Section 3.7). Regression slopes for the two dry cellulose runs are statistically similar, but yield different intercepts. The dry vs. wet cellulose experiment yielded similar results for zirconium.

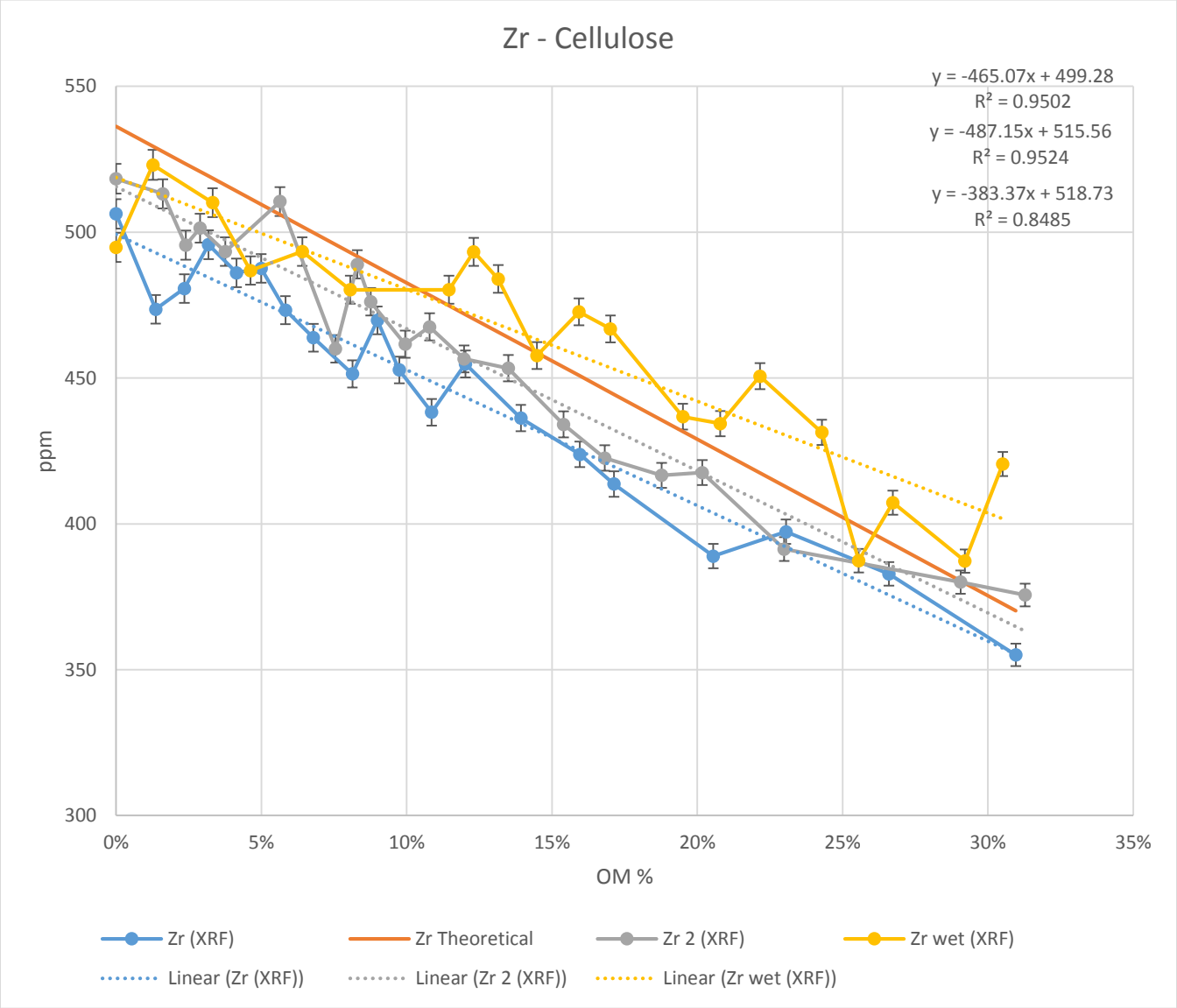

Figure 3.37 Zirconium concentration versus cellulose organic matter fraction.

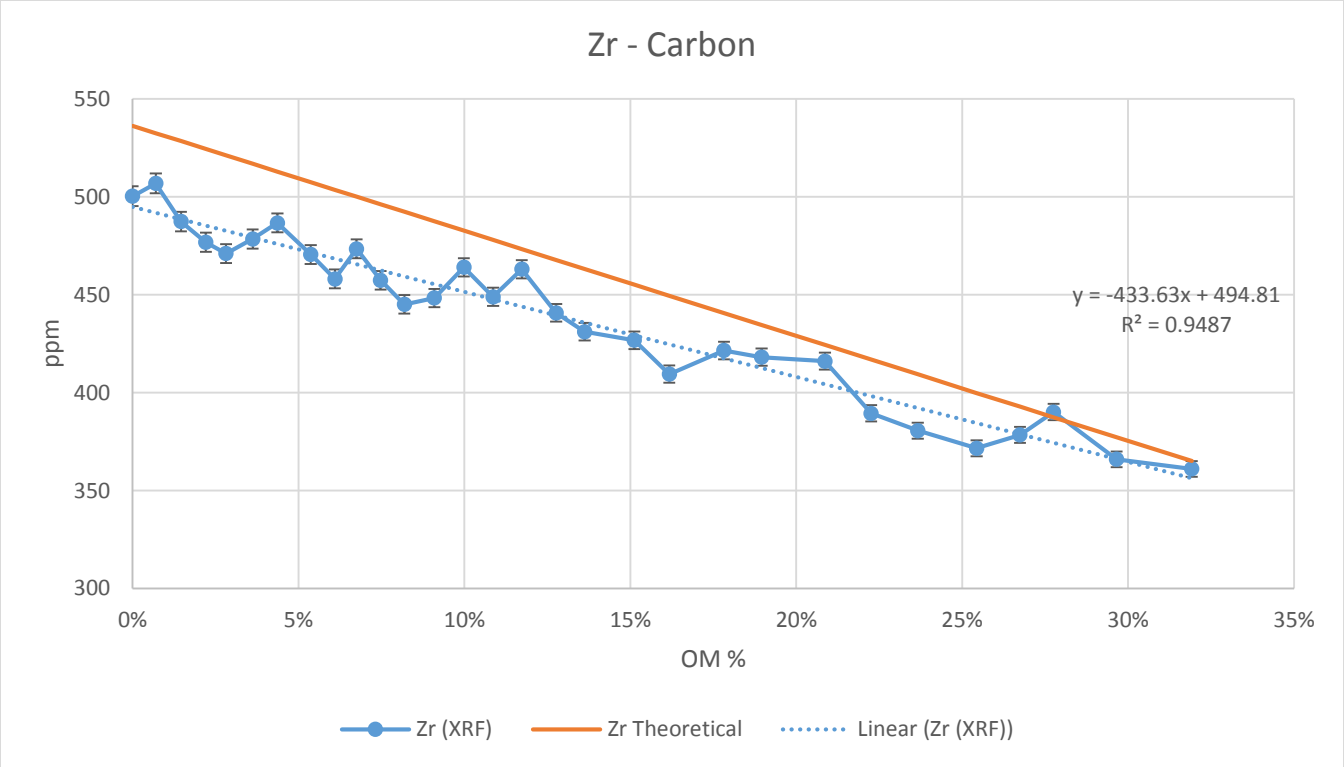

Figure 3.38 Zirconium concentration versus carbon organic matter fraction.

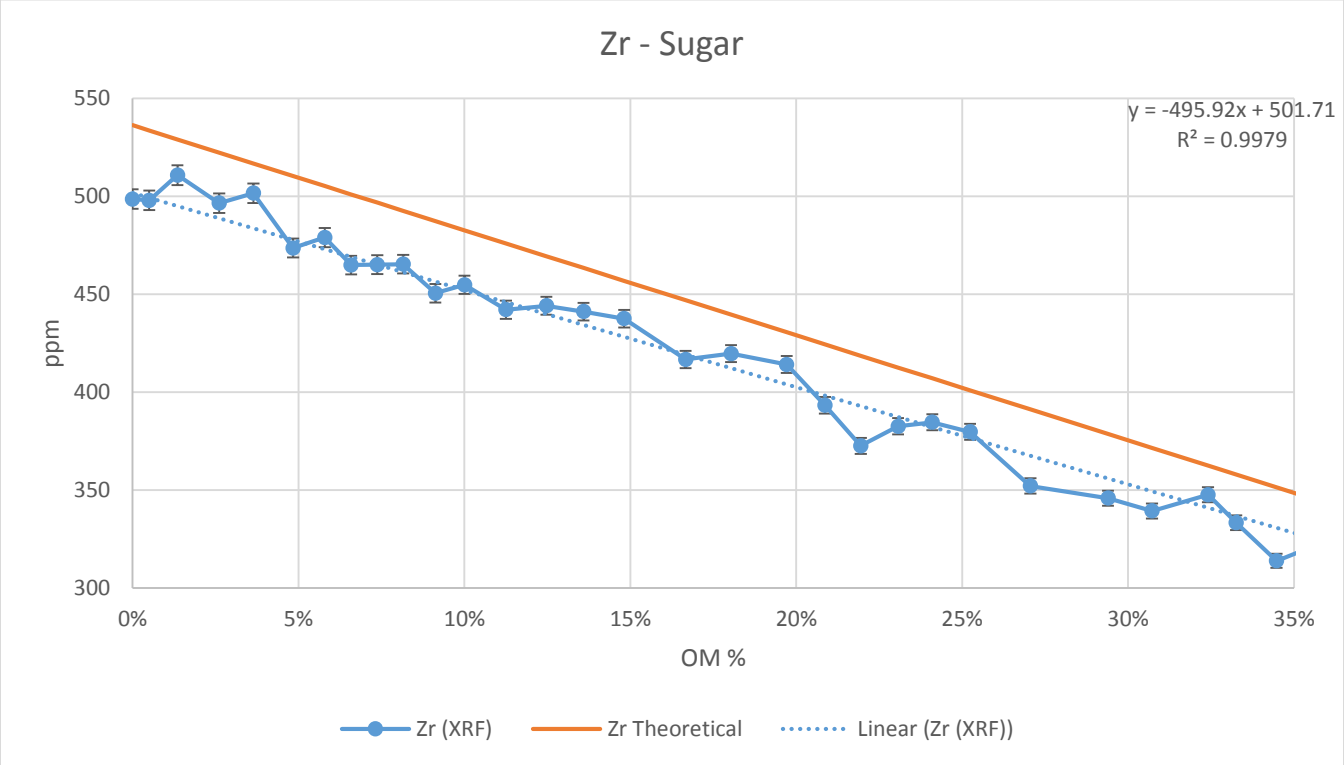

Figure 3.39 Zirconium concentration versus sugar organic matter fraction.

3.6 ANOVA: Carbon

Table 3.6 summarizes the results for the analysis of variance conducted on the carbon samples. Figure 3.40 illustrates the results summarized in Table 3.6. The sample heterogeneity factor for Pb and Cu are <.001%. Elements with large analytical variance (As, Cr, Cu, Pb, Th, and V) display correspondingly large error bars on the preceding plots of pXRF concentrations versus organic matter fraction.

Table 3.6 Carbon ANOVA results: Percent Variances

	As	Cr	Cu	Fe	Mn	Pb	Rb	Sr	Th	Ti	V	Zn	Zr
Geochemical	74.5	41.0	67.7	97.7	94.1	79.3	94.5	98.5	38.0	42.9	22.7	90.7	90.2
Heterogeneity	4.0	6.6	<.001	1.7	3.1	<.001	0.9	0.5	7.7	52.7	11.8	3.1	9.1
Analytical Variance	21.5	52.3	32.3	0.6	2.8	20.7	4.6	1.00	54.4	4.5	65.6	6.2	0.7

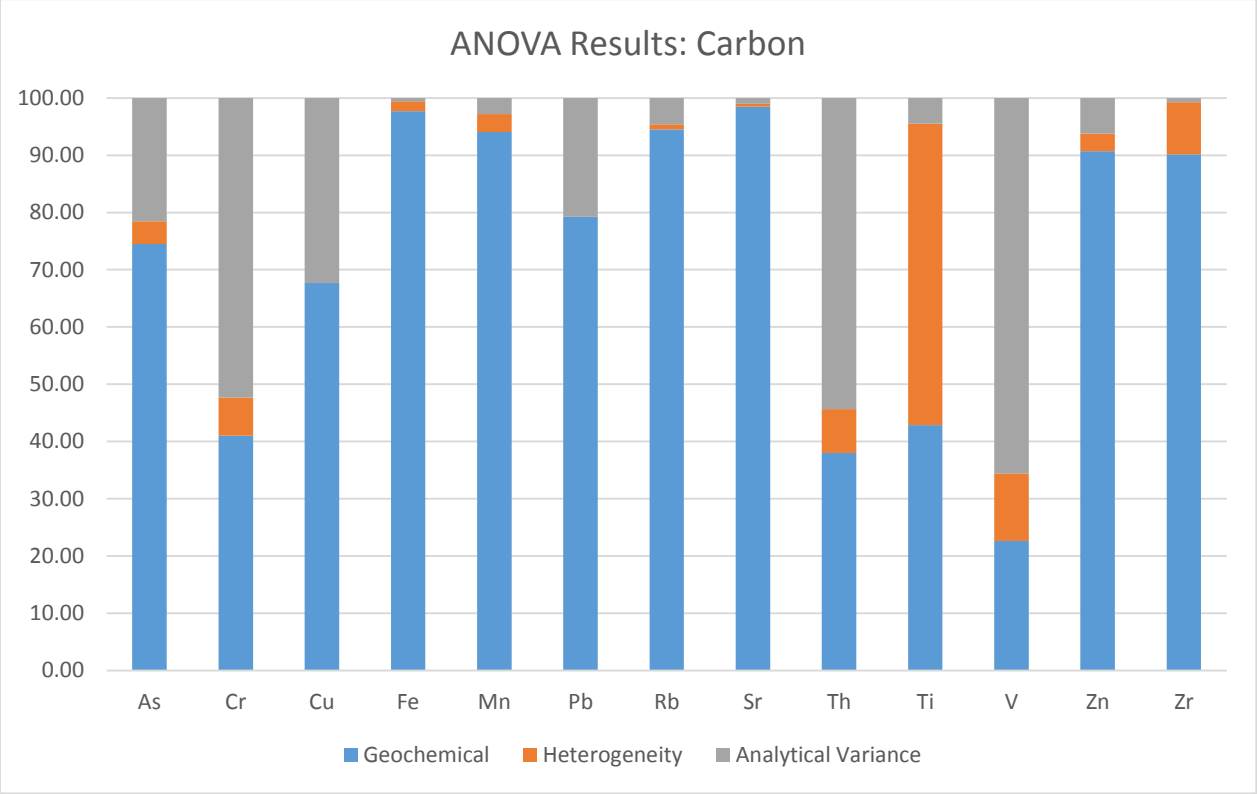

Figure 3.40 Carbon ANOVA results.

3.7 Regression Coefficients

The linear regression coefficients for plots in Figures 3.1-3.39 are summarized in Table 3.7. Regressions were computed via excel. The r^2 value presented in the table refers to the correlation coefficient. The correlation coefficients for the theoretical lines were all 1.0. P-Value significance test results comparing the regressions are also presented in Tables 3.8 and 3.9.

Table 3.7 Table of regression coefficients

	Theoretical		**Cellulose 1**			**Cellulose 2**			**Cellulose Wet**			**Carbon**			**Sugar**		
	Slope	Int	Slope	Int	r^2	Slope	Int	r^2	Slope	Int	r^2	Slope	Int	r^2	Slope	Int	r^2
As	-19.2	19.2	-24.6	20.2	0.87	-24.0	20.3	0.88	-27.5	19.8	0.91	-24.1	20.1	0.96	-21.8	19.2	0.95
Cr	-69.4	69.4	-71.7	62.5	0.89	-70.4	62.5	0.88	28.5	56.8	0.16	-38.9	60.1	0.75	-57.0	61.2	0.85
Cu	-50.2	50.2	-106	63.8	0.92	-78.0	60.0	0.88	-90.2	59.2	0.96	-66.7	59.0	0.92	-73.6	59.7	0.97
Fe	-51400	51400	-47100	46300	0.98	-45600	46400	0.98	-44900	46000	0.96	-49000	46200	1.00	-43700	44100	1.00
Mn	-1517	1517	-1999	1545	0.97	-1941	1530	0.98	-2285	1512	0.98	-1803	1510	0.99	-1590	1438	1.00
Pb	-23.5	23.5	-30.9	24.8	0.92	-30.1	24.5	0.93	-36.1	24.3	0.95	-29.3	24.2	0.97	-28.3	23.9	0.95
Rb	-47.0	47.0	-45.0	42.1	0.99	-43.2	42.4	0.99	-50.0	42.3	0.99	-42.9	42.1	0.99	-41.6	40.9	1.00
Sr	-311	311	-307	305	1.00	-306	308	1.00	-313	306	0.99	-280	302	1.00	-296	299	1.00
Th	-5.98	5.98	-10.4	6.02	0.79	-10.9	6.09	0.71	-11.6	6.21	0.81	-7.40	5.71	0.52	-7.82	5.92	0.76
Ti	-6400	6400	-1860	5730	0.47	-1650	5960	0.55	4160	5680	0.43	-1770	5490	0.70	-5100	6210	0.92
V	-106	106	-42.8	121	0.27	-96.0	131	0.68	-29.1	122	0.09	-49.3	113	0.63	-61.3	121	0.80
Zn	-105	105	-115	98.9	0.97	-113	99.4	0.98	-127	98.8	0.98	-111	98.3	0.98	-104	94.6	0.99
Zr	-536	536	-465	499	0.95	-487	516	0.95	-383	519	0.85	-434	495	0.95	-496	502	1.00

P-Value significance tests were performed using Minitab statistical analysis software. P-Values less than .01 are considered significant and are highlighted in Tables 3.8 and 3.9. Significant values (<.01) signal that the regression coefficient is different for the respective comparison being conducted; i.e., if the p-value is less than 0.01 then the regression coefficient is deemed to be different with a greater than 99% confidence. These values are highlighted in yellow in Tables 3.8 and 3.9.

Table 3.8 P-Value Significance Tests (Slopes)

Factor		As	Cr	Cu	Fe	Mn	Pb	Rb	Sr	Th	Ti	V	Zn	Zr
OM Type vs Theoretical Line	Cellulose vs Theoretical	0.019	0.702	0.000	0.006	0.000	0.002	0.075	0.305	0.001	0.000	0.001	0.056	0.007
	Carbon vs Theoretical	0.000	0.000	0.000	0.001	0.000	0.000	0.000	0.000	0.326	0.000	0.000	0.033	0.000
	Sugar vs Theoretical	0.005	0.004	0.000	0.000	0.000	0.000	0.000	0.000	0.017	0.000	0.000	0.543	0.000
Repeatability	Dry Run 1 vs Dry Run 2	0.530	0.874	0.007	0.456	0.570	0.795	0.297	0.777	0.810	0.723	0.025	0.751	0.543
Coating	Dry 1 vs Wet	0.345	0.000	0.067	0.411	0.011	0.084	0.007	0.559	0.523	0.000	0.626	0.073	0.088
Elemental Dependence	Carbon vs Cellulose	0.784	0.000	0.000	0.171	0.016	0.479	0.092	0.000	0.131	0.843	0.687	0.459	0.326
	Carbon vs Sugar	0.143	0.009	0.144	0.000	0.000	0.568	0.276	0.000	0.798	0.000	0.281	0.092	0.000
	Cellulose vs Sugar	0.231	0.104	0.000	0.068	0.000	0.330	0.049	0.039	0.121	0.008	0.282	0.069	0.165

Table 3.9 P-Value Significance Tests (Intercepts)

Factor		As	Cr	Cu	Fe	Mn	Pb	Rb	Sr	Th	Ti	V	Zn	Zr
OM Type vs Theoretical Line	Cellulose vs Theoretical	0.004	0.000	0.000	0.000	0.021	0.000	0.000	0.000	0.855	0.000	0.000	0.000	0.000
	Carbon vs Theoretical	0.000	0.000	0.000	0.000	0.205	0.000	0.000	0.000	0.167	0.000	0.000	0.000	0.000
	Sugar vs Theoretical	0.845	0.000	0.000	0.000	0.000	0.108	0.000	0.000	0.739	0.102	0.000	0.000	0.000
Repeatability	Dry Run 1 vs Dry Run 2	0.666	0.950	0.012	0.772	0.303	0.452	0.209	0.000	0.808	0.013	0.004	0.564	0.004
Coating	Dry 1 vs Wet	0.396	0.042	0.001	0.473	0.063	0.315	0.562	0.601	0.525	0.772	0.766	0.933	0.013
Elemental Dependence	Carbon vs Cellulose	0.867	0.030	0.000	0.828	0.004	0.081	0.742	0.003	0.265	0.001	0.002	0.442	0.347
	Carbon vs Sugar	0.002	0.389	0.417	0.000	0.000	0.392	0.000	0.000	0.416	0.000	0.000	0.000	0.038
	Cellulose vs Sugar	0.012	0.378	0.001	0.000	0.000	0.049	0.000	0.000	0.733	0.015	0.915	0.000	0.497

Chapter 4

Analysis and Discussion

4.0 Introduction

This chapter presents a discussion of the results presented in Chapter 3 along with an analysis of correction factors accounting for pXRF response to varying organic matter fractions generated for each element. A discussion of the nested ANOVA results is also included. The chapter concludes with an evaluation of the hypothesis presented in the first chapter of this thesis and recommendations for future work related to quantification of the effects of organic matter on XRF soil metal measurements.

4.1 Instrument Resolution Effects

The resolution of the detector on the Niton XL3t GOLDD+ pXRF instrument is 185 electron volts (eV). This has important implications for the measurements rendered by the pXRF. It is widely recognized in the pXRF community that elements with similar peaks may interfere with one another and lead to inaccurate results if using the X-Ray fluorescence method of analysis (Goulding and Jaklevic, 1973). The culprit in these types of interference errors is in part the instrument detector because the pXRF can only decipher and differentiate between peaks separated by an energy greater than the instrument resolution (185 eV in this case). When the peaks fall within or near 185 electron volts of one another, the detector may fail to appropriately assign the measurement counts. This may in turn affect the results rendered by the system's algorithms.

Carbon contains a single X-Ray emission line at an energy of 0.277 keV. Because the resolution of our detector is 0.185 keV, the distance from the peak to the through should be within +/- 92.5 eV (instrument resolution divided by 2). This means emission photons from carbon are not easily distinguished by the detector within the limits of 184.5 and 369.5 eV, and can be interpreted anywhere in between those values. Similarly, oxygen has a single X-Ray emission line at 524.9 eV. This means emission photons from oxygen are not easily distinguished by the detector within the limits of 432.4 and 617.4 eV. These limits are under ideal circumstances and neglect to take into account that Compton scattering may

modify the photon energy emanations from these light elements. Compton scattering further complicates and blurs the lines between carbon and oxygen peaks. As a result, the effective pXRF resolution is degraded, making it more difficult to distinguish among peaks and leading to additional measurement error.

Table 4.1 lists the specific X-Ray lines the Niton XL3t instrument takes into account with its algorithms in rendering concentration values. All values are in keV and the information was obtained directly from the instrument's control console when connected to a lap top computer. For each element of interest, the peaks which the instrument may misinterpret for oxygen emanations have been highlighted in yellow (value between 524.9 eV and 617.4 eV).

Table 4.1 Instrument elemental peaks (in keV)

Element	Ka1	Ka2	Kb1	Kb2	Kb3	La1	La2	Lb1	Lb2	Lg	Ll	Ma1
As	10.544	10.508	11.726	11.864	11.72	1.282	1.282	1.317	-	-	1.12	-
Cr	5.415	5.405	5.947	-	5.947	0.573	0.573	0.583	-	-	0.500	-
Cu	8.048	8.028	8.905	-	8.905	0.93	0.93	0.95	-	-	0.811	-
Fe	6.404	6.391	7.058	-	7.058	0.705	0.705	0.718	-	-	0.615	-
Mn	5.899	5.888	6.49	-	6.49	0.637	0.637	0.649	-	-	0.556	-
Pb	*	*	*	*	*	10.449	12.614	12.623	14.764	9.184	2.345	-
Rb	13.395	13.336	14.961	15.185	14.952	1.694	1.693	1.752	-	-	1.482	-
Sr	14.165	14.098	15.836	16.085	15.825	1.807	1.805	1.871	-	-	1.582	-
Th	*	*	*	*	*	12.969	12.81	16.81	15.624	18.982	11.119	2.996
Ti	4.511	4.505	4.932	-	4.932	0.452	0.452	0.458	-	-	0.395	-
V	4.952	4.945	5.427	-	5.427	0.511	0.511	0.519	-	-	0.446	-
Zn	8.639	8.616	9.572	-	9.572	1.012	1.012	1.035	-	-	0.884	-
Zr	15.775	15.691	17.668	17.97	17.654	2.042	2.04	2.124	2.219	2.303	1.792	-

*Lines which exceeded 50keV limit of instrument

4.2 Organic Matter Corrections

Figures 3.1-3.39 in the preceding chapter document the response of the pXRF versus the organic matter fraction of each sample analyzed. In some instances, the pXRF response behaved as one would expect given the mass dilutions with the organic matter surrogates that were conducted. In other instances, the pXRF response as a function of surrogate fraction presence diverged from the predicted response (Tables 3.8 and 3.9). Based on these empirical observations, correction factors were generated by dividing the theoretical value by the measured value at the various organic matter surrogate dilution fraction points along the cellulose 1 run. Plots of these correction factors (Figures 4.1 – 4.13) were generated and subsequently modeled via excel using second order polynomial regression.

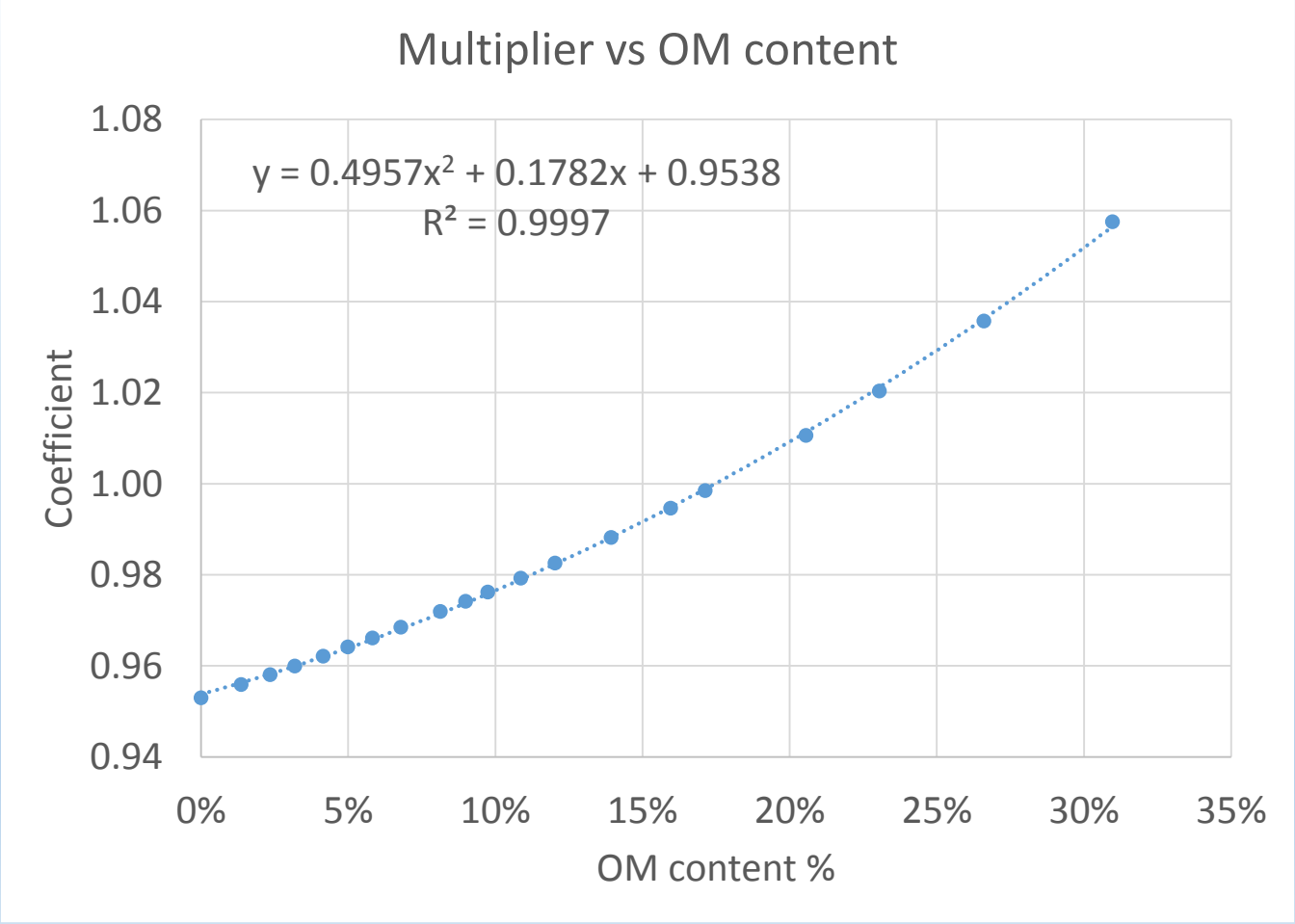

Figure 4.1 Arsenic correction coefficient versus organic matter content

The arsenic signal overestimates the theoretical value at zero percent organic matter by approximately 5%. This is reflected in Figure 4.1 by the y-intercept of the regression at 0.954. The 5% overestimation is attributable to instrumental bias because the sample is free of organic matter and other complicating factors (grain size, moisture content, geometry, etc.) have been controlled. It is noteworthy that the pXRF response, as reflected by the polynomial regression, varies as a function of organic matter content of the sample. This means that the addition of organic matter affects the correction factor that must be applied in order to adjust the measured pXRF value to the theoretical value. In the case of arsenic, a crossover point where no correction is required occurs at approximately 17% organic matter content.

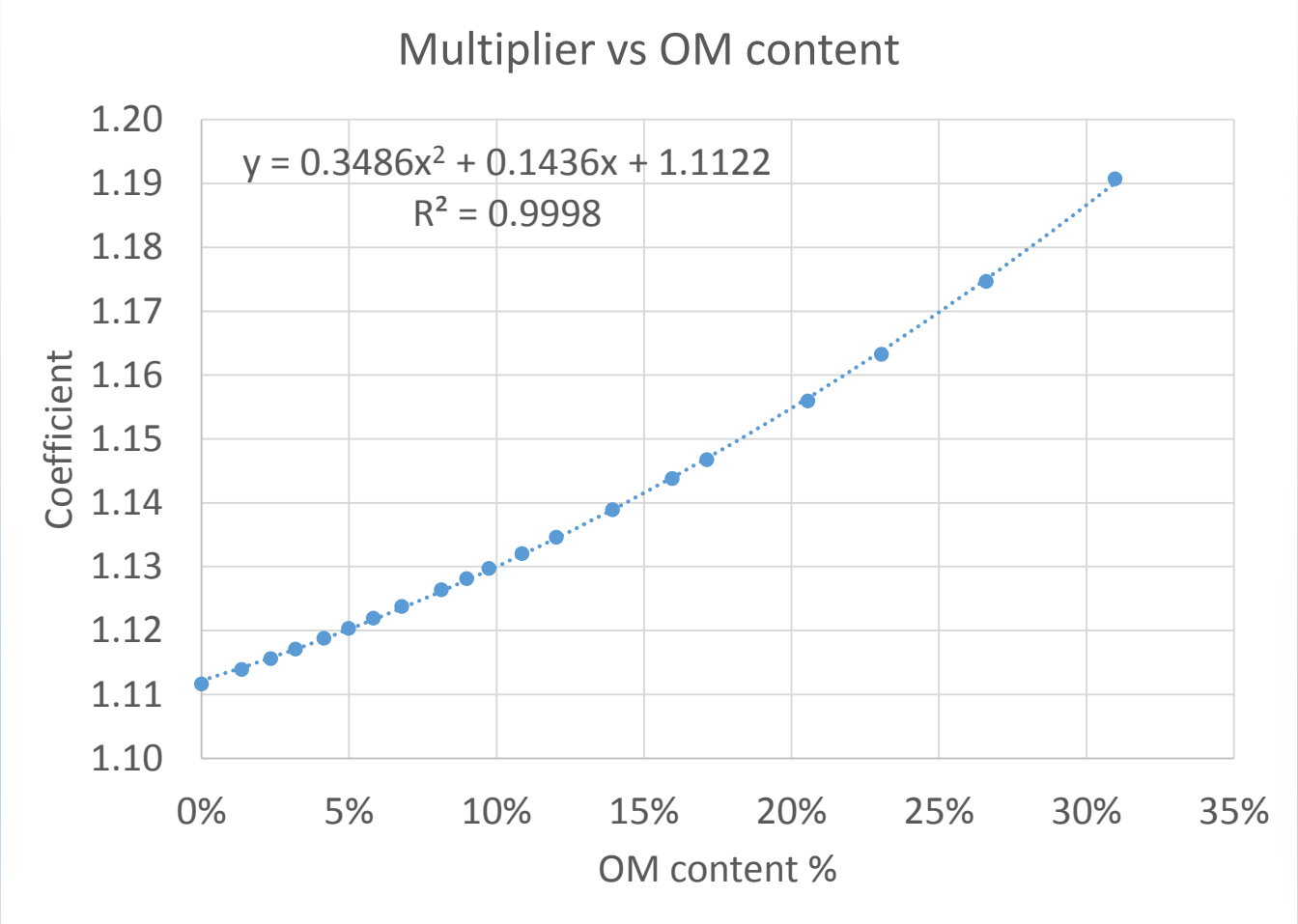

Figure 4.2 Chromium correction coefficient versus organic matter content

In the absence of organic matter, the pXRF measurement for chromium underestimates the certified chromium concentration by approximately 11% (Figure 4.2). The magnitude of the correction factor required to adjust measured Cr concentrations to the theoretical cellulose dilution curve increases from approximately 1.11 to 1.19 across the range of OM fractions measured. Therefore, with the addition of increasing dry cellulose OM fraction, the degree of underestimation is amplified, as shown by the upward trend of the regression line in Figure 4.2. This behavior is also reflected in the plot of Cr concentration vs OM fraction (Figure 3.4) which shows a steeper slope for the cellulose dry 1 linear regression compared to the theoretical curve resulting in an increasing divergence between the two lines with increasing OM fraction.

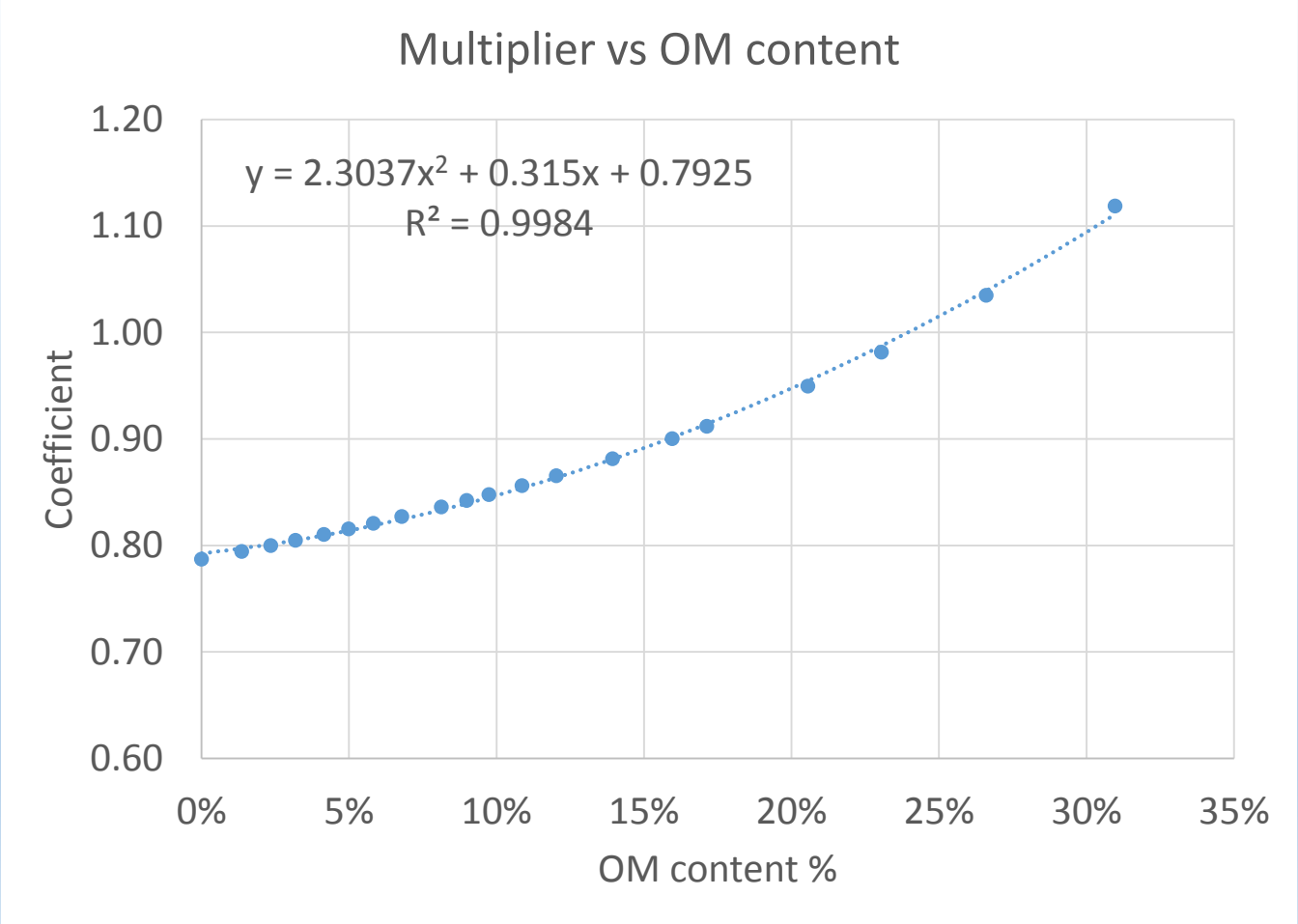

Figure 4.3 Copper correction coefficient versus organic matter content

The copper signal overestimates the theoretical value at zero percent organic matter by approximately 20% (Figure 4.3). The correction factor for copper increases and reaches a crossover point at approximately 24% organic matter content.

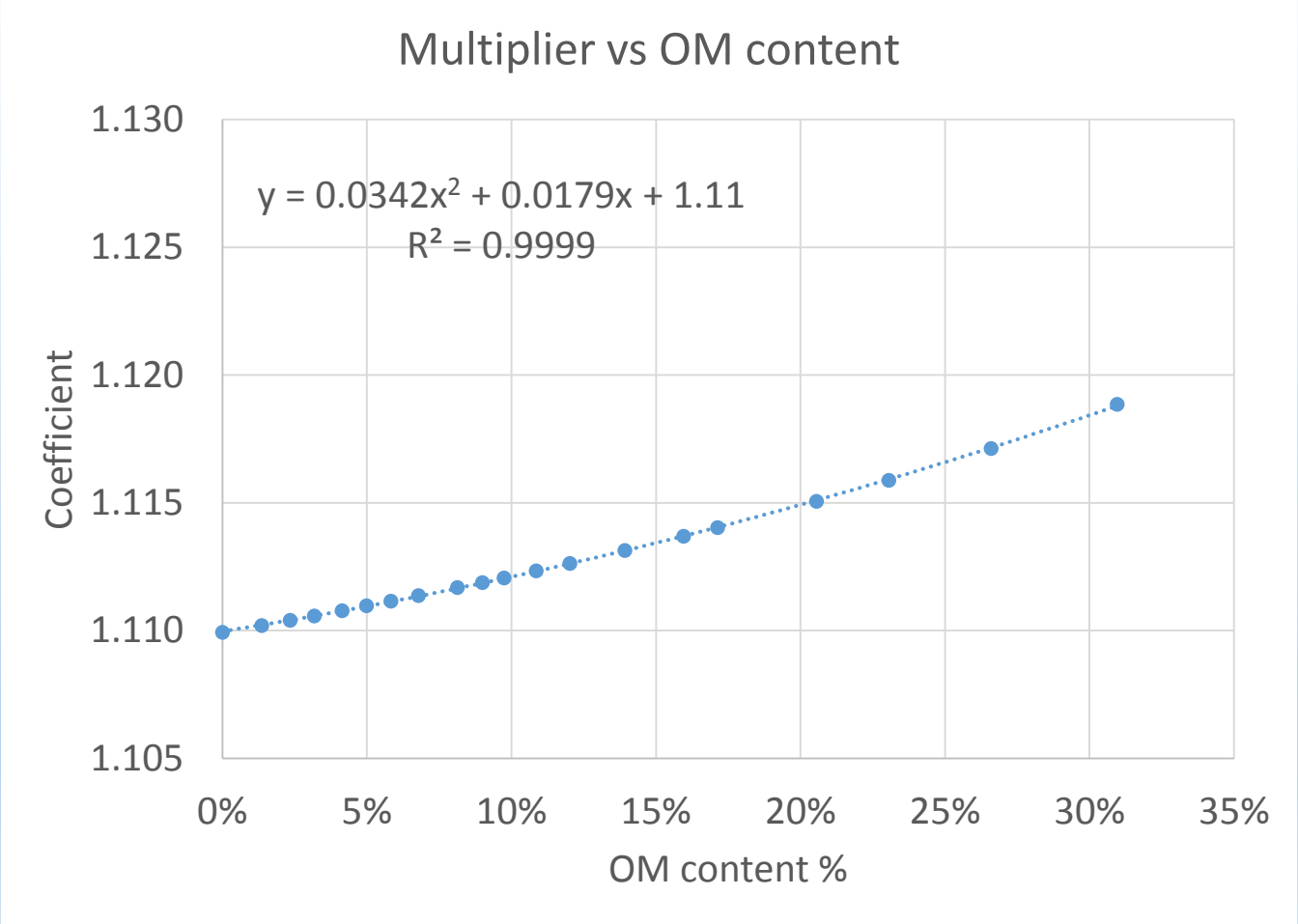

Figure 4.4 Iron correction coefficient versus organic matter content

The iron signal underestimates the theoretical value at zero percent organic matter by approximately 11% (Figure 4.4). The correction coefficient does not change in response to OM addition as much as the other elements discussed thus far. The correction coefficient line remains relatively flat meaning instrument bias accounts for much of the underestimation and that the addition of organic matter only mildly affects the response of the pXRF, potentially due to a relatively high abundance of iron within the sample (on the order of 5%).

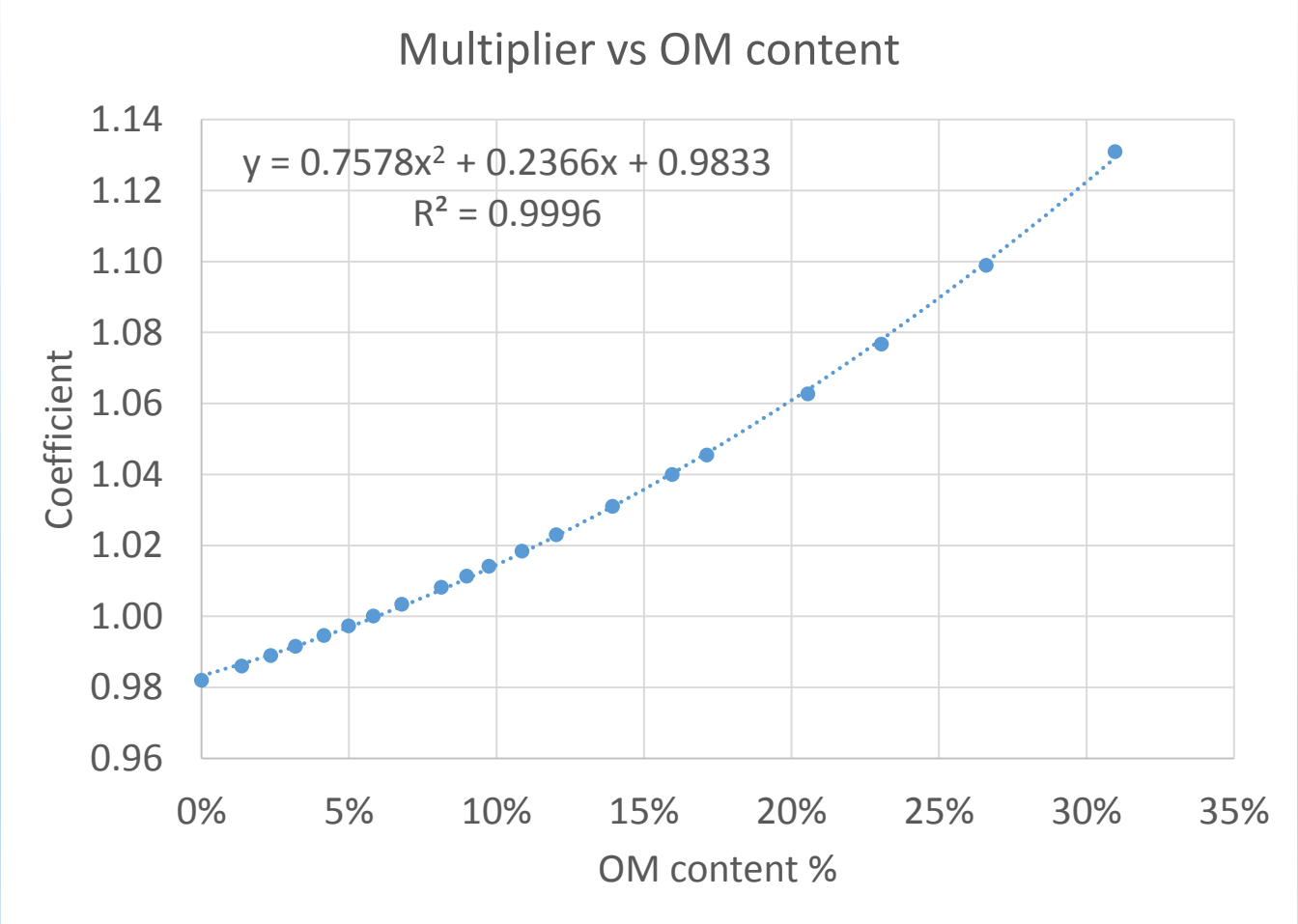

Figure 4.5 Manganese correction coefficient versus organic matter content

The manganese signal overestimates the theoretical value at zero percent organic matter by approximately 2% (Figure 4.5). The crossover point is at approximately 6% organic matter content for manganese.

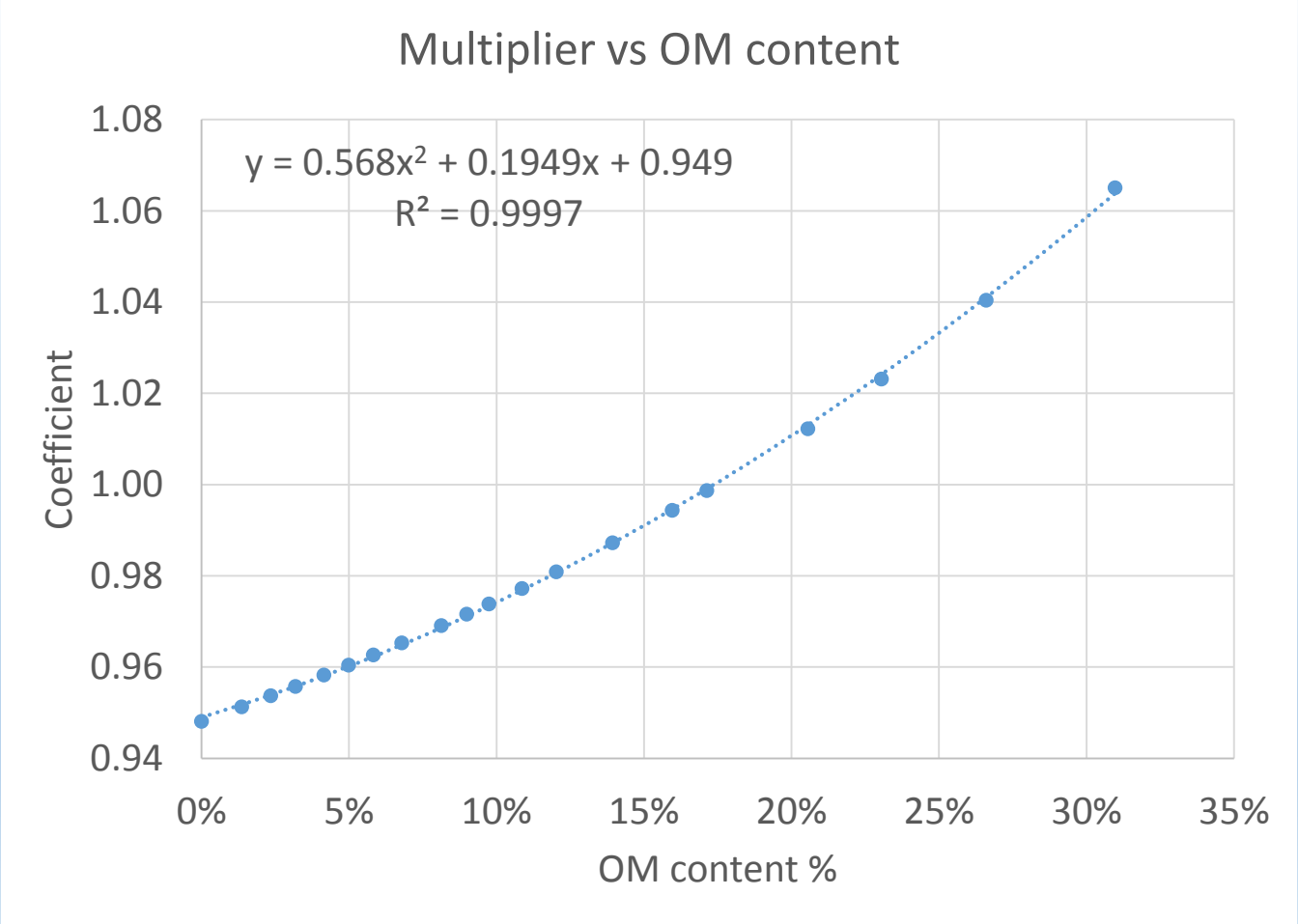

Figure 4.6 Lead correction coefficient versus organic matter content

The lead signal overestimates the theoretical value at zero percent organic matter by approximately 5% (Figure 4.6). The crossover point for lead is at approximately 17% organic matter content.

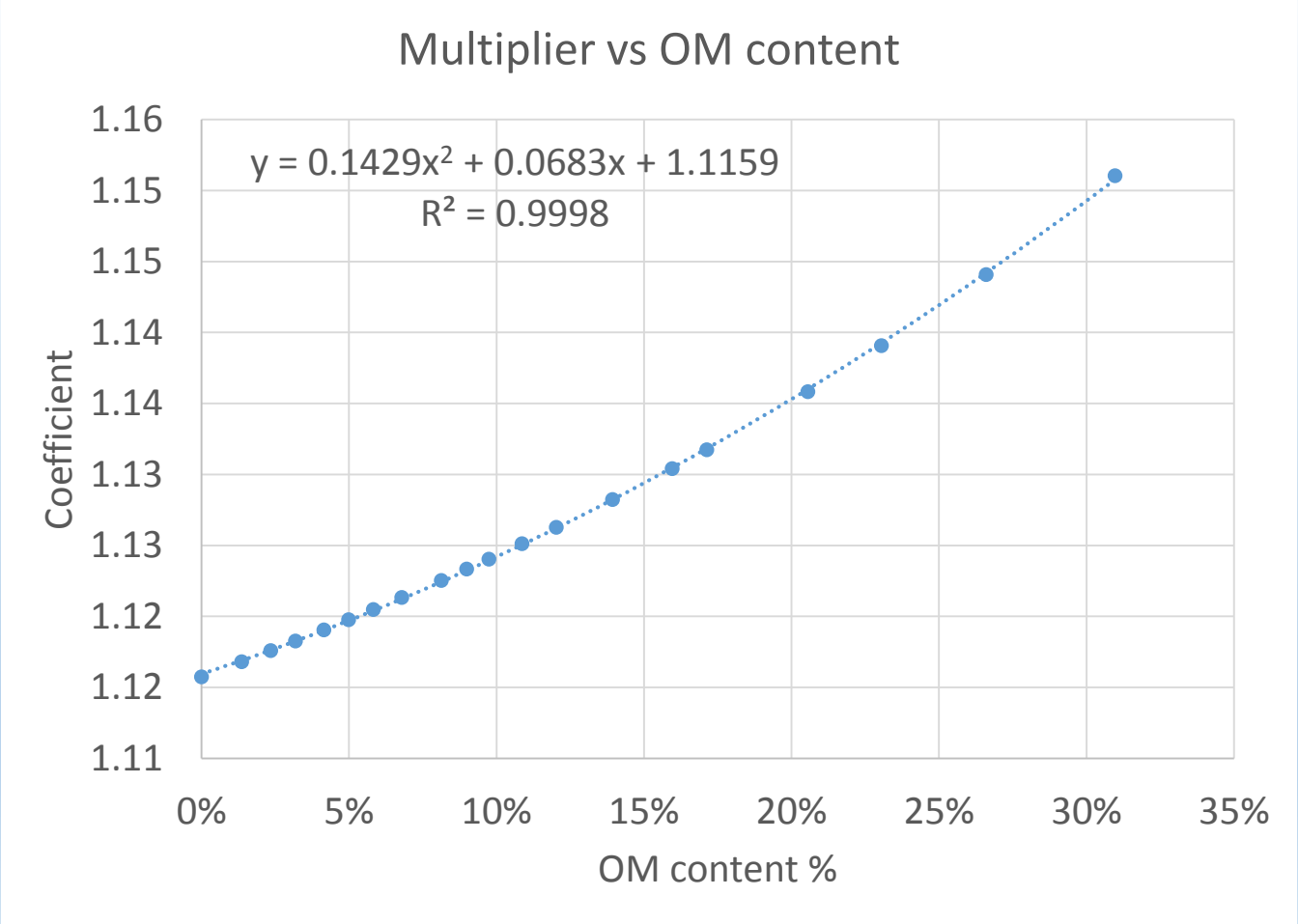

Figure 4.7 Rubidium correction coefficient versus organic matter content

The rubidium signal underestimates the theoretical value at zero percent organic matter by approximately 12% and does so consistently at an increasing rate with the addition of organic matter (Figure 4.7).

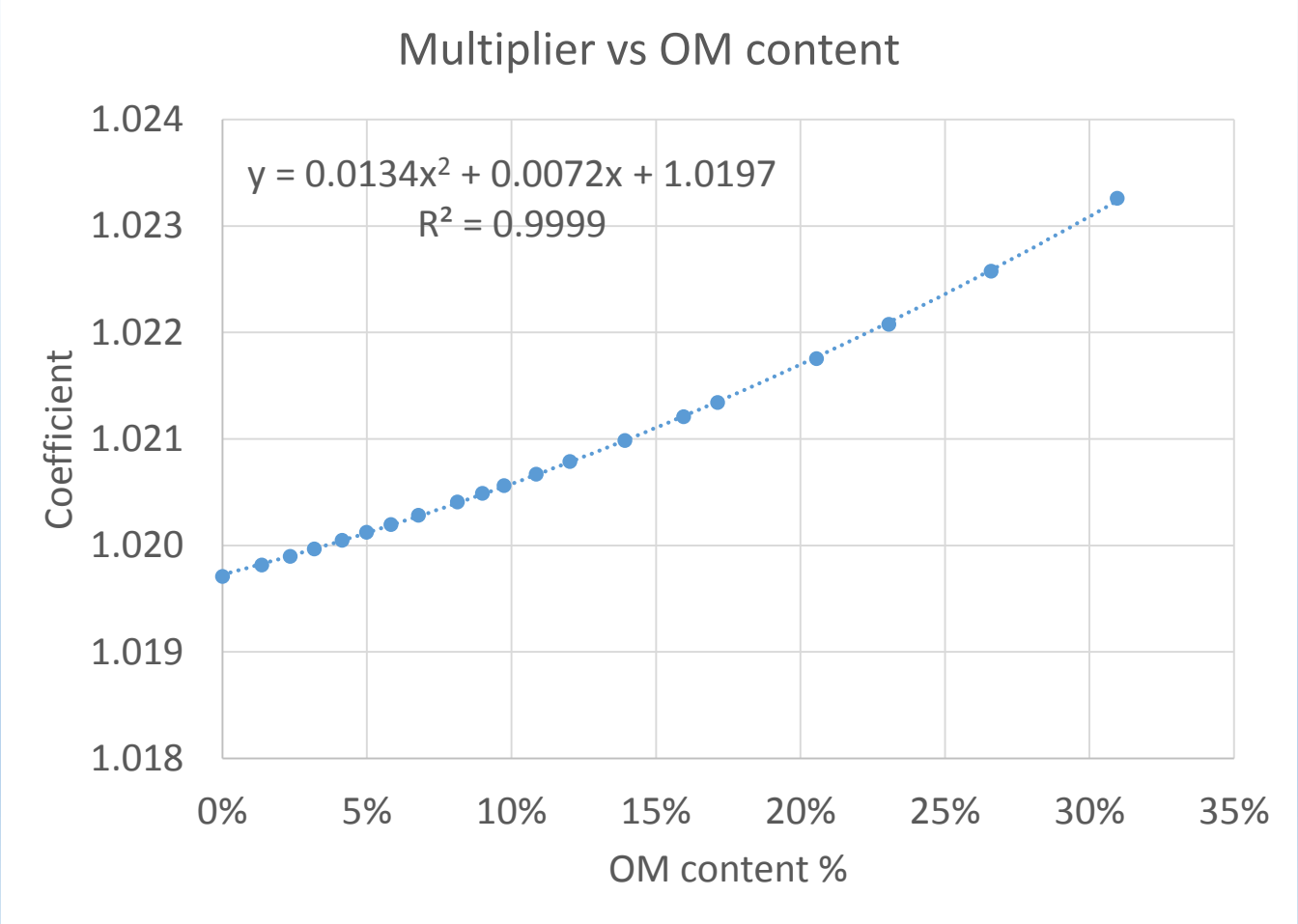

Figure 4.8 Strontium correction coefficient versus organic matter content

The strontium signal underestimates the theoretical value at zero percent organic matter by approximately 2% and does so consistently at an increasing rate with the addition of organic matter (Figure 4.8).

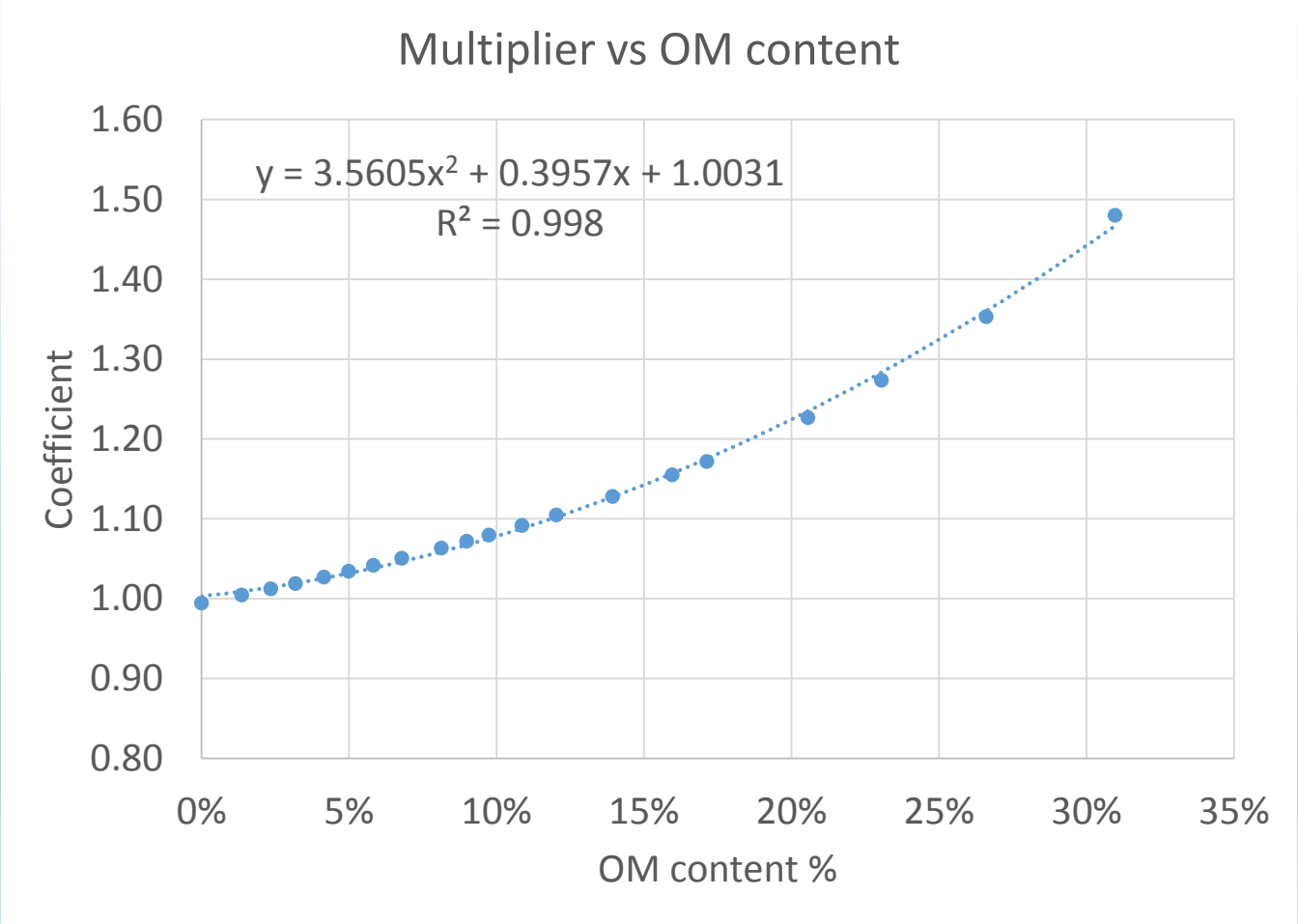

Figure 4.9 Thorium correction coefficient versus organic matter content

The thorium signal does a good job at estimating the theoretical value in the absence of organic matter and begins underestimating the theoretical levels with the addition of organic matter (Figure 4.9). It is noteworthy that the thorium levels in the standard used (Till-1) were near the detection limit of the instrument giving rise to potential errors associated with the instrumental limits.

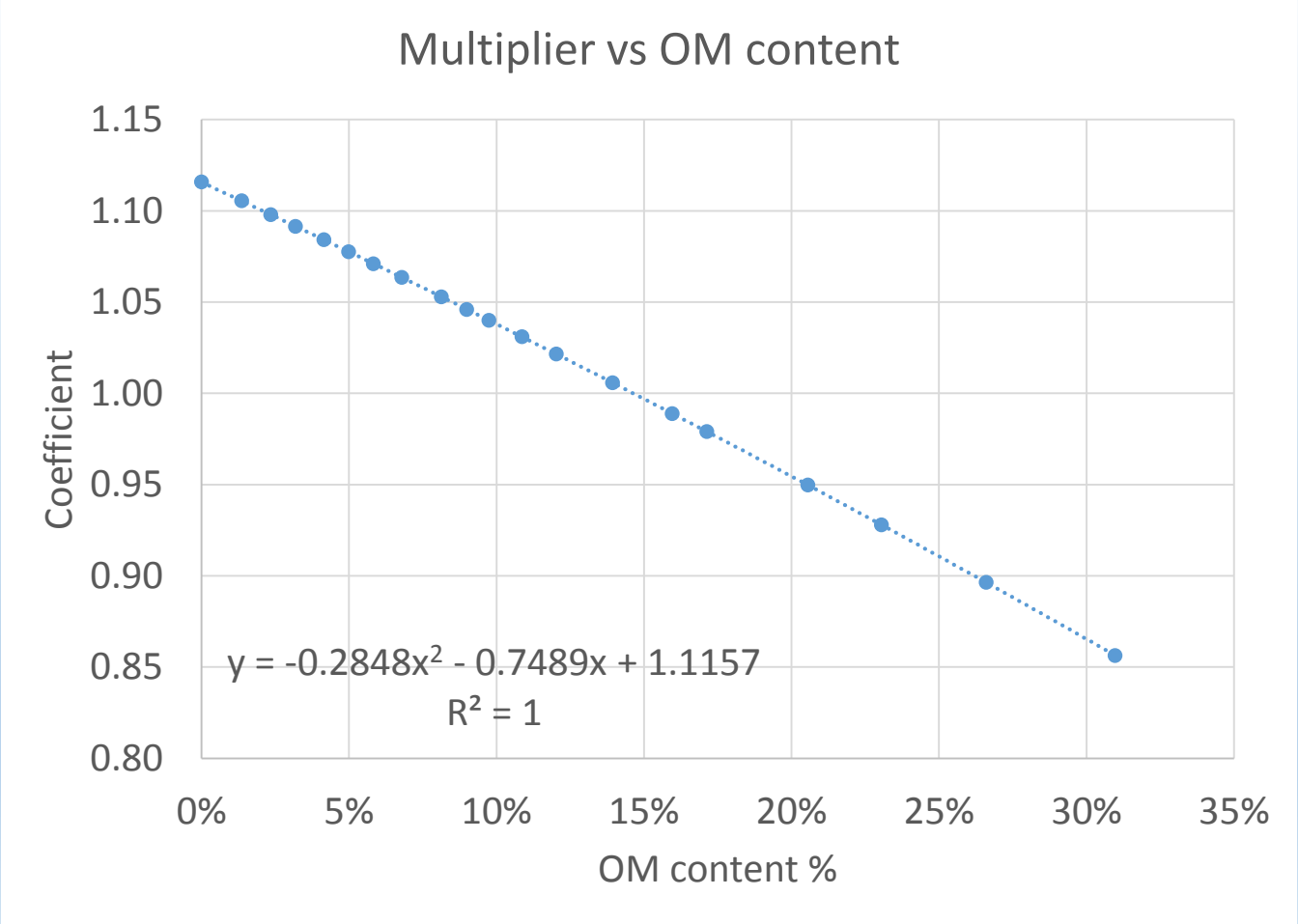

Figure 4.10 Titanium correction coefficient versus organic matter content

The titanium signal underestimates the theoretical value by approximately 12% at zero percent organic matter (Figure 4.10). The crossover point at which no correction is necessary for titanium is approximately 15% organic matter content. Titanium, along with vanadium and zirconium, is one of three elements investigated in this study that increasingly overestimate metal concentration in response to the addition of organic matter. This results in the negative slope of the regression shown in Figure 4.10.

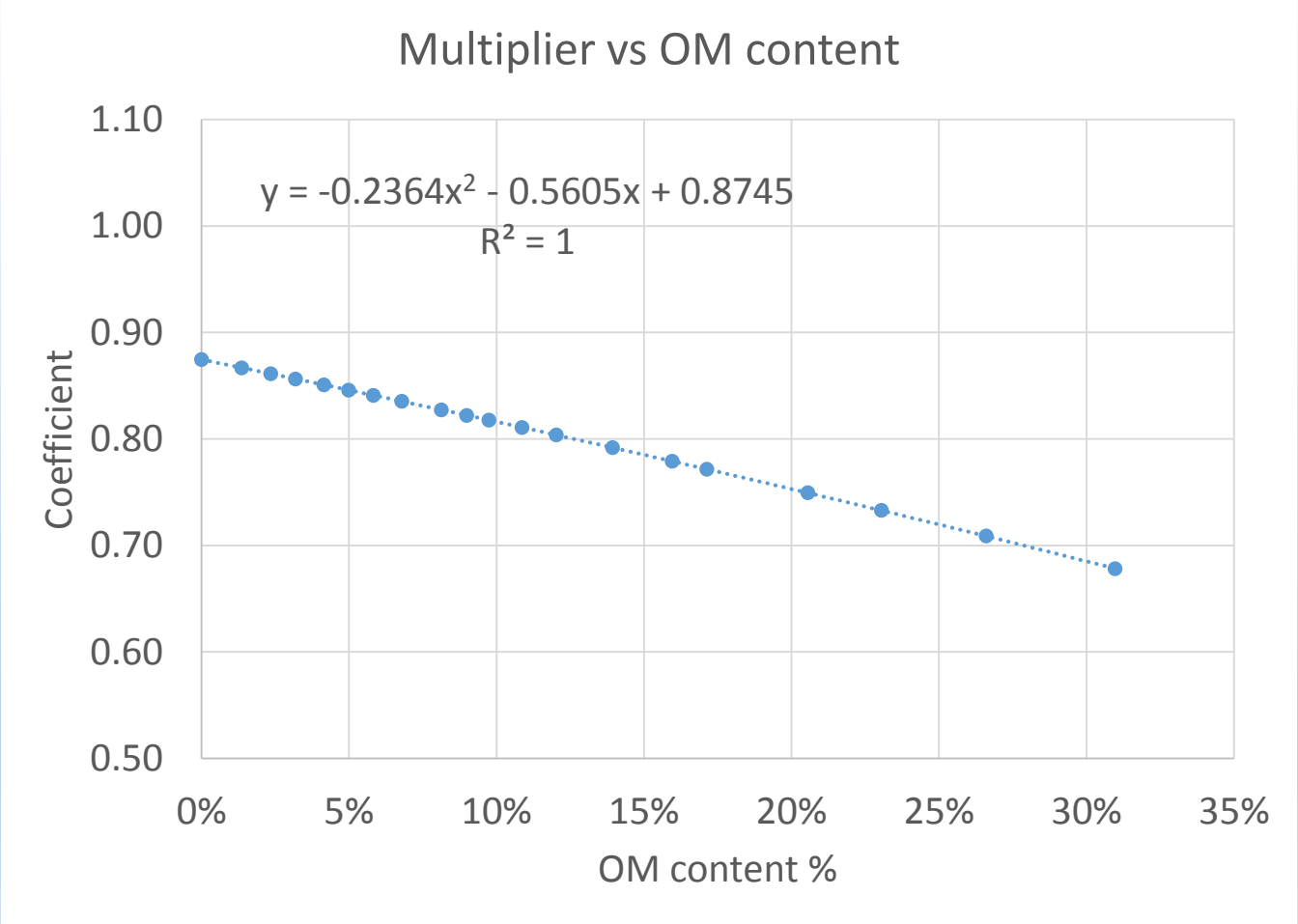

Figure 4.11 Vanadium correction coefficient versus organic matter content

The vanadium signal overestimates the theoretical value at zero percent organic matter by 13% (Figure 4.11). From there, as for titanium, the pXRF increasingly overestimates the theoretical value with the addition of cellulose organic matter surrogate.

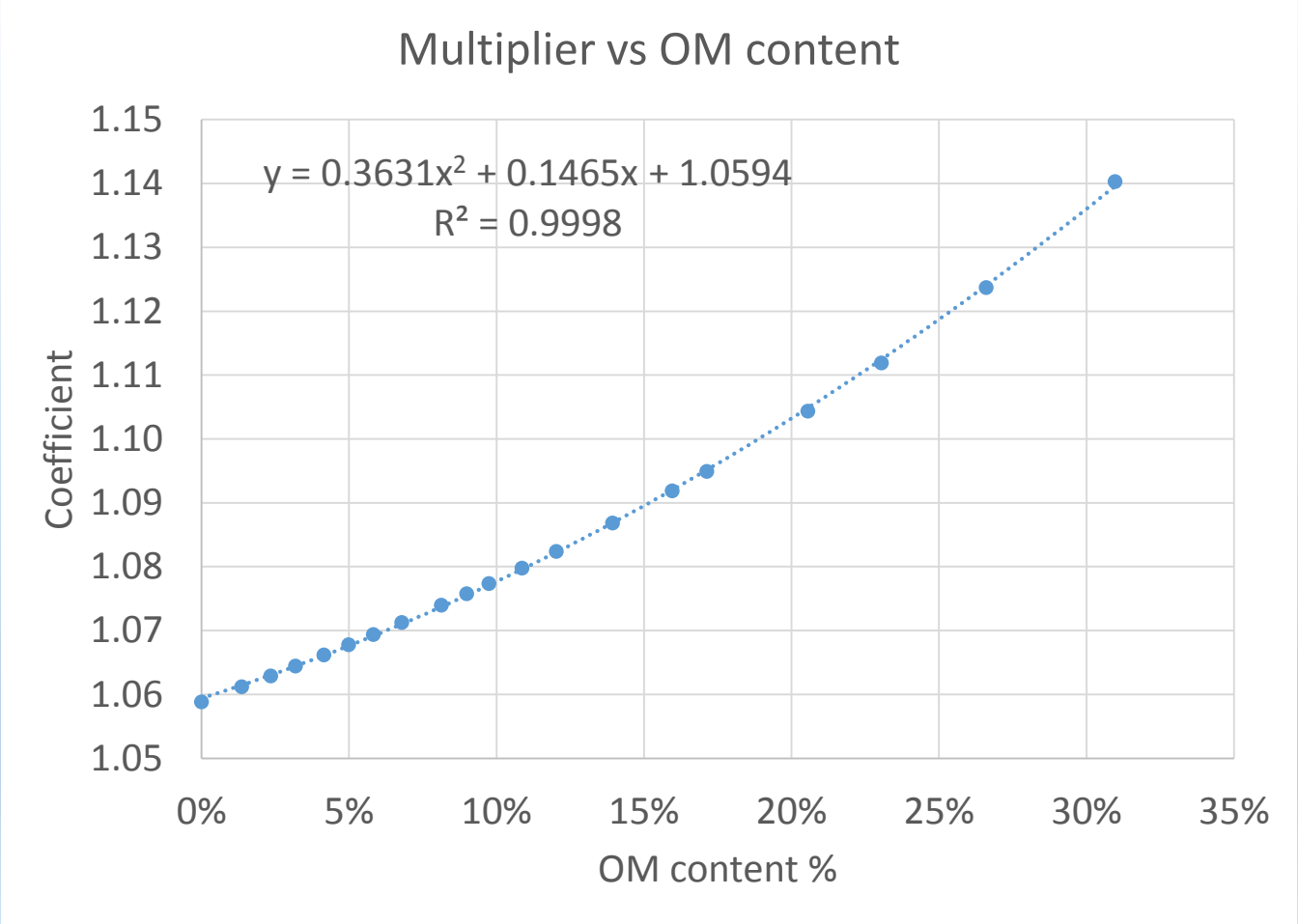

Figure 4.12 Zinc correction coefficient versus organic matter content

The zinc signal underestimates the theoretical value at zero percent organic matter by approximately 6% (Figure 4.12). The pXRF underestimates the zinc concentration at an increasing rate with the addition of organic matter.

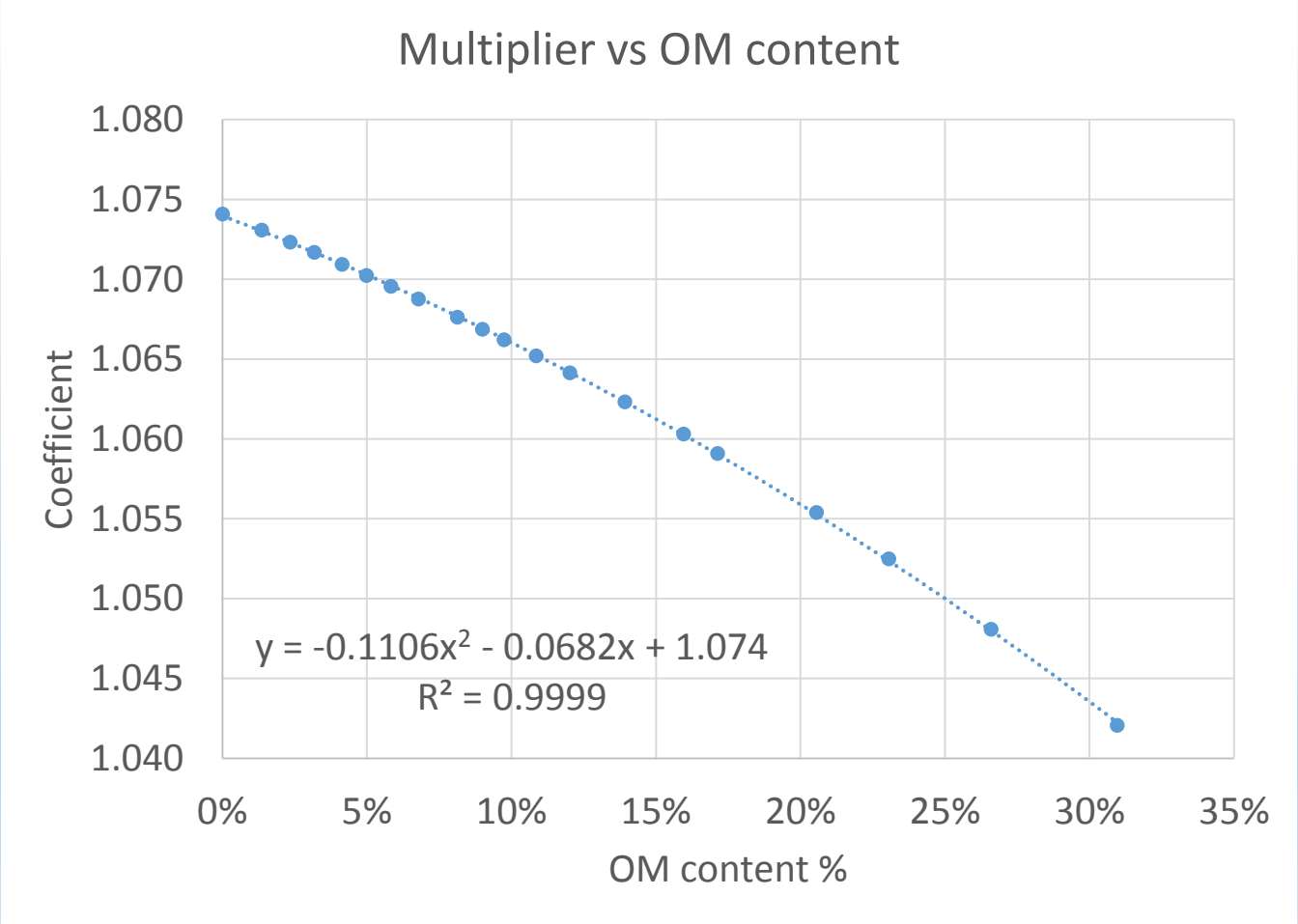

Figure 4.13 Zirconium correction coefficient versus organic matter content

The zirconium signal underestimates the theoretical value at zero percent organic matter by approximately 7% and it increasingly overestimates metal concentration in response to the addition of organic matter (Figure 4.13).

Table 4.2 lists the computed correction polynomials for the 13 elements of interest to this investigation, where y is the correction coefficient to be applied to the measured XRF response and where x is the measured organic matter fraction of the sample analyzed. Correlation coefficients for all second order polynomials were >.99 for all elements. All elements under investigation exhibited positive regression polynomial slopes with the exception of titanium, vanadium and zirconium indicating the pXRF signal was amplified with the addition of organic matter for these three elements.

Table 4.2 Correction Polynomials Summary Table.

	Correction Polynomial
As	$y = 0.4957x^2 + 0.1782x + 0.9538$
Cr	$y = 0.3486x^2 + 0.1436x + 1.1122$
Cu	$y = 2.3037x^2 + 0.315x + 0.7925$
Fe	$y = 0.0342x^2 + 0.0179x + 1.11$
Mn	$y = 0.7578x^2 + 0.2366x + 0.9833$
Pb	$y = 0.568x^2 + 0.1949x + 0.949$
Rb	$y = 0.1429x^2 + 0.0683x + 1.1159$
Sr	$y = 0.0134x^2 + 0.0072x + 1.0197$
Th	$y = 3.5605x^2 + 0.3957x + 1.0031$
Ti	$y = -0.2848x^2 - 0.7489x + 1.1157$
V	$y = -0.2364x^2 - 0.5605x + 0.8745$
Zn	$y = 0.3631x^2 + 0.1465x + 1.0594$
Zr	$y = -0.1106x^2 - 0.0682x + 1.074$

4.3 Evaluation of OM Corrections

The correction coefficient polynomials were evaluated by analyzing four unaltered Natural Resources Canada standards (Till-1, Till-2, Till-3, Till-4) using the pXRF.

Results are presented in a series of plots (Figures 4.14 – 4.26) that compare certified values for each standard (blue bars) with traditional XRF-corrected values (yellow bars) and OM-corrected values (green bars). Traditional corrected values (yellow bars) were calculated using calibration curves generated with a set of seven standard reference materials (Appendix B). The OM-corrected XRF values (green bars) were computed using the correction polynomials (Table 4.2) and the certificate organic matter fraction (Table 4.3) for each standard. The error bars depicted on each plot represent the two sigma (95%) confidence interval.

Table 4.3 Organic matter fractions for Natural Resources Canada Till standards.

	Certificate (LOI %)
Till - 1	6.3%
Till - 2	6.8%
Till - 3	3.6%
Till - 4	4.4%

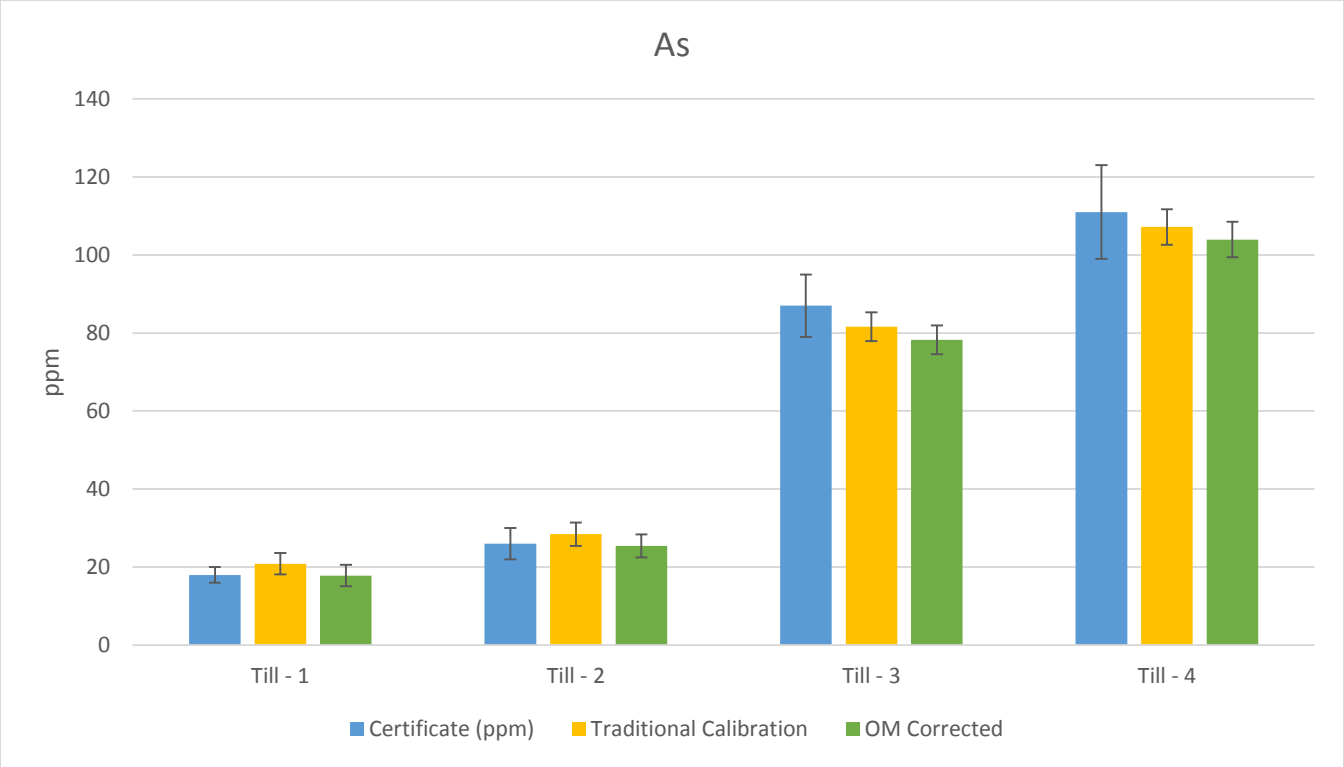

Figure 4.14 Arsenic OM correction evaluation chart

Although the OM correction method adjusts the consensus value closer to the certificate value for Till-1 and Till-2, for arsenic (Figure 4.14), both correction methods do a good job of correcting the XRF generated value (all values are located within each other's 95% confidence interval). This is likely due to the fact that arsenic (atomic number 33) is among the heavier elements investigated within this study, thus it contains more protons and the electrons within its K and L shells are more tightly bound to the nucleus of the atom. This results in fluorescence photons of higher energy that are less likely to be attenuated by lighter elements such as oxygen, nitrogen and carbon. Arsenic does not share similar peaks with carbon or oxygen, which can explain why the regression plots presented in Chapter 3 (Figures 3.1 – 3.3) follow the theoretical line closely. Arsenic shares a peak with lead which may lead to interference effects. However, concentrations of lead in the standards used in the experiments do not exceed 10 times the arsenic concentration, suggesting that interference effects should be minimal (USEPA, 2007a).

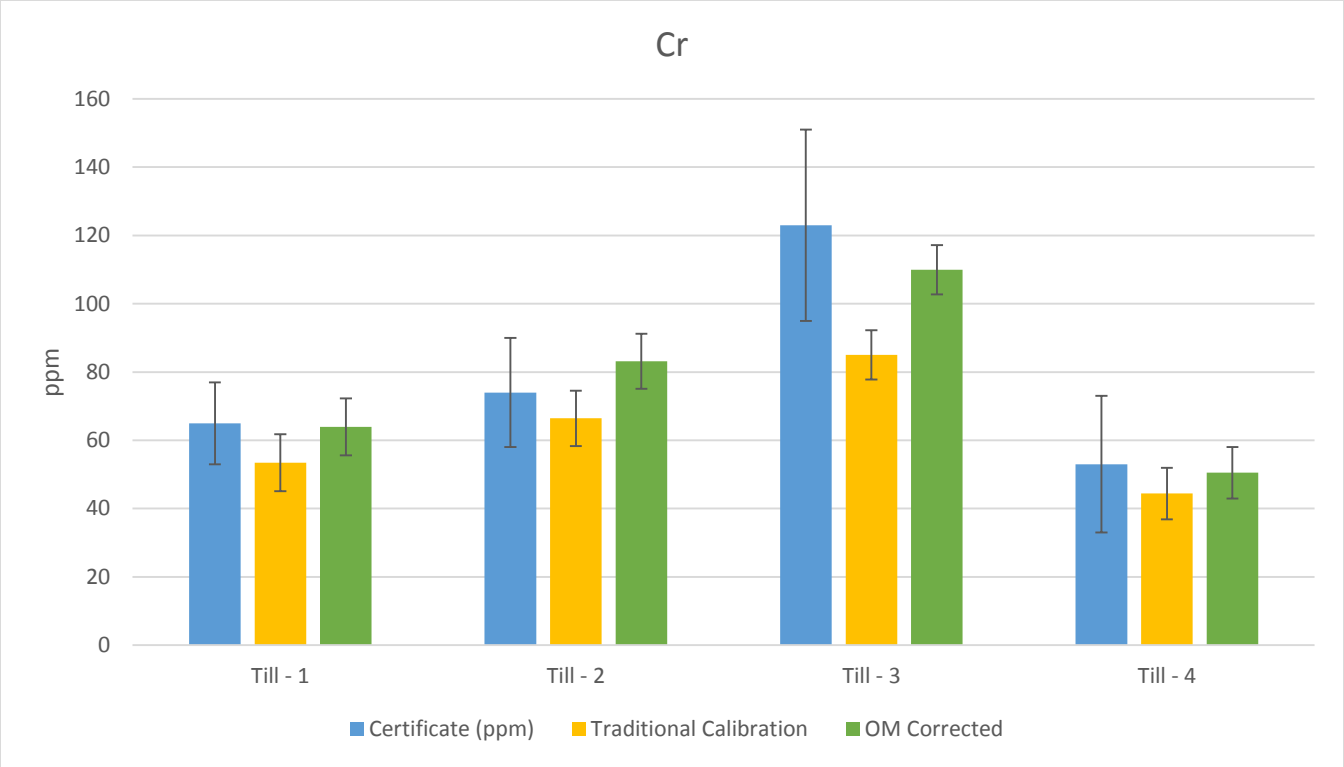

Figure 4.15 Chromium OM correction evaluation chart

For chromium, OM corrections adjust 3 out of 4 measurements closer to their certificate value compared to the traditional correction (Figure 4.15). The OM correction works especially well for the Till-3 standard where adjustment using the traditional correction method yields a value outside the 95% confidence interval of the certified value.

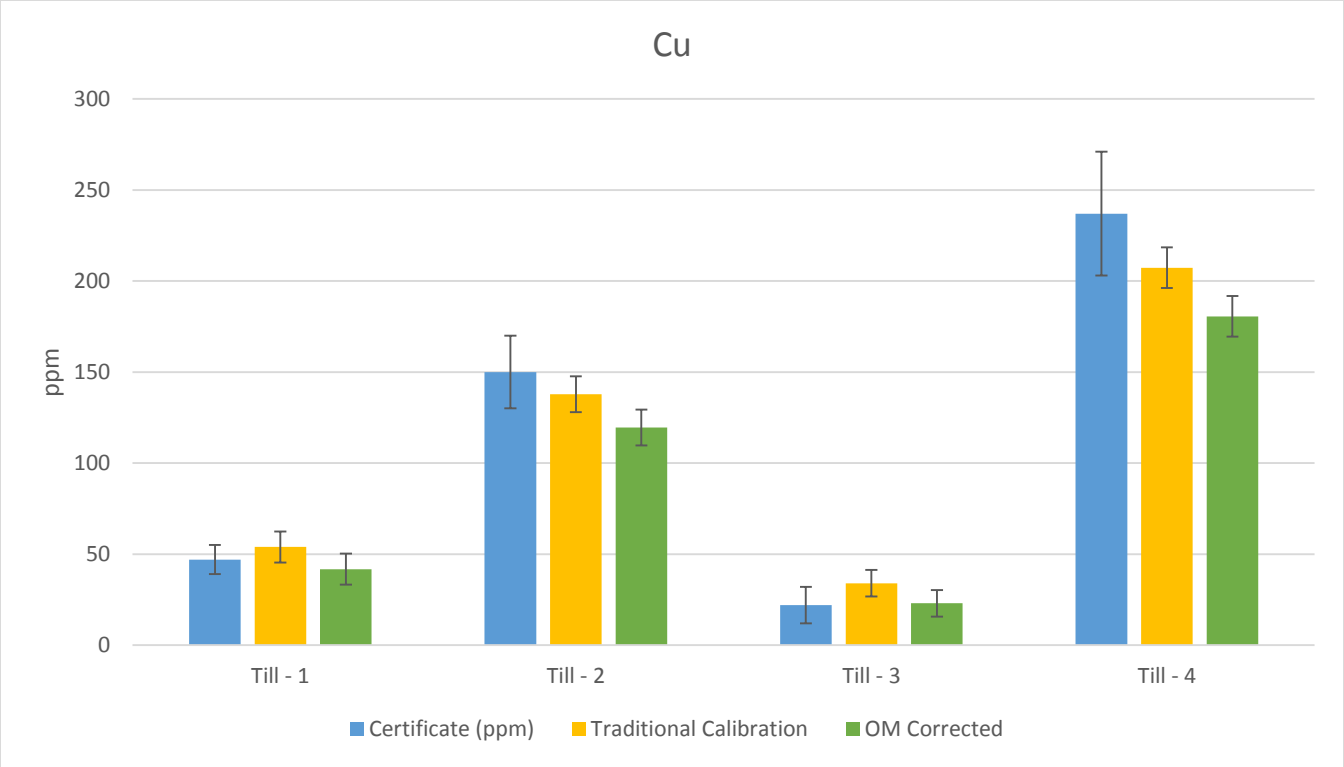

Figure 4.16 Copper OM correction evaluation chart

In the case of copper, the traditional method of correction performs better than the OM correction because all traditional corrections fall within the 95% confidence interval of the certificate values (Figure 4.16). The OM corrections adjust two of the four till measurements outside the 95% confidence interval surrounding their certified values.

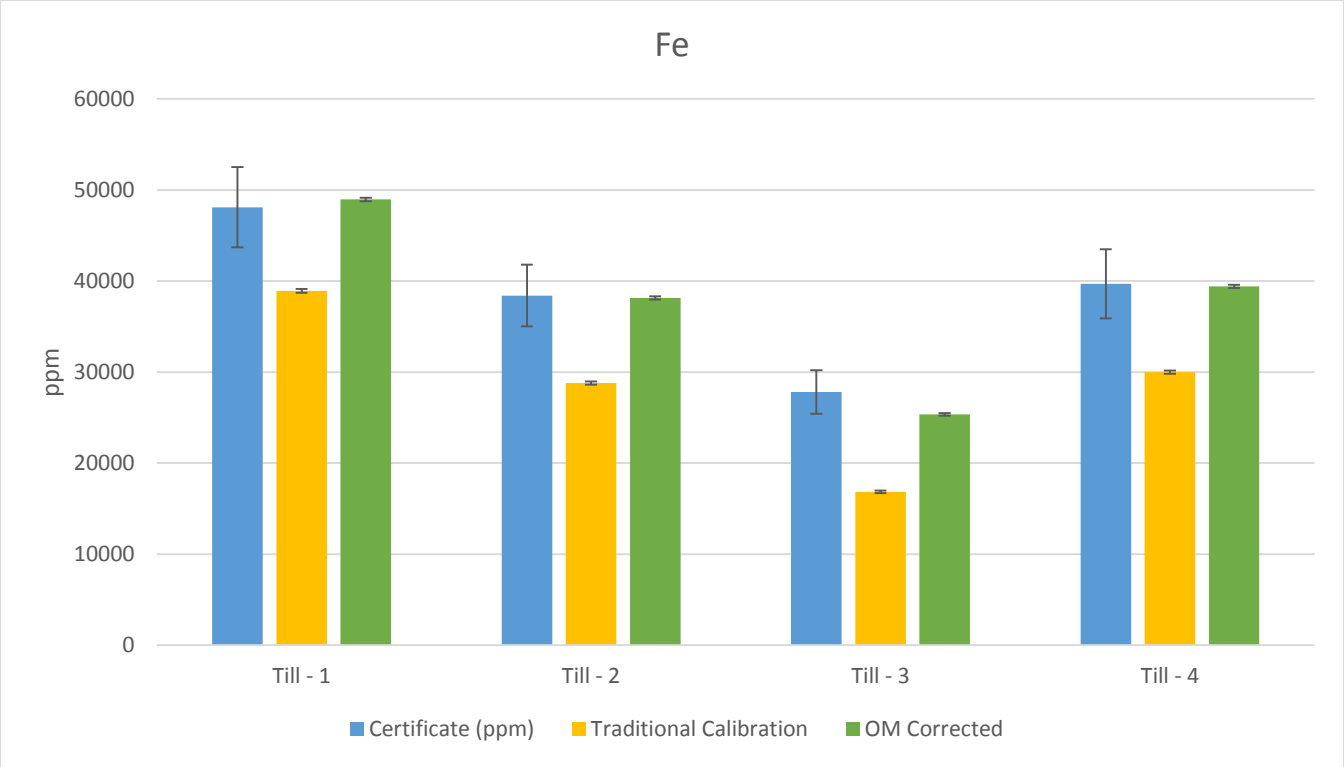

Figure 4.17 Iron OM correction evaluation chart

The traditional method of corrections grossly underestimates the certificate value across the board for iron (Figure 4.17). The OM corrections put all four of the measurement values within the 95% confidence interval of the certificate values and perform better than the traditional method of correction.

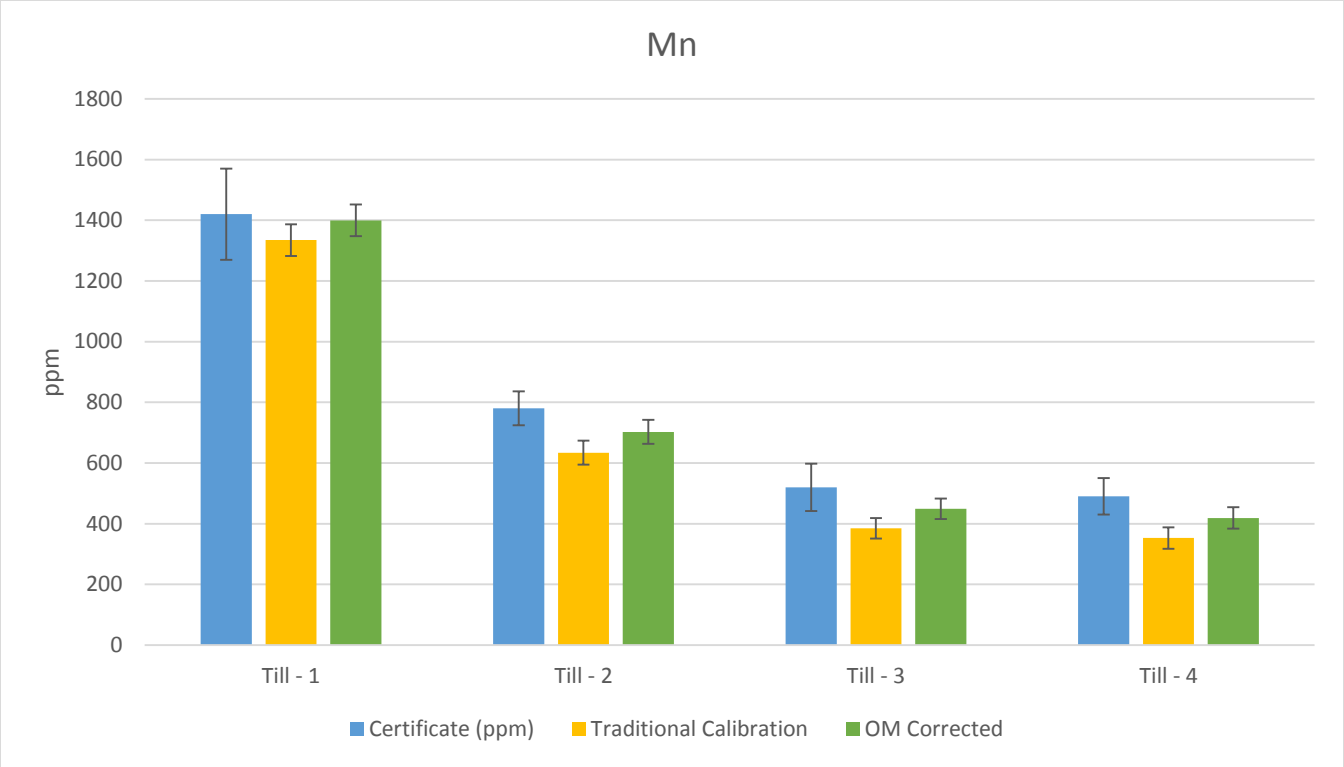

Figure 4.18 Manganese OM correction evaluation chart

Using the traditional correction method for manganese, three out of four measurements (Till-2, Till-3, and Till-4) fell outside the certificate 95% confidence interval (Figure 4.18). Using the OM correction method, all four till measurements fell within their respective certificate's 95% confidence interval.

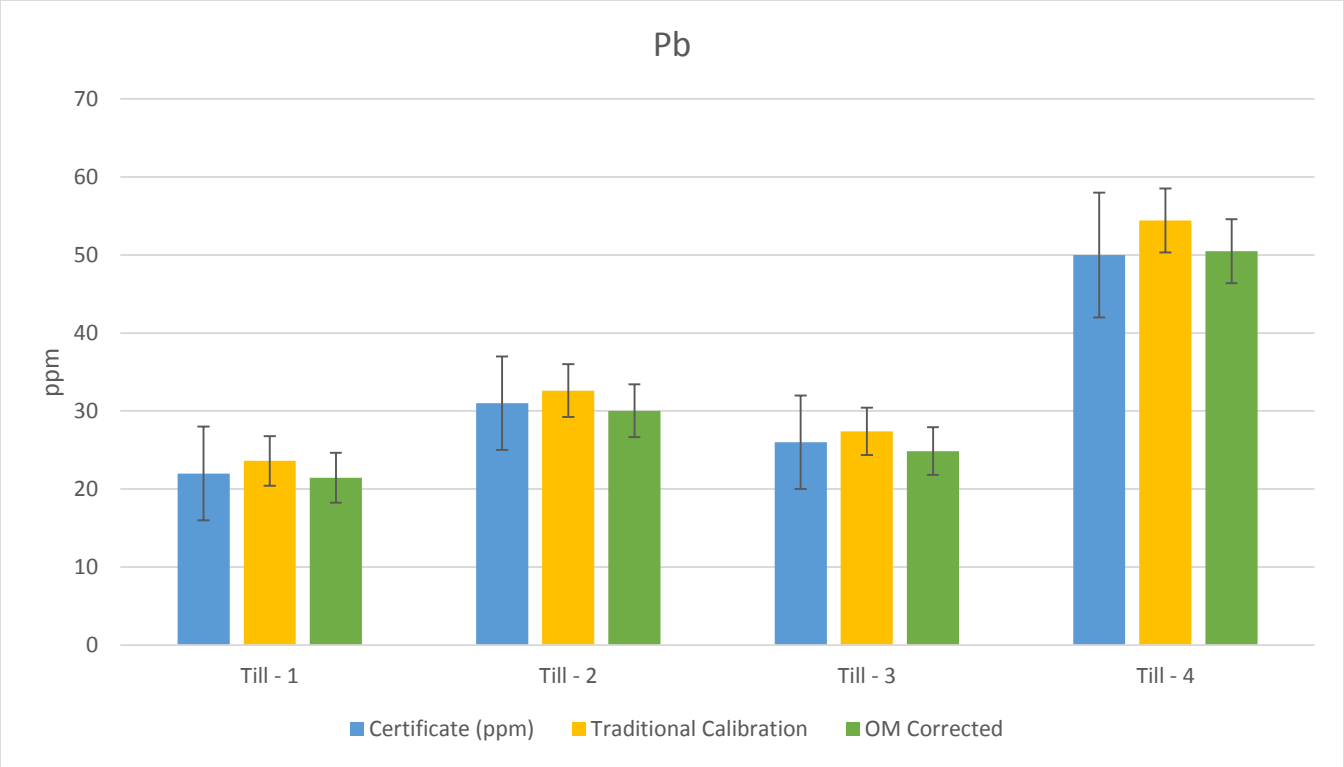

Figure 4.19 Lead OM correction evaluation chart

Both traditional and OM corrections work well for lead, however, the traditional corrections tend to overestimate the certificate values. The organic matter corrections put all four till standard measurements closer to their respective certificate's consensus value compared to the traditional correction (Figure 4.19).

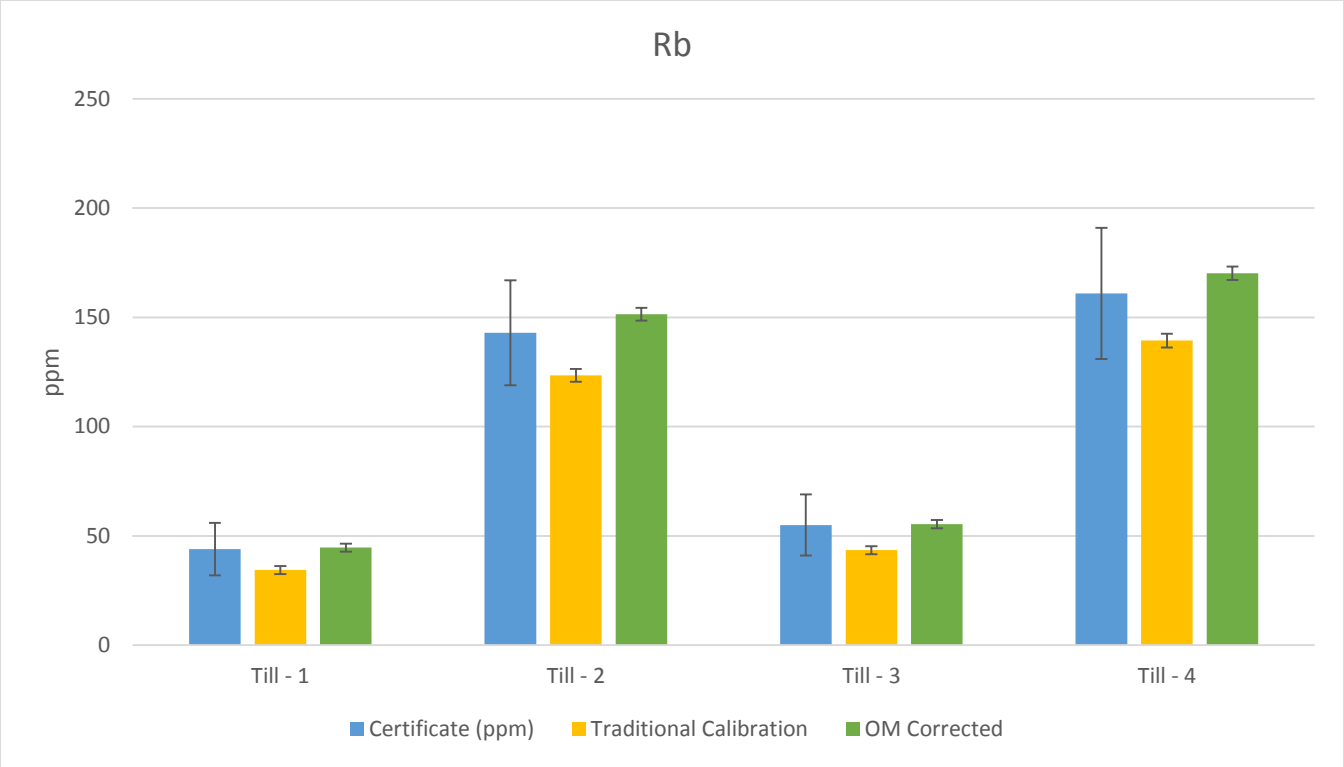

Figure 4.20 Rubidium OM correction evaluation chart

For rubidium, the OM correction moves all four measurements closer to their certificate consensus value compared to the traditional correction. The traditional correction also tends to consistently underestimate the certificate consensus values of the standards, although all estimates fall within the 2σ certificate confidence interval (Figure 4.20).

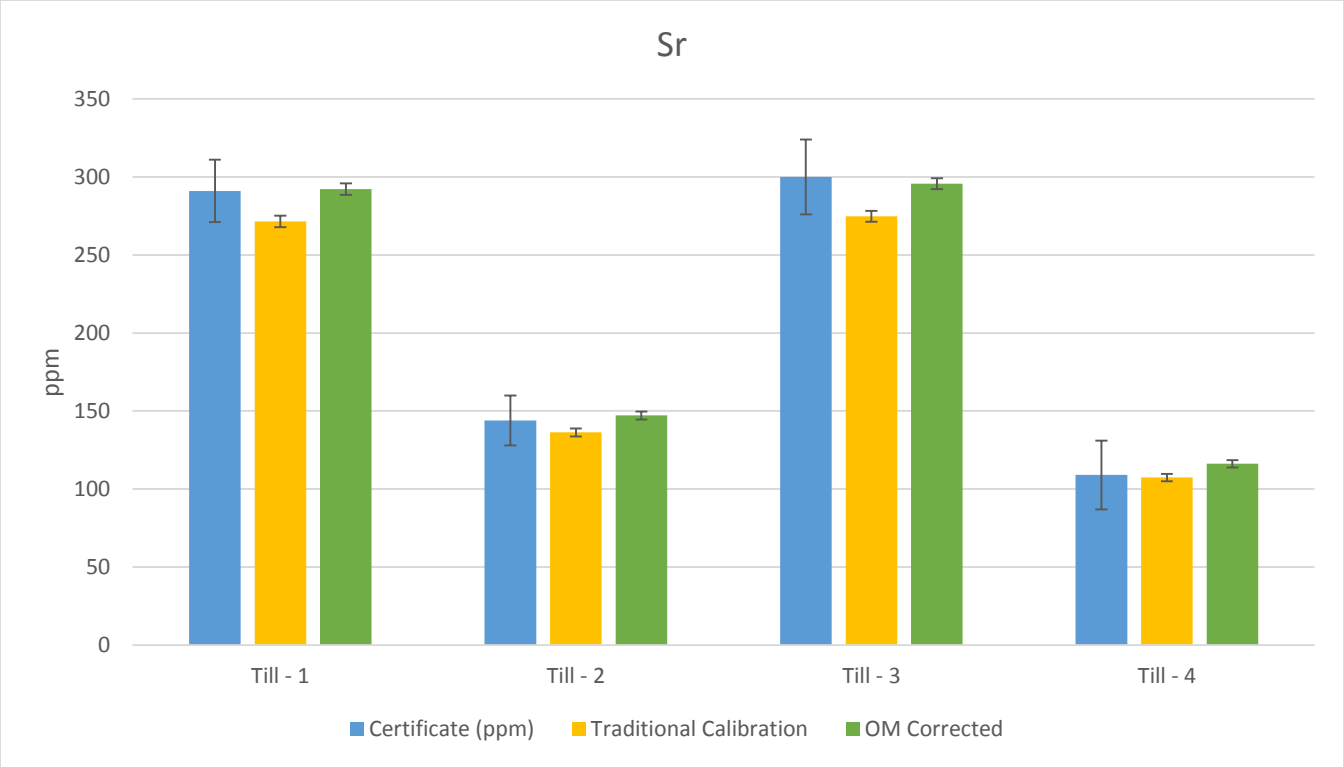

Figure 4.21 Strontium OM correction evaluation chart

For strontium, all estimates fall within the two sigma confidence interval. However, the organic matter corrections move three out of four measurements (Till-1, Till-2, and Till-3) closer to their certificate consensus value.

The strontium nucleus itself consists of 38 protons making it one of the heavier elements under investigation. This gives its electrons relatively high binding energies and thus it has high energy K and L lines which are less likely to be misconstrued for or attenuated by lighter elements.

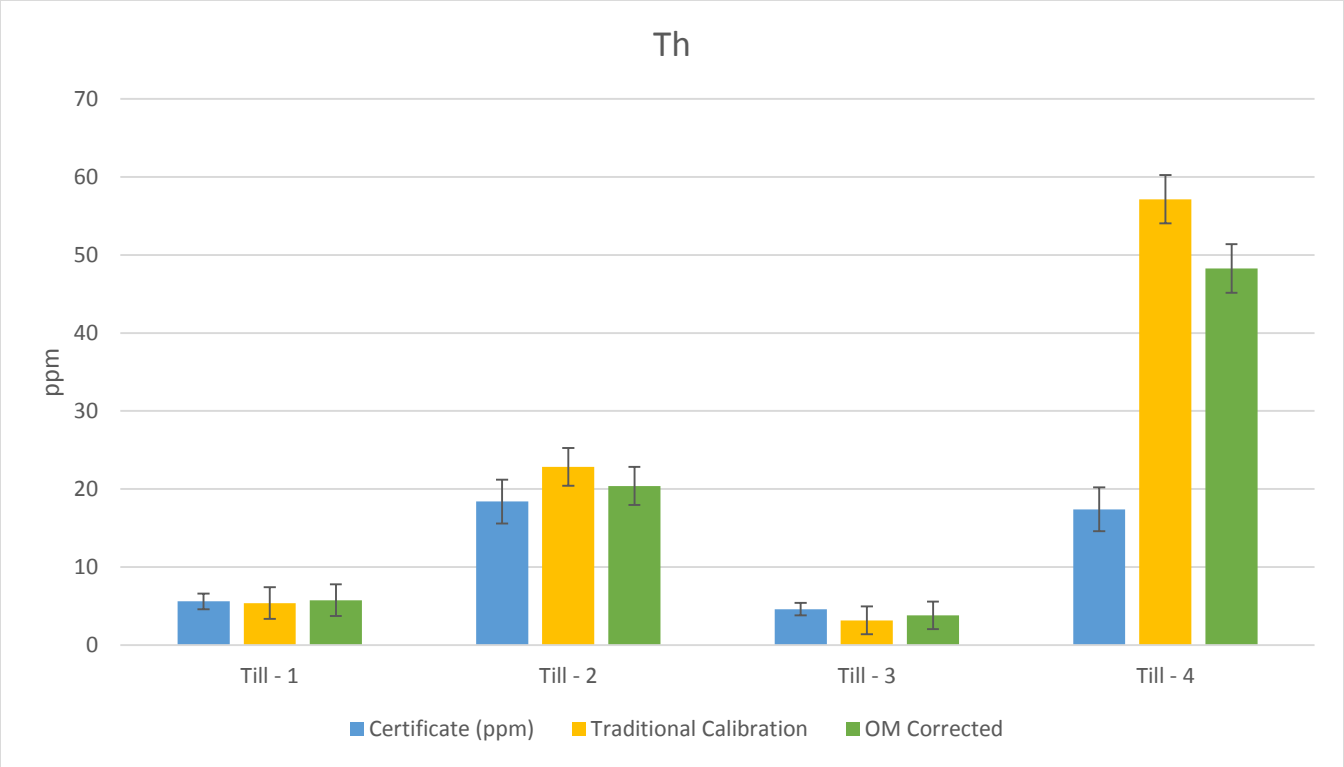

Figure 4.22 Thorium OM correction evaluation chart

For strontium, the OM corrections for the Till-1, Till-2 and Till-3 standards moved the measured values closer to their certified values (Figure 4.22). The Till-4 measurements grossly overestimate their certificate value for both traditional and OM corrections. A second Till-4 standard vial was prepared and re-tested with the pXRF but the results were similar to the first experiment. Hence, the Till-4 standard measurements for thorium are considered outliers.

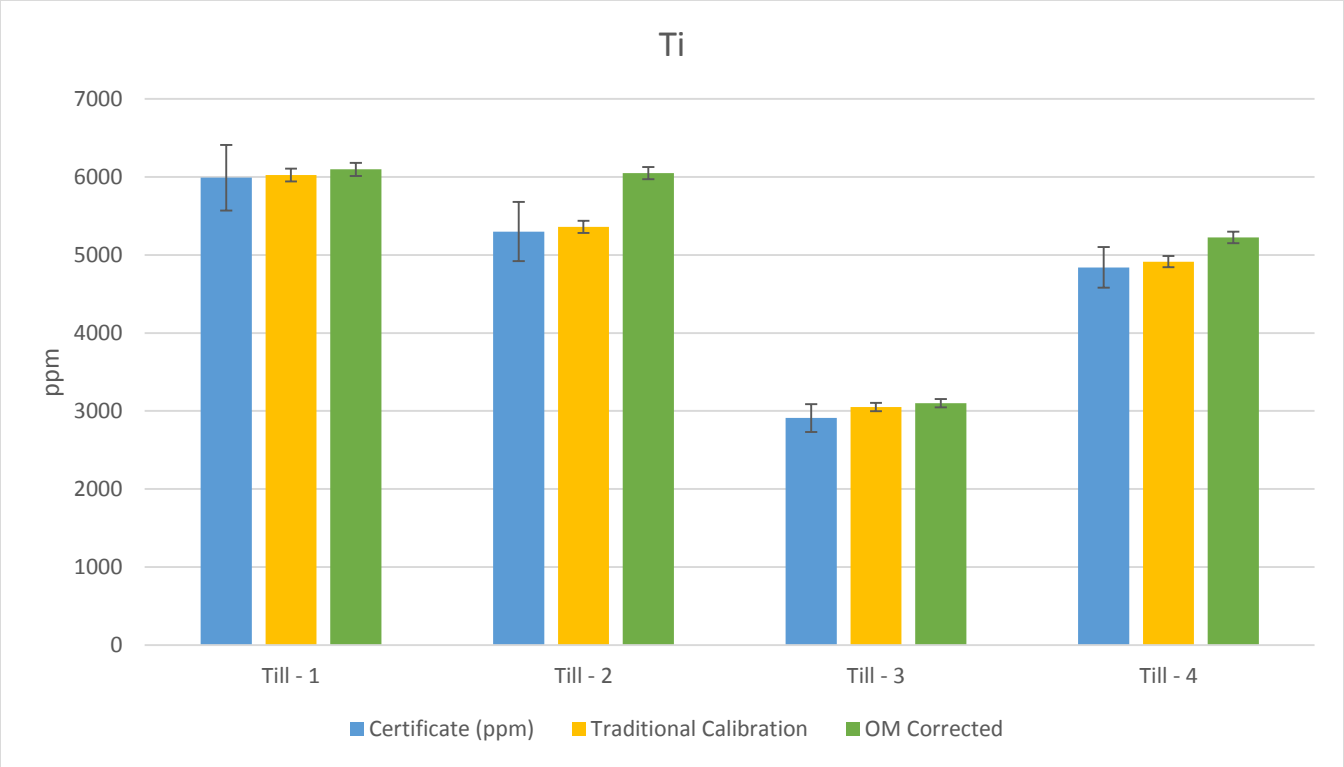

Figure 4.23 Titanium OM correction evaluation chart

In the case of titanium, the OM corrections perform poorly compared to their traditional correction counterparts. The traditional corrections put the consensus values of the measurements closer to their certified values (Figure 4.23). The poor performance of the OM corrections is attributable to the poor correlation coefficients for the cellulose regressions (Table 3.1) from which the OM correction polynomials were generated. These complications may stem from the fact that titanium shares many similar peaks with oxygen which may interfere with the results generated by the pXRF.

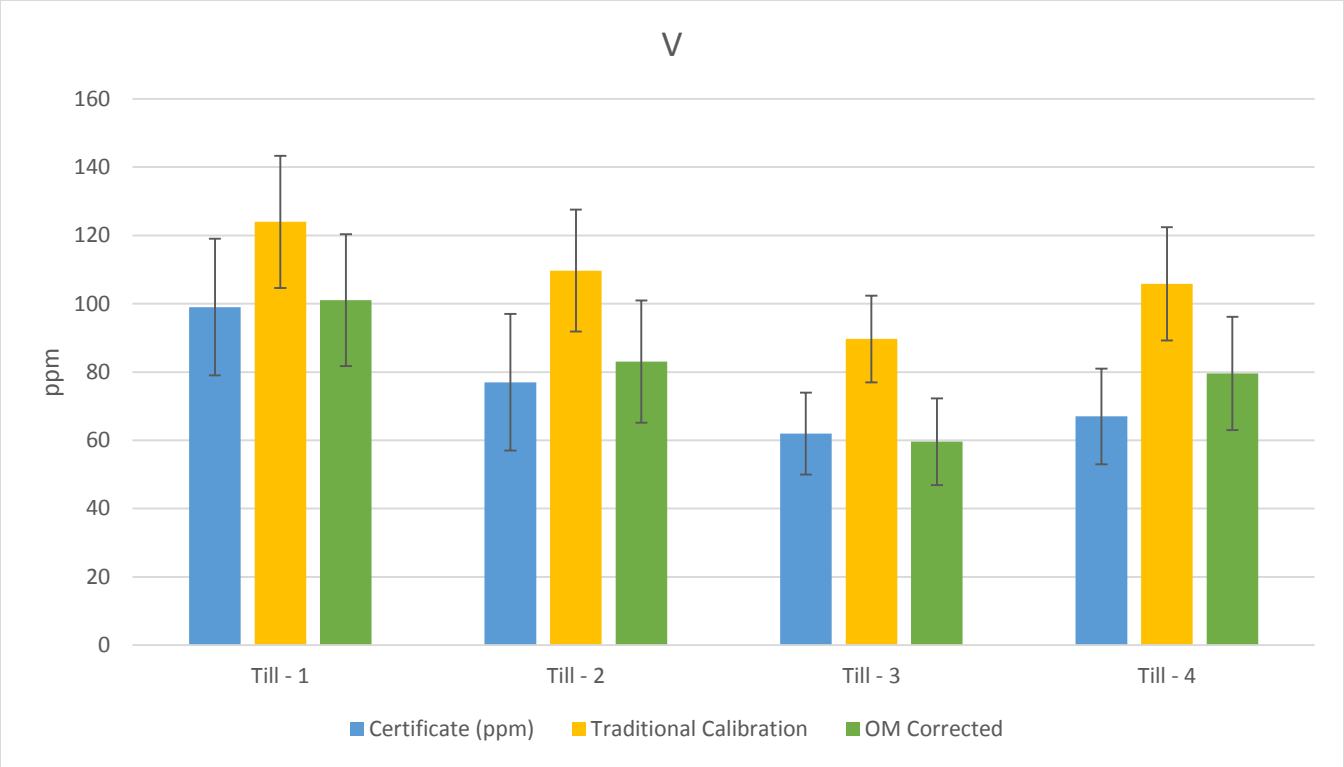

Figure 4.24 Vanadium OM correction evaluation chart

The organic matter corrections perform better than the traditional corrections for vanadium (Figure 4.24). The organic matter corrections move all four till standard measurements closer to their respective certificate values. The organic matter corrections work especially well for the Till-3 and Till-4 standard where the values for the traditional correction exceed their respective certificate 95% confidence intervals. The vanadium dry 1 cellulose regression line from which the vanadium correction polynomial was constructed had a low correlation coefficient (Table 3.7). Nevertheless, pXRF measurements consistently overestimated theoretical vanadium concentrations for all the surrogates used (Figures 3.31 – 3.33).

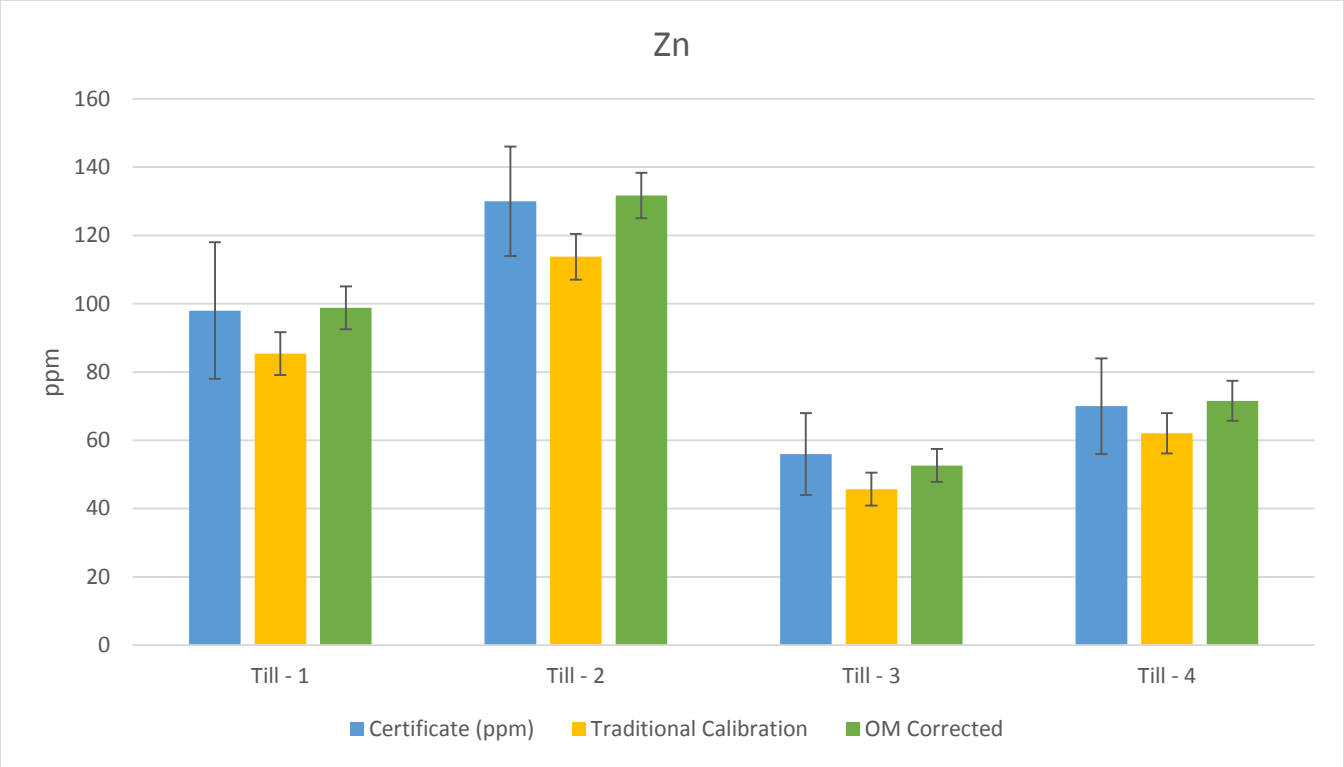

Figure 4.25 Zinc OM correction evaluation chart

For zinc, all estimates fall within the two sigma confidence interval. However, the traditional correction method consistently underestimates the consensus value of the certificates for all four till standards (Figure 4.25). For all four till standards, the OM correction moves the measurement values closer to their certificate consensus value.

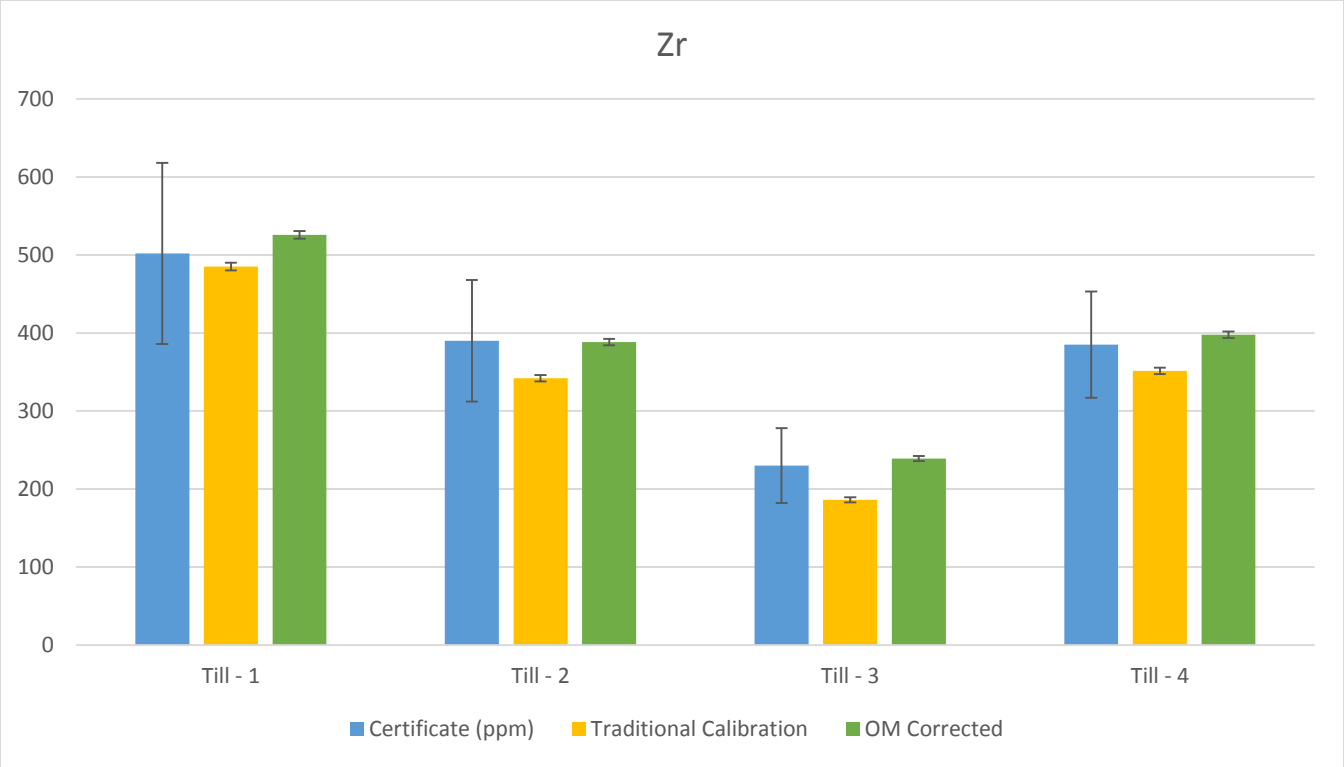

Figure 4.26 Zirconium OM correction evaluation chart

The OM corrections moves three out of four measurements closer to their certificate values (Figure 4.26). The traditional corrections tend to underestimate the consensus value of the certificates as exhibited by Till-2, Till-3 and Till-4.

4.4 ANOVA: Carbon

A nested analysis of variance was conducted on the carbon surrogate using Minitab statistical software to assess the relative contributions of three variability components, i.e. geochemical variability, sample heterogeneity variability, and analytical variability (Table 3.6 and Figure 3.40). Most of the variability stems from the geochemical variability for As, Cu, Fe, Mn, Pb, Rb, Sr, Zn and Zr. However, Cr, Ti, V, and Th do not behave as expected due to complications caused by the analyte concentrations present in the samples and the peak similarities they share with organic matter.

Chromium, titanium and vanadium are relatively light elements that share similar peaks/emissions with organic matter which is why they exhibit high analytical variability. The detector on the pXRF has difficulty distinguishing between their peaks, which in turn affects the interpretation of the counts and their translation into concentration measurements.

Thorium is present within the samples at relatively low levels which give rise to its high analytical and heterogeneity variance. When dealing with a solid medium while performing any type of stochastic analysis, heterogeneity is an important factor because the lack of movement contributes to a lack of signal averaging within samples that gives rise to a higher degree of randomness for metals present at very low levels as is the case with thorium. The analytical variance may also be attributed to the fact that the concentrations of thorium present were very close to the limits of detection for the instrument.

4.5 Hypothesis Evaluation

It was hypothesized that **pXRF metal concentration measurements are attenuated with increasing soil organic matter in proportion to the fraction of organic matter present.** The hypothesis was supported for all elements under investigation, the slopes for all regressions were negative (Table 3.7) meaning the signal was weakened by the addition of organic matter as expected.

Table 3.8 illustrates 8 out of 13 elemental cellulose slope regression values which significantly diverge from their respective theoretical values [Cu, Fe, Mn, Pb, Th, Ti, V, Zr] and Table 3.9 illustrates that 11 out of 13 [As, Cr, Cu, Fe, Pb, Rb, Sr, Ti, V, Zn, Zr] cellulose regression intercepts significantly deviated from their respective theoretical values. In most instances, the theoretical regression lines did not match with the actual pXRF measurement regression lines. This was a common trend not only for cellulose but for carbon and sugar as well. The results presented in Table 3.9 suggest that in all instances, measurement calibrations should be applied to pXRF measurements because 11 out of 13 intercept values were significantly divergent even with zero organic matter present to complicate measurements. When organic matter is present, it is insufficient to apply flat correction factors and the applied calibration must be a function of organic matter fraction present within the sample analyzed.

Results of this investigation demonstrate that pXRF measurements for each element are affected by the addition of organic matter in different ways. For example, it was observed that each surrogate's regression line exhibited different slopes. This may be due to differing ratios of carbon and oxygen atoms present within the surrogates with which the standard is spiked with. On a fundamental level, what makes "cellulose" in fact cellulose is the presence of 6 carbon atoms along with 10 hydrogens and 5 oxygens in molecular form. The X-Ray fluorescence technique is an elemental analysis technique, so it makes sense that each surrogate would affect the XRF signal in different ways given that each surrogate is comprised of different numbers of different types of atoms. The slope of the regression lines among each surrogate are different (Table 3.8) because on a fundamental (elemental) level, each surrogate is comprised of different numbers of carbon and oxygen atoms leading to signal interplay.

The findings of this thesis point to pXRF response as a function of organic matter presence, or more specifically, presence of carbon and oxygen atoms (the primary constituents of organic matter). The empirical observations enabled the construction of plots and calculation of algorithms tailored for pXRF measurement corrections based on organic matter fraction present within the sample being analyzed – specifically with the Niton XL3t+ 950 instrument in soils analysis mode. When tested using four NRCan standard reference soils (Till-1, Till-2, Till-3, and Till-4), in most instances the OM correction algorithms performed better than the traditional correction method. In the case of vanadium, iron, and chromium, *traditional corrections* failed to generate estimated concentrations within their respective certificate 95% confidence intervals for one or more of the standard reference soils. In the case of copper and titanium, some of the OM corrections generated estimated concentrations outside their respective certificate's 95% confidence intervals. Nevertheless, the results of this investigation demonstrate the usefulness of applying elementally dependent OM correction factors for trace metal concentrations in organic rich soils.

4.6 Future Work

The results of this thesis point to XRF response as a function of organic matter presence. This opens many doors for future research because traditionally, application of corrections based on organic matter have not been considered. In this section several ideas for future research are presented.

4.6.1 Bake Samples Prior to XRF

The presence of organic matter affects pXRF response. One could avoid this complication by baking samples to purge them of organic matter prior to XRF analyses. This would require the analyst to keep track of mass loss during the burn so that s/he could back calculate the concentrations from XRF values. This would also require the analyst to calibrate their instrument by constructing calibration curves with standards purged of OM for whom concentrations were adjusted according to their respective mass loss.

4.6.2 Create Certified Standards Pure of OM

Some researchers have called for the creation of certified soil standards with varying organic matter content (Shand and Wendler, 2014). It may be unfeasible for the NIST or others to create soil standards for every conceivable organic matter fraction encounter able in the field. Alternatively, organic matter-free standards could be generated. This would save analysts time and effort by eliminating the need to purge their own standards of organic matter and applying the calculations necessary to render adjusted (concentrated) certificate values.

4.6.3 Pyrolysis

Pyrolysis (to determine carbon, oxygen and nitrogen content) in conjunction with pXRF can prove to be a potent combination. One of the limitations of this investigation was the fact that organic matter was generalized as either carbon, cellulose, or sugar. In the field one may encounter thousands of varying types of organic matter all with different C, N, and O contents. Gas chromatography could conceivably be used in a similar study to isolate and investigate the effects of C, N and O content in natural samples to determine the their effects on pXRF response (as opposed to being chained to the ratios of carbon and oxygen present in the surrogates used in this experiment). One could also investigate the effects of C, N and O by substituting different compounds for the surrogates used in this experiment however, this would not replicate the ratios of organic matter potentially encountered in the field. Use of gas chromatography along with pXRF could potentially help isolate the effects of light elements on pXRF response and enable more accurate correction methods.

4.6.4 Non-Solid Signal Elemental Isolation

The effects of pure carbon content on pXRF response have been detailed and isolated within this investigation. It is conceivable to use the carbon signal plot along with the cellulose plot to isolate the effects of pure oxygen by taking into account the ratios of oxygen and carbon present in cellulose and subtracting the carbon signal out of the cellulose signal thus isolating the oxygen signal. If this method is to be pursued it does not suffice to think of the surrogates in terms of a compound, one would need to begin keeping track of how many physical atoms of carbon and oxygen have been added to the sample. The same method could be employed for nitrogen. One could subtract the effects of carbon from that of cellulose resulting in the isolation of the oxygen signal response. This method would be useful for nitrogen and oxygen signal isolation because they are not found in solid form when they are pure elements at room temperature. If these tests were carried out, it is conceivable to generate algorithms which take site specific determined C, N, and O contents and translate them into an elementally dependent correction factor for pXRF measurements.

APPENDIX A

Acid Digestion Procedure, McElmuury Lab (Wayne State University)

Standard Operating Procedure (SOP)

Microwave Assisted Soil Lead Nitric Acid Digestion

Initially created by: Michael Bickel
Last revised by: S. McElmurry, July 2, 2014

This method is intended to completely extract/solubilize metals from soil samples allowing for the determination of the total lead (Pb) content. Please note that this method will not completely extract lattice bound minerals. SOP is based on US EPA Method 3051A Microwave Assisted Acid Digestion of Sediments, Sludges, Soils, and Oils and is specifically written for use on the CEM MARS Express Microwave Digester.

Notes:

- Procedures in this document require trace metal cleaning. Please see the trace metal cleaning SOP (SOP-Trace Metal Acid Washing.docx) for details.
- Samples and digestion tubes should be completely dry before digestion.
- All sets of samples being run should contain a NIST standard, two blanks, and a spiked and unspiked control.

Materials:

- Light duty tissue wipes (i.e. KimWipes) (VWR 82003-820)
- Trace metal washed 50 ml centrifuge tubes (VWR 89039-662)
- Trace metal washed 30 ml HOPE wide mouth bottles (VWR 414004-110)
- Trace metal washed 30 ml syringes
- Trace metal washed syringe 0.45µm PTFE filters (Microliter Analytical supplies Inc. F25- 1045)
- Purple nitrile gloves (VWR 32930-744)
- NIST Standard 2586, Trace Elements in Soil Containing Lead from Paint
- One un-spiked control sample
- One spiked control sample
- 10 ml pipette
- Disposable scoops (VWR 80081-190)
- Two 8 qt plastic containers

Preclean filters:

1. Prepare a OOmL 6.8% solution of trace metal grade nitric acid in nanopure water (l0mL of nitric acid + 90ml nanopure) and two 1OOmL beakers filled with nanopure water.

2. Using a new trace metal clean syringe (SOP-Trace Metal Acid Washing.docx). draw "'20ml of air into syringe followed by 5ml of 6.8% nitric acid solution.
3. Attach new filter.
4. Pass the Sml of nitric acid through syringe - *taking care not to allow the black plunger not to contact the bottom 5ml of syringe.*
5. Remove filter
6. Draw "'20ml of air into syringe followed by SmL of first nanopure rinse solution.
7. Pass the 5ml of noanopure water through syringe - *taking care not to allow the black plunger not to contact the bottom 5ml of syringe.*
8. Remove filter
9. Draw "'20ml of air into syringe followed by Sml of second nanopure rinse solution.
10. Pass the Sml of noanopure water through syringe - *taking care not to allow the black plunger not to contact the bottom 5ml of syringe.*
11. The filter is now clean. Place filter on new KimWipe to dry in hood, covered by second KimWipe.
12. Repeat steps 2-11 using the same solution for up to 50 new filters.
13. When complete, dispose of nanopure rinses down drain with water and nitric acid solution in hazardous waste container.

Digesting the sample:

1. Remove the cap from a digestion tube, place it on a scale, zero the scale.
2. Slowly add approximately 0.50 g soil (0.45-0.55 g) using the scoop
3. Over the sink, rinse the scoop with nano water and dry it well with a light duty tissue wipe.
4. Repeat this process with each of the samples, making sure to record the exact mass of each sample being put into the digestion tube. Do not put the caps back on the tubes.
5. After all of the digestion tubes have soil in them, move them over to the hood, and, while wearing acid washing gear, add 10ml of 68% Nitric Acid to each tube (from the pump located in the hood with the Flame AA), put both caps back on securely, then put the tubes in the canister.
6. Place the canister in the microwave for digestion, making sure that the space between 17 and 18 is centered.
7. Pick the digestion program that corresponds to the number of samples being tested from the following list, and press start.

EPA Method 3051Xpress for 8-24 Samples

EPA Method 3051A_40 MODI Xpress For 24-40 Samples

8. Leave the digestion tubes in the microwave overnight, or at the very least for a few hours, to make sure they have cooled down enough to handle.

Diluting/Centrifuging the Samples:

- Label an empty trace metal washed centrifuge tube for each sample and weigh the tubes, record the weight.
- Using a pipette, add 10 ml of nano-water to each centrifuge tube.
- Wearing acid washing gear, move digestion canister from the microwave to the hood.
- Carefully pour the contents of each digestion tube into its corresponding centrifuge tube.
- Rinse each digestion tube, using 10 ml of nano-water and the pipette, then pour into centrifuge tube.
- Repeat the above step, so there is a total of 40 ml in the centrifuge tubes creating a 17% nitric acid solution.
- Place the empty digestion tubes into one of the 8 qt containers and the tops the other 8 qt container
- Weigh and record the weight of the full centrifuge tubes.
- Put samples in the wrist action shaker, for twenty minutes each (up to 12 samples can be shaken simultaneously).
- Put samples in the centrifuge (only 4 at a time), and let the samples centrifuge for 20 minutes at 4000 rpm (there is a line indicating this point on the machine).
- Clean digestion tubes (SOP-Trace Metal Acid Washing.docx).

Filteringthe Samples:

1. Move centrifuge tubes to the hood, along with the appropriate number of 30 ml bottles (labeled with the sample number AND centrifuge tube number), plastic syringes,and filters.

2. Secure a filter to the bottom of syringe, remove the plunger of the syringe,pour in 15 ml of the sample, and push it through the syringe in clean 30mlbottle (SAFETY NOTE: Be sure to angle the syringe away from you so that if acid were to squirt out, it would not be directed toward you)

3. Repeat the above step, for the same sample, with another 15 ml (There should be 30 ml of sample in each bottle and 10 mlof sample left in the bottom of the centrifuge, tube).

4. Discard empty syringes and filters in the trash.

5. Repeat steps 1-4 for all the samples.

6. Pour the excess sample from the centrifuge tubes into the waste bin and label it.

APPENDIX B

XRF Calibration Tables
(Till-1, Till-2, Till-3, Till-4, NIST 2586, NIST-2709a, NIST-2711a)

Plots included in Appendix C were generated using the following data.

	As Reference	As XRF	Cr Reference	Cr XRF	Cu Reference	Cu XRF	Fe Reference	Fe XRF
	Mn Reference	Mn XRF	Pb Reference	Pb XRF	Rb Reference	Rb XRF	Sr Reference	Sr XRF
Till 1	1420	1393	22	22	44	41	291	286
Till 2	780	694	31	33	143	134	144	143
Till 3	520	449	26	26	55	50	300	291
TILL 4	490	473	50	53	161	149	109	111
NIST 2586	1000	900	432	425	N/A	45	84	76
NIST 2709a	529	490	17	17	99	82	239	215
NIST 2711a	675	551	1400	1421	120	109	242	223

	Th Reference	Th XRF	Ti Reference	Ti XRF	V Reference	V XRF	Zn Reference	Zn XRF
Till 1	5.6	6.2	5990	5505	99	113	98	92
Till 2	18.4	20.4	5300	5822	77	107	130	119
Till 3	4.6	4.3	2910	2958	56	74	56	51
TILL 4	17	49	4840	5144	67	95	70	65
NIST 2586	7	7	6050	6090	160	149	352	329
NIST 2709a	11	10	3360	3753	110	120	103	92
NIST 2711a	15	20	3170	2953	81	78	414	379

	Zr Reference	Zr XRF
Till 1	502	500
Till 2	390	365
Till 3	230	215
TILL 4	385	364
NIST 2586	N/A	280
NIST 2709a	195	139
NIST 2711a	N/A	N/A

APPENDIX C

XRF Calibration Plots
(Till-1, Till-2, Till-3, Till-4, NIST 2586, NIST-2709a, NIST-2711a)

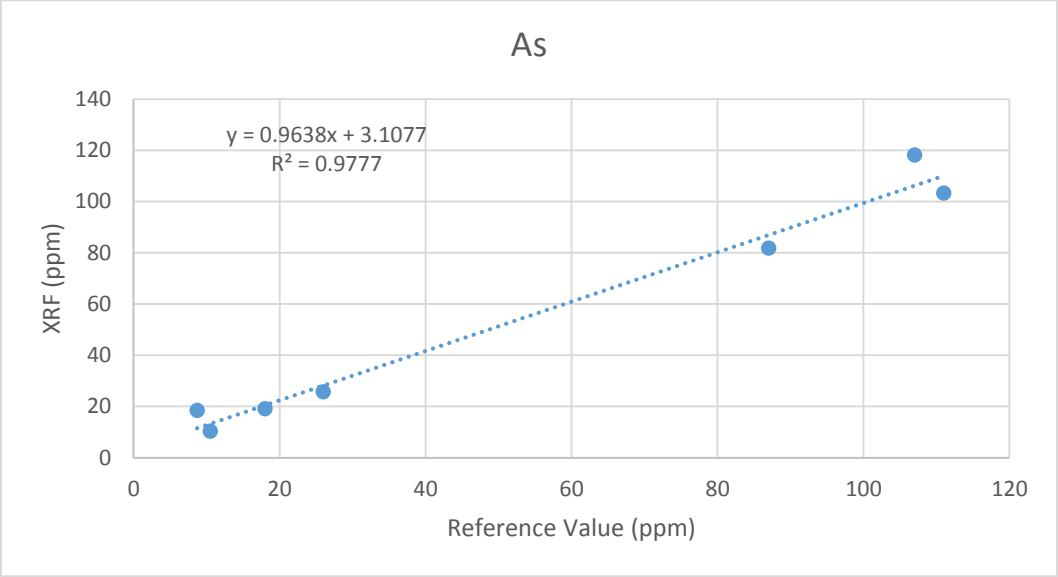

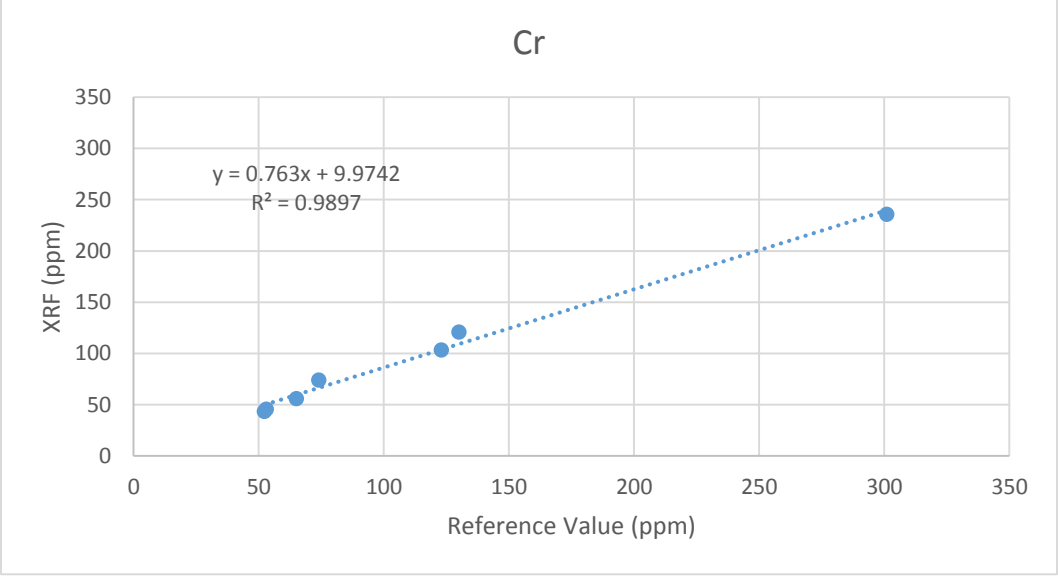

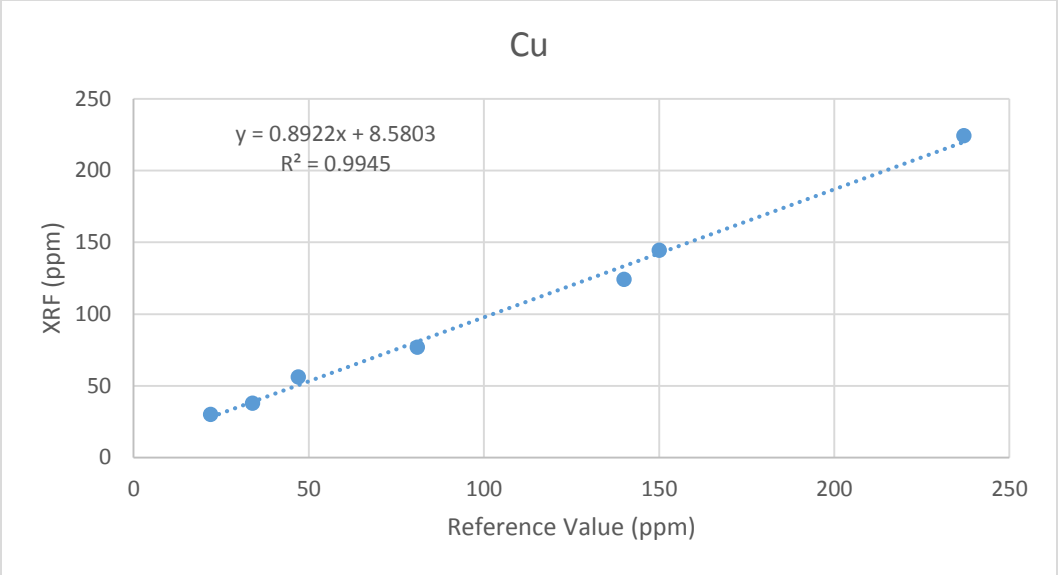
Cu
y = 0.8922x + 8.5803
R² = 0.9945
XRF (ppm)
Reference Value (ppm)
0
50
100
150
200
250

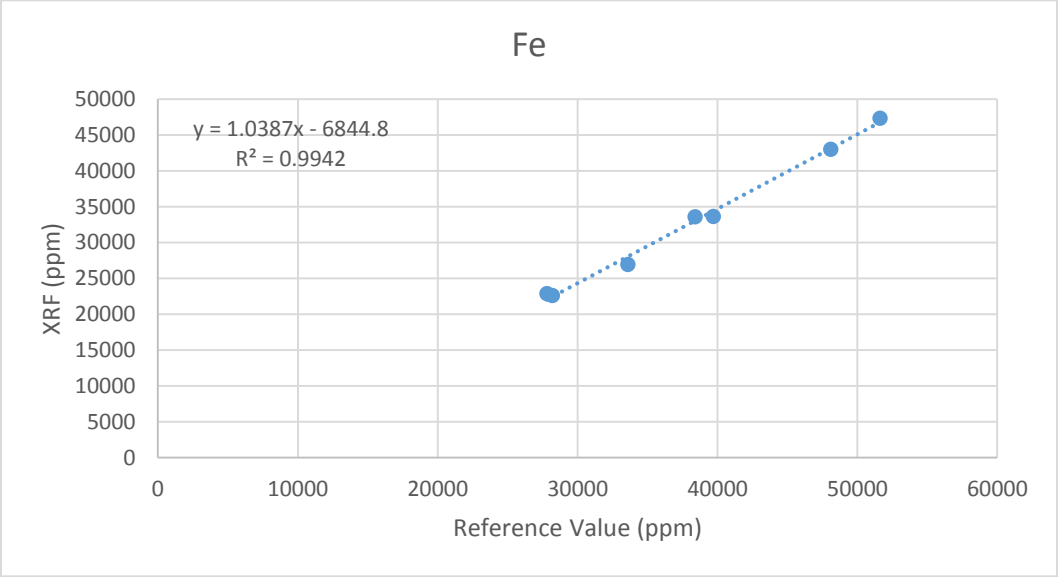
Fe
y = 1.0387x - 6844.8
R² = 0.9942
XRF (ppm)
Reference Value (ppm)
0
5000
10000
15000
20000
25000
30000
35000
40000
45000
50000
60000

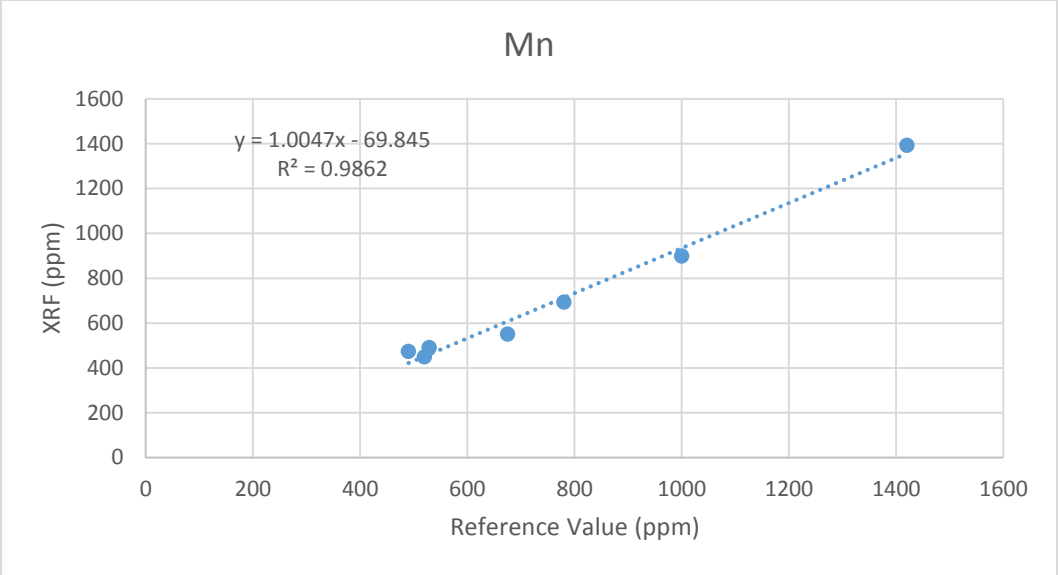
Mn
y = 1.0047x - 69.845
R² = 0.9862
XRF (ppm)
Reference Value (ppm)
0
200
400
600
800
1000
1200
1400
1600

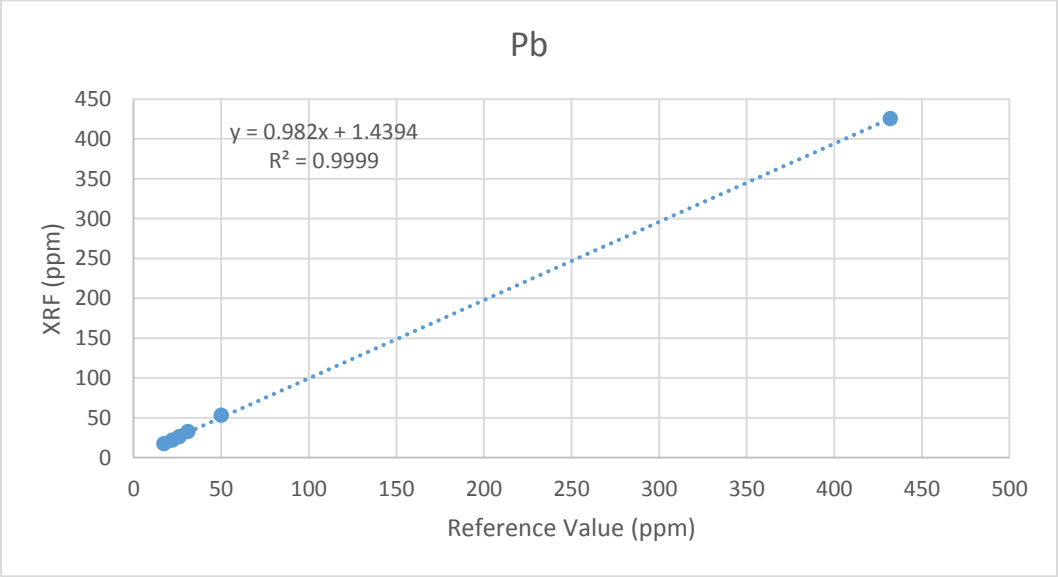
Pb
y = 0.982x + 1.4394
R² = 0.9999
XRF (ppm)
Reference Value (ppm)
0
50
100
150
200
250
300
350
400
450
500

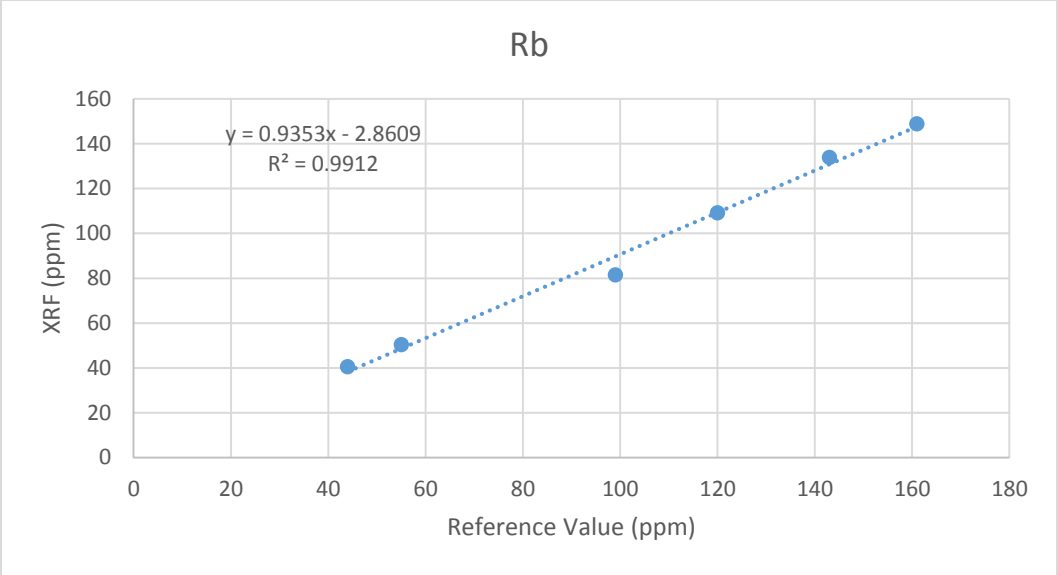
Rb
y = 0.9353x - 2.8609
R² = 0.9912
XRF (ppm)
Reference Value (ppm)
0
20
40
60
80
100
120
140
160
180

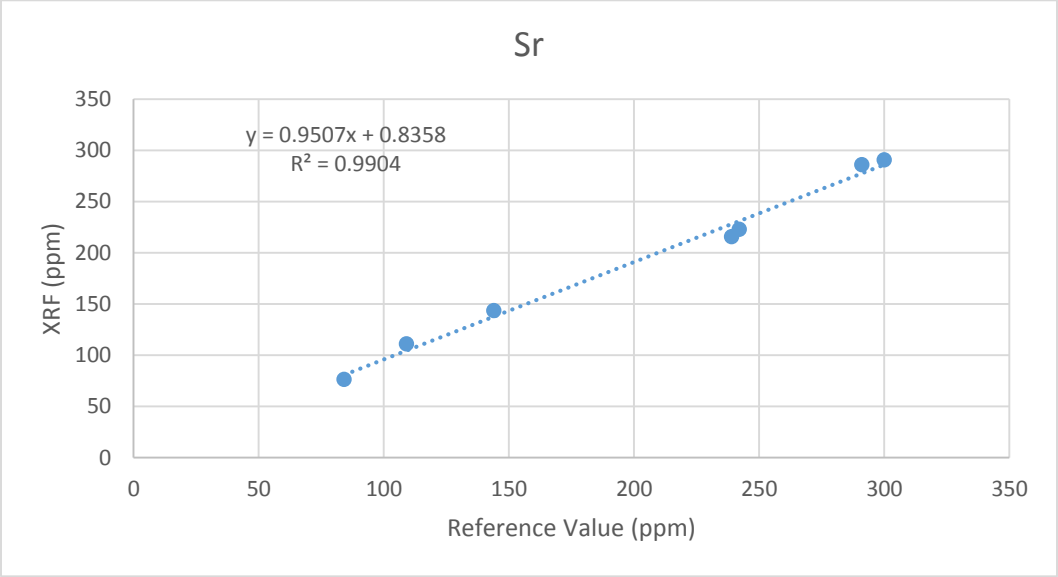
Sr
y = 0.9507x + 0.8358
R² = 0.9904
XRF (ppm)
Reference Value (ppm)
0
50
100
150
200
250
300
350

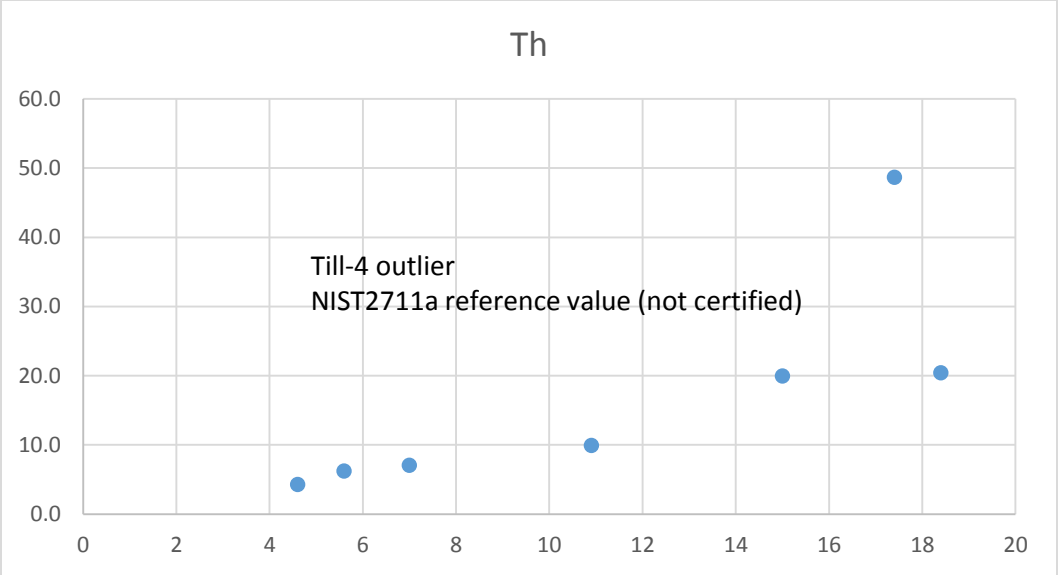
Th
60.0
50.0
40.0
30.0
20.0
10.0
0.0
0
2
4
6
8
10
12
14
16
18
20
Till-4 outlier
NIST2711a reference value (not certified)

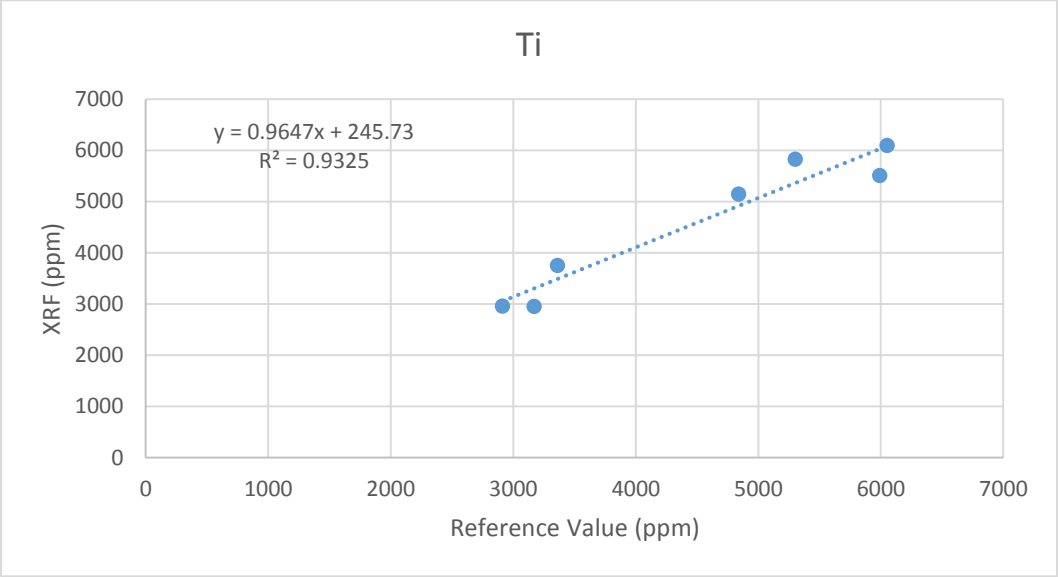
Ti
y = 0.9647x + 245.73
R² = 0.9325
XRF (ppm)
Reference Value (ppm)
7000
6000
5000
4000
3000
2000
1000
0
0
1000
2000
3000
4000
5000
6000
7000

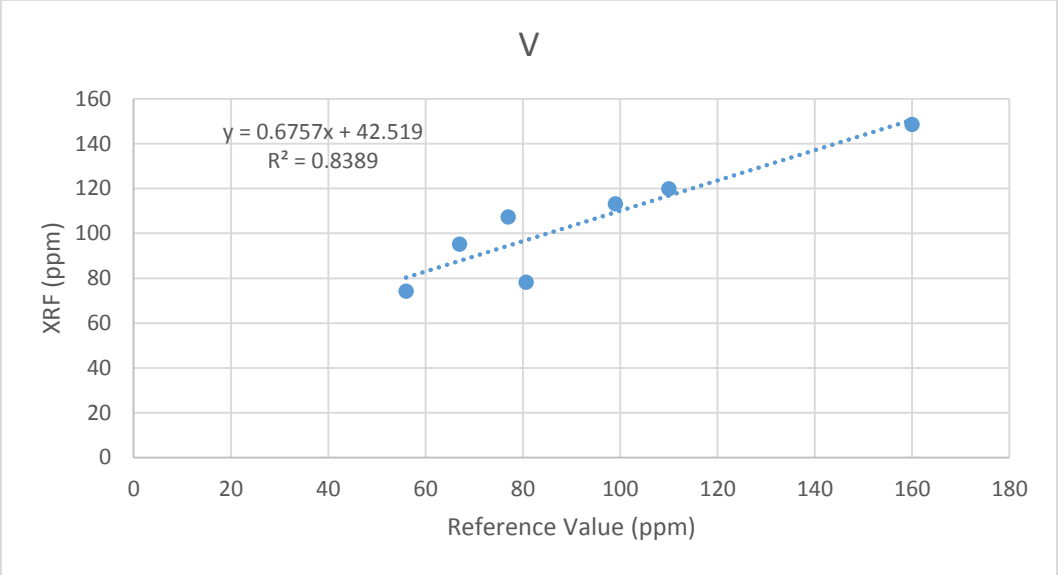
V
y = 0.6757x + 42.519
R² = 0.8389
XRF (ppm)
Reference Value (ppm)
0
20
40
60
80
100
120
140
160
180

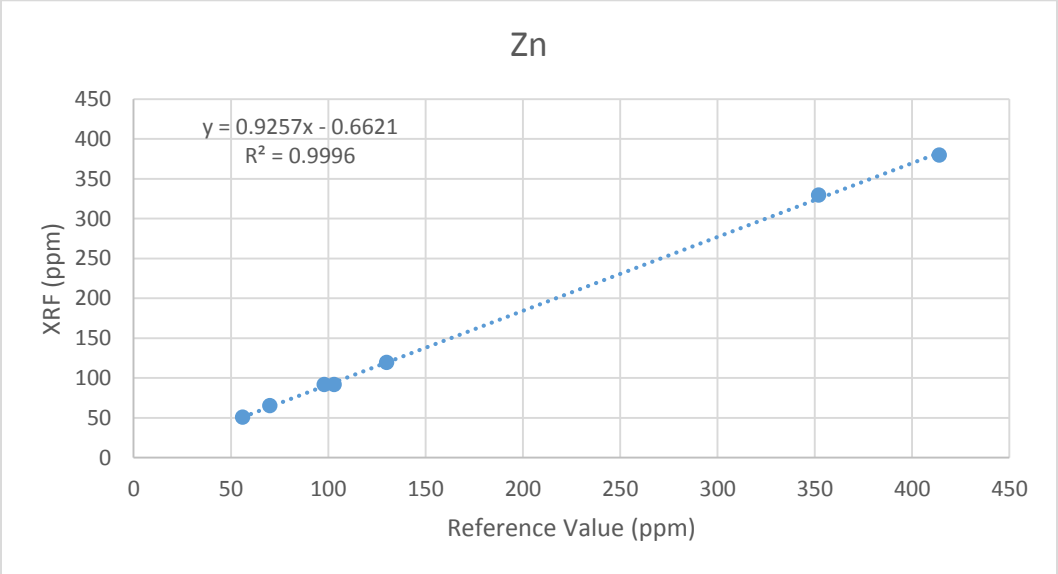
Zn
y = 0.9257x - 0.6621
R² = 0.9996
XRF (ppm)
Reference Value (ppm)
0
50
100
150
200
250
300
350
400
450

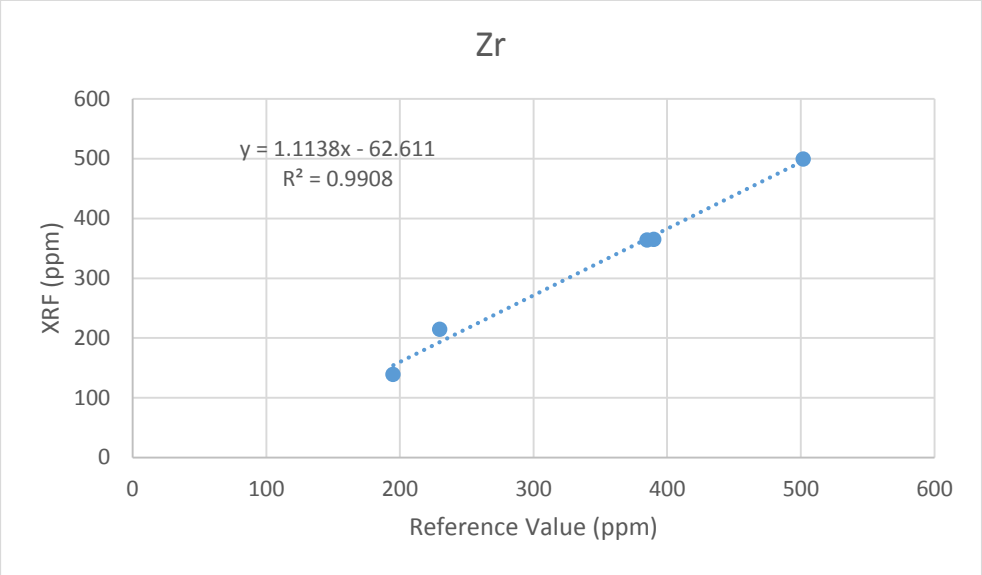
Zr
y = 1.1138x - 62.611
R² = 0.9908
XRF (ppm)
Reference Value (ppm)
0
100
200
300
400
500
600

REFERENCES

ASTM, 2014, Standard Test Methods for Moisture, Ash, and Organic Matter of Peat and Other Organic Soils, Volume D2974 - 14, ASTM International

Böning, P., Bard, E., and Rose, J., 2007, Toward direct, micron-scale XRF elemental maps and quantitative profiles of wet marine sediments: Geochemistry, Geophysics, Geosystems, v. 8, no. 5.1525-2027. 10.1029/2006GC001480

Brand, N., and Brand, C., 2014, Performance comparison of portable XRF instruments: Geochemistry: Exploration, Environment, Analysis, p. 2012-2172.1467-7873.

Brumbaugh, W. G., Tillitt, D. E., May, T. W., Javzan, C., and Komov, V. T., 2013, Environmental survey in the Tuul and Orkhon River basins of north-central Mongolia, 2010: metals and other elements in streambed sediment and floodplain soil: Environmental Monitoring and Assessment, v. 185, no. 11, p. 8991-9008.1573-2959. 10.1007/s10661-013-3229-9

Congiu, A., Perucchini, S., and Cesti, P., 2013, Trace metal contaminants in sediments and soils: comparison between ICP and XRF quantitative determination: E3S Web of Conferences, v. 1, p. 1-4

Goulding, F., and Jaklevic, J., 1973, Photon-excited energy-dispersive X-ray fluorescence analysis for trace elements: Annual review of nuclear science, v. 23, no. 1, p. 45-74.0066-4243.

Iwanczyk, J. S., and Patt, B. E., 1999, New X-ray detectors for XRF analysis: Adv. X-Ray Anal, v. 41, p. 951

Jenkins, R., 1988, X-Ray Fluorescence Spectrometry, Wiley, Chemical Analysis.9780471836759

Kalnicky, D. J., and Singhvi, R., 2001, Field portable XRF analysis of environmental samples: Journal of Hazardous Materials, v. 83, no. 1–2, p. 93-122.0304-3894. http://dx.doi.org/10.1016/S0304-3894(00)00330-7

Kenna, T. C., Nitsche, F. O., Herron, M. M., Mailloux, B. J., Peteet, D., Sritrairat, S., Sands, E., and Baumgarten, J., 2011, Evaluation and calibration of a Field Portable X-Ray Fluorescence spectrometer for quantitative analysis of siliciclastic soils and sediments: Journal of Analytical Atomic Spectrometry, v. 26, no. 2, p. 395-405.0267-9477. 10.1039/C0JA00133C

Lachance, G. R., and Claisse, F., 1995, Quantitative X-Ray Fluorescence Analysis: Theory and Application, New York, Wiley.ISBN 9780471951674

Löwemark, L., Chen, H. F., Yang, T. N., Kylander, M., Yu, E. F., Hsu, Y. W., Lee, T. Q., Song, S. R., and Jarvis, S., 2011, Normalizing XRF-scanner data: A cautionary note on the interpretation of high-resolution records from organic-rich lakes: Journal of Asian Earth Sciences, v. 40, no. 6, p. 1250-1256.1367-9120. http://dx.doi.org/10.1016/j.jseaes.2010.06.002

NRCan, 1995, TILL-1, TILL-2, TILL-3 and TILL-4 Geochemical Soil and Till Reference Materials: Natural Resources Canada.http://www.nrcan.gc.ca/mining-materials/certified-reference-materials/certificate-price-list/8137.

Piorek, S., 1998, Determination of Metals in Soils by Field-Portable XRF Spectrometry, *in* Lopez-Avila, V., Barcelo, D., Beckert, W., Goheen, S., Jinno, K., Keith, L. H., and Rittenberg, J. H., eds., Current Protocols in Field Analytical Chemistry, Wiley.ISBN 9780471176091.

Potts, P., 1999, Portable X-ray fluorescence analysis, Industrial and environmental applications of nuclear analytical techniques, Volume IAEA-TECDOC--1121, International Atomic Energy Agency (IAEA), p. 67

Radu, T., and Diamond, D., 2009, Comparison of soil pollution concentrations determined using AAS and portable XRF techniques: Journal of Hazardous Materials, v. 171, no. 1–3, p. 1168-1171.0304-3894. http://dx.doi.org/10.1016/j.jhazmat.2009.06.062

Ramsey, M., 1998, Sampling as a source of measurement uncertainty: techniques for quantification and comparison with analytical sources: Journal of Analytical Atomic Spectrometry, v. 13, no. 2, p. 97-104.0267-9477. 10.1039/A706815H

Shand, C. A., and Wendler, R., 2014, Portable X-ray fluorescence analysis of mineral and organic soils and the influence of organic matter: Journal of Geochemical Exploration, v. 143, p. 31-42.0375-6742. http://dx.doi.org/10.1016/j.gexplo.2014.03.005

Tjallingii, R., Röhl, U., Kölling, M., and Bickert, T., 2007, Influence of the water content on X-ray fluorescence core-scanning measurements in soft marine sediments: Geochemistry, Geophysics, Geosystems, v. 8, no. 2, p. 1-12.1525-2027. 10.1029/2006GC001393

Troeh, F. R., 2005, Soils and Soil Fertility, Wiley.9780813809557

USEPA, 2007a, EPA Method 3051a Microwave Assisted Aced Digestion of Sediments, Sludges, Soils, and Oils: United States Environmental Protection Agency, Revision 1

-, 2007b, EPA Method 6200 Field Portable X-Ray Fluorescence Spectrometry for the Determination of Elemental Concentrations in Soil and Sediment: United States Environmental Protection Agency, Revision 0

VanCott, R. J., McDonald, B. J., and Seelos, A. G., 1999, Standard soil sample preparation error and comparison of portable XRF to laboratory AA analytical results: Nuclear Instruments and Methods in Physics Research Section A: Accelerators, Spectrometers, Detectors and Associated Equipment, v. 422, no. 1–3, p. 801-804.0168-9002. http://dx.doi.org/10.1016/S0168-9002(98)01000-6

Weindorf, D. C., Zhu, Y., Chakraborty, S., Bakr, N., and Huang, B., 2012, Use of portable X-ray fluorescence spectrometry for environmental quality assessment of peri-urban agriculture: Environmental Monitoring and Assessment, v. 184, no. 1, p. 217-227.1573-2959. 10.1007/s10661-011-1961-6

ABSTRACT

PORTABLE X-RAY FLUORESCENCE MEASUREMENT VIABILITY IN ORGANIC RICH SOILS: PXRF RESPONSE AS A FUNCTION OF ORGANIC MATTER PRESENCE

by

ROOZBEH RAVANSARI

AUGUST 2016

Advisor: Dr. Lawrence D. Lemke

Major: Geology

Degree: Master of Science

Portable X-Ray fluorescence provides a cost effective method for producing rapid geochemical data. With advancements in X-Ray generation and detection technology, pXRF has become feasible for use on pedologic materials. Factors affecting pXRF soil measurements such as heterogeneity, moisture content, object geometry, and matrix interferences are widely recognized. However, the influence of organic matter on pXRF soil measurements is poorly understood.

This study examined the influence of organic matter fraction on pXRF trace metal measurements in a soil matrix. Incremental addition of three organic matter surrogates (cellulose, graphite powder, and confectioner's sugar) was used to investigate the influence of increasing organic matter content up to approximately 30%. Each organic matter surrogate was independently added to and homogenized with samples of Natural Resources Canada Till-1 standard reference material that was initially expunged of organic matter through combustion. Incremental addition was performed 20 times for each surrogate, and concentrations of arsenic,

chromium, iron, manganese, lead, rubidium, strontium, thorium, titanium, vanadium, zinc and zirconium were measured as a function of varying organic matter fractions using a Thermo Scientific Niton XL3t GOLDD+ 950 XRF analyzer.

Results demonstrate attenuation of the pXRF signal and elementally-dependent deviation from the expected concentration with increasing sample organic matter fraction. Based on the results, a pXRF organic matter fraction-dependent calibration method was developed and its performance was evaluated using four unmodified NRCan soil standards (Till-1, Till-2, Till-3, Till-4) with known organic matter content. In general, the new method improved measurement accuracy compared to conventional pXRF calibration methods. Because soils inherently contain varying amounts of organic matter, these results suggest more accurate geochemical data can be generated via pXRF if soil organic matter fraction is quantified and taken into account during measurement calibration.

AUTOBIOGRAPHICAL STATEMENT

I, Roozbeh Ravansari was born and raised in San Diego, California. Growing up, I spoke Farsi at home because my mother and father are immigrants from Iran. I attended the Language Academy from elementary through middle school where I was enrolled in a French immersion program. This is where I learned to speak, read and write in French. I attended the San Diego High School of International Studies where I was enrolled in their International Baccalaureate program. In 2007, I earned my high school diploma in addition to an International Baccalaureate diploma. In 2013 I graduated from the University of California San Diego earning a Bachelor of Science in Earth Sciences. In 2016 I graduated from Wayne State University in Detroit, Michigan earning a Master of Science in Geology.